ISBN 0-315-55720-6

CONSTRAINTS ON THE FORMATION OF DEPOSITIONAL PLACER ACCUMULATIONS IN COARSE ALLUVIAL BRAIDED RIVER SYSTEMS

by

© JOHN PETER BURTON ©

A THESIS

SUBMITTED TO THE FACULTY OF GRADUATE STUDIES AND RESEARCH IN PARTIAL FULFILMENT OF THE REQUIREMENTS FOR THE DEGREE OF MASTER OF SCIENCE

DEPARTMENT OF GEOLOGY

LAKEHEAD UNIVERSITY

THUNDER BAY, ONTARIO

NOVEMBER, 1989

ABSTRACT

Placer accumulations are formed by the preferential sedimentation of heavy minerals from the general population of detritus being transported by a fluid. The depth, velocity, and grain size conditions under which placers form on beaches, sand-dominated meandering, and braided fluvial systems is at present only partially understood. Our knowledge of the controls on alluvial placer formation in gravel-dominated longitudinal bars of braided rivers is even more poorly developed despite their obvious economic importance.

The accumulation of heavy minerals in coarse-grained longitudinal gravel bars was studied by examining and sampling surficial and matrix sediments from modern, naturally occurring bars, and by simulating these bars under a variety of controlled flow conditions in a sediment-water recirculating flume.

Two processes dominated the deposition of sediments in both the natural and artificial systems studied: 1) suspension rain out; and 2) avalanche face progradation. Sediments which were deposited as a result of avalanche face progradation were found to contain significantly higher concentrations of heavy minerals in both the naturally occurring and experimental longitudinal gravel bars. Data also indicate that the difference in heavy mineral content amongst sediments deposited as a result of these two processes will increase substantially with increasing density of the detrital minerals present. This suggests that denser heavy minerals are more likely to be deposited amongst less dense surficial sediments whereas less dense heavy minerals are more likely to be vertically distributed throughout the bar sequence.

In the natural systems studied, heavy mineral content was found to be much higher in poorly sorted, coarse-grained sediments deposited amongst pebble sized clasts. Flume tank experimentation similarly revealed that detrital lead content was highest amongst pebble sized clasts during the fastest velocity runs. In addition, an increase in clast size resulted in a decrease in the amount of heavy minerals accumulating in surficial sediments.

This study has also highlighted two processes which result in the formation of alluvial depositional placer accumulations in coarse-grained braided river systems. The first process occurs as a result of heavy minerals in channel bottom sediments becoming progressively enriched through the winnowing of less dense sediments, resulting in the formation of an erosional placer deposit. Flume experimentation revealed that when high concentrations of heavy minerals armouring the stream-bed were reached, this often

resulted in the initiation of their movement downstream. This process can also be triggered by catastrophic events such as large floods or regional tectonic uplift. A sudden increase in energy typically associated with such events results in the flushing of erosional placers and their eventual deposition in areas of higher preservation potential. Therefore, a catastrophic adjustment helps to flush out erosional placer deposits into the basin to form a depositional placer accumulation. The second process of depositional placer formation results from heavy minerals travelling in bed load transport, while less dense sediments are kept mostly in suspension. With a decrease in velocity, heavy minerals are sedimented with hydraulically equivalent sized, less dense sediments in open framework gravels.

TABLE OF CONTENTS

LIST OF TABLES

LIST OF FIGURES

ACKNOWLEDGEMENTS

I wish to extend a special thanks to Dr. P. W. Fralick for his advice and efforts in supervising the work throughout. I am grateful for his time he freely gave to me on so many occasions. I also wish to thank Dr. W. E. L. Minter of the University of Capetown, South Africa, for his constructive comments on the manuscript. I am particularly indebted to the following people for their help at various times over the study: Anne Hammond for her help in sample preparations and magnetic separations; Prof. Brian Spenceley for allowing me access to the darkroom facilities of the Physics Department; Phil Gaudino who wrote the computer programme I used on numerous occasions to analyse the data obtained from countless grain size analyses; Sam Spivack who drafted the diagrams; Linda Siczkar who assisted me with the computer graphics; and to Anne LaRoche who helped me on many occasions with the manuscript during its preliminary stages. Their help is gratefully acknowledged.

Financial support for this study was provided by an Ontario Geoscience Research Grant from the Ministry of Northern Development and Mines. Special thanks are also extended to Environment Canada, Parks Division, Western Region, for granting me permission to collect sediment samples in Banff National Park.

Finally, I wish to thank my family, and particularly my parents, for their constant encouragement and inspiration throughout the entire course of study; for their support, I am especially indebted.

CHAPTER 1: INTRODUCTION

1.1: Purpose and Objectives:

The primary objective of this study is to identify the fundamental conditions present in braided gravel-dominated fluvial systems that maximise the concentration of economic heavy minerals in longitudinal gravel bars.

Traditionally, most research concerning placer development in coarse grained gravel bars has centred on the Witwatersrand palaeoplacers of South Africa (see Minter, 1970, 1978; Pretorius, 1976, 1981; Smith and Minter, 1980; Smith and Beukes, 1983; and Krapez, 1985). These vast palaeoplacer deposits are significant as they alone have contributed over half the gold mined by man, some 1.4 billion Troy ounces, in a little over one hundred years of exploitation (Pretorius, 1981).

Considering the obvious economic importance of placer deposits, it is surprising that such occurrences have not been the subject of more sedimentological research. As one recent paper stated, "...the physical processes responsible for concentrating heavy minerals have attracted little attention and are poorly understood. The mechanisms of sediment sorting in rough mobile beds under turbulent flows are complex, and present transport theory provides useful but only limited assistance to the problem" (Smith and Beukes, 1983, p. 1342). These constraints have led most researchers to focus their attention on sandy braided systems that are inherently less turbulent (Kartashov, 1971; Minter, 1970, 1978; Smith and Minter, 1980; Pretorius, 1976, 1981; Slingerland, 1977, 1984; Slingerland and Smith, 1986), or on the accumulation of placer lag deposits (Cheney and Patterson, 1967; Gunn, 1968; Krook, 1968; Tuck, 1968; Kolesov, 1975; Mosley and Schumm, 1977) formed as a result of erosional processes rather than the depositional accumulation of heavy minerals in coarse-grained longitudinal bars. Such gravel bars are areas of high turbulence, a condition that should not be favourable for heavy mineral concentration, yet there are numerous examples of placer deposits that have formed under these conditions (see Pretorius, 1981).

The first direct experiments on the processes involved in heavy mineral deposition in gravel bars were conducted by Minter and Toens (1970). In this study, magnetite was used in a flume to simulate the behaviour of detrital gold in a coarse-grained fluvial system. Different sized pebbles were used to construct a simulated gravel bar in each of three separate runs. Results from these experiments indicated that significant heavy mineral enrichment of gravel beds did not occur, at least under the flow conditions studied.

In the present study, field work was carried out in two contrasting environmental settings to compliment data obtained from 27 experimental flume runs to further investigate the results obtained by Minter and Toens (1970).

The first braided river system examined was that of the North Saskatchewan River located in Banff National Park, Alberta. The underlying reason for selecting this particular section of river was for the presence of a large unvegetated braided outwash plain which continues downstream for over 75 kilometres from its source, the Saskatchewan Glacier. Such extensive unvegetated outwash plains contain a multitude of longitudinal gravel bars (see Gustavson, 1974; Miall, 1977; Smith, 1985). A total of five longitudinal gravel bars were randomly selected and sampled over the 55 kilometre section of the river examined. This sample programme was conducted in order to understand the processes operating which result in the deposition of surficial and matrix sediments in coarse-grained longitudinal bars. It was theorised that a modern glaciofluvial system that has developed in a largely unvegetated braided outwash plain would be analogous to the system that resulted in the palaeoplacer deposits of Elliot Lake in Ontario. This system produced thick sequences of quartz-pebble conglomerates containing economic concentrations of uraninite during the Proterozoic. However, the predominance of limestone and dolomite in the source terrain of the North Saskatchewan River system resulted in few heavy minerals found in the sediments sampled in this study. This is in contrast to the relatively plentiful supply made available from the granitic plutons exposed during the Proterozoic to the north of Elliot Lake.

The second portion of this study involved the examination and sampling of three separate rivers in proximity to Lake Superior in Ontario. The rivers examined were: The Jackpine, Agawa, and Mississagi. Although these rivers do not compare to the North Saskatchewan River with respect to the presence of large glacial outwash plains, they were each selected because they exhibit classic braided sections containing coarse-grained longitudinal gravel bars. Compared to the North Saskatchewan River, these rivers also inherently contain proportionally higher concentrations of heavy minerals which is the result from flowing through Pleistocene aged glacial deposits derived from the Canadian Shield.

The third portion of this study involved the simulation of natural braided river systems by means of flume experimentation. This was conducted in order to determine the conditions operating which result in maximum heavy mineral accumulation in longitudinal gravel bars. Detrital magnetite and lead grains were added to the predominantly quartz and pyroxene rich sand used in the flume to simulate the behaviour

of detrital uraninite and gold in these systems. The controlled (independent) variables included bed roughness (gravel size), bed shear stress, and sand grain size. The uncontrolled (dependent) variable was the amount of pyroxene, magnetite, and lead found concentrated in both surficial and matrix sediments of the gravel bar following each run. A series of 27 flume runs using various combinations of controlled variables were conducted in order to identify the conditions which result in the highest accumulation of heavy minerals.

1.2: Regional Setting

1.2.1: The North Saskatchewan River

The North Saskatchewan River originates at the Saskatchewan Glacier, one of several valley glaciers emanating from the Columbia Icefields which straddle the continental divide and whose meltwaters supply the Atlantic, Pacific, and Arctic Oceans (see Figure 1). The river flows in a southeasterly direction through a highly mountainous terrain in Banff National Park, Alberta, with relief from valley floor to mountain tops often approaching 1500 metres. The river is a large, mostly unvegetated, braided river system whose outwash plain often reaches one kilometre in width. Owing to the predominantly glacial source of meltwater, this river experiences large fluctuations in discharges, both diurnally and seasonally (Smith, 1972; Burton, 1986) which contributes to the development of this type of fluvial system (Miall, 1977). The river receives a substantial supply of coarse-grained clastic sediments consisting of limestone, dolomite, shale, and quartzite (Smith, 1972) from the Saskatchewan Glacier. However, coarse sediments also reach the river by the many tributaries entering the North Saskatchewan river system, and from colluvial debris delivered to the river by talus slope processes.

1.2.2: The Jackpine River

The Jackpine River, located approximately 130 kilometres east of Thunder Bay, Ontario, (see Figure 1) was selected due to the presence of a readily accessible longitudinal gravel bar. The river originates predominantly from lake and groundwater discharge from the north and empties into Lake Superior to the south. A large seasonal variation in discharge exists, owing to a significant contribution from spring runoff that allows gravel bars, such as the one studied, to become submerged during maximum spring discharge events. During such events, these bars experience both erosion and

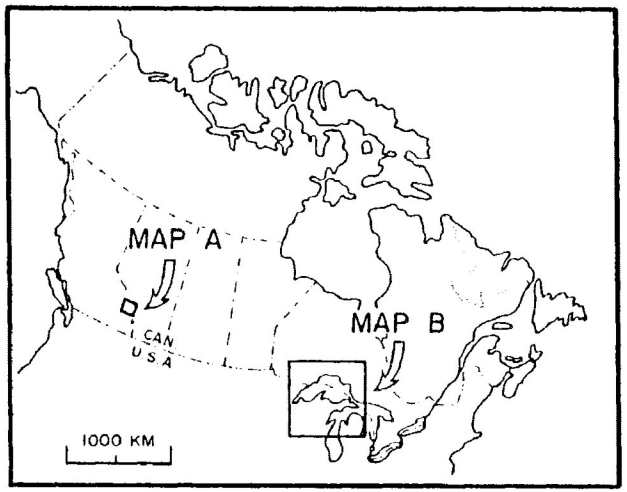

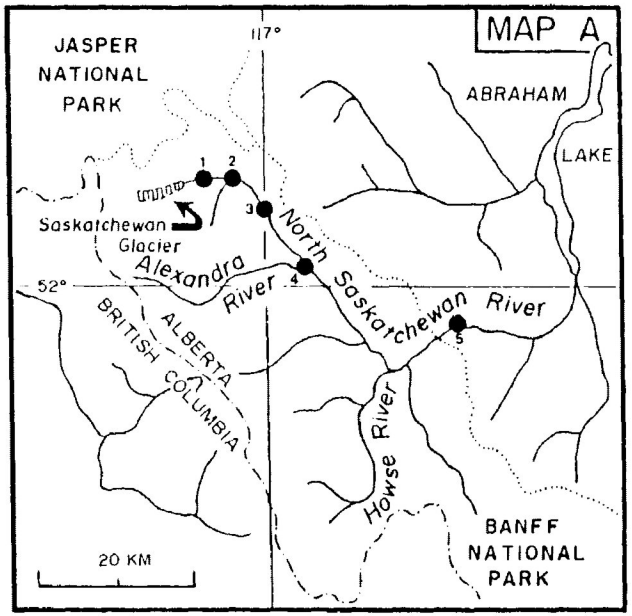

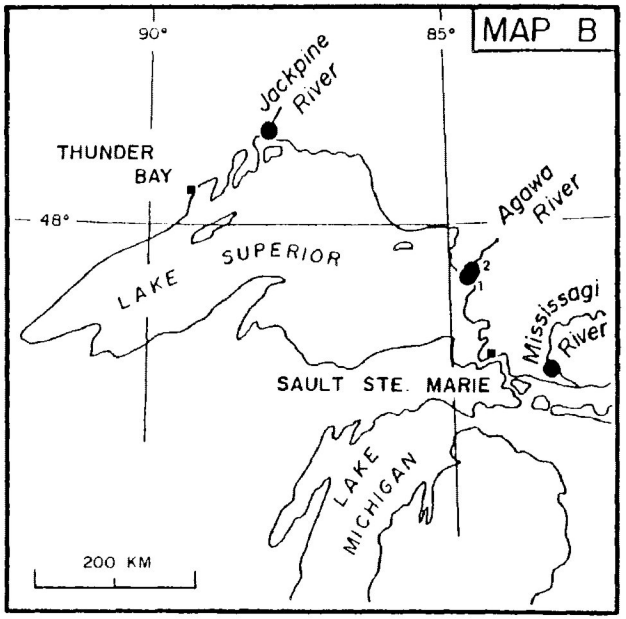

Figure 1. Location maps of areas studied.

deposition of sediments. Rock units present along the length of the river include Pleistocene tills, Early Precambrian granites, syenites, and pegmatites, together with minor conglomerates, sandstones, mudstones, chert, iron formation, and related migmatites (OGS Map 2506, 1986). Such rock types account for the higher percentages of magnetite encountered in the sediments sampled.

1.2.3: The Agawa River

The Agawa River, located approximately 120 kilometres north of Sault Ste Marie, Ontario, (see Figure 1) was the second of three rivers examined in the Lake Superior study area. This river originates from the north east and eventually empties into Lake Superior. A total of two longitudinal gravel bars were examined and subsequently sampled from this river. Both bars are submerged during high annual spring discharges, during which time, they are modified by erosional and depositional processes. The first bar sampled was located approximately 200 metres upstream of the Highway 17 bridge over the Agawa River. The second was located approximately five kilometres upstream of the first. Both bars were separated from the bank, and aligned parallel to the dominant flow direction. Major rock types in the region include granite, syenite, pegmatites, metasedimentary and minor metavolcanic migmatite, with minor basaltic and andesitic flows, tuffs, and breccias (OGS Map 2506, 1986).

1.2.4: The Mississagi River

A longitudinal gravel bar was selected and subsequently sampled on the Mississagi River approximately 100 kilometres north east of Sault Ste Marie, Ontario (see Figure 1). This river contains numerous longitudinal bars, of which, one was randomly selected for this study. This river eventually drains into the North Channel of Lake Huron. The river flows predominantly through granitic rock with syenite, pegmatite, and migmatite with minor metasedimentary and minor metavolcanic migmatite (OGS Map 2506, 1986).

1.3: Methodology

Modern natural braided rivers were examined and flume experimentation conducted in order to investigate the distribution and concentration of detrital heavy minerals in surficial and matrix sediments in coarse-grained longitudinal gravel bars.

Due to the complex and ever changing nature of braided river systems, sampling was restricted to well developed longitudinal bars. Once a bar had been selected, each

was measured, sketched, photographed, and sampled. At each sample site, where present, the long and short axis of the ten largest clasts in a one metre square area were measured. This was conducted in order to determine the variation in clast size over the length of the bar as well as in relation to other variables such as the mean grain size and sorting of matrix materials. Following these measurements, sediments were collected from between and under these clasts. This procedure was repeated at various locations over the length of the bar. Samples were also collected from bar edge sand wedges, chute channels, and chute channel delta sands, where present. Each sample contained 250 ml of sediment to which heavy mineral separation and grain size analysis was conducted. A total of 129 samples were collected from 9 longitudinal bars. During sediment analysis, samples were divided into surficial and matrix, depending on the site deposition.

The simulation of natural braided river systems by means of flume experimentation was carried out in a sediment-water recirculating flume at the Department of Geology, Lakehead University. This was undertaken in order to understand the processes operating in coarse-grained braided river systems that result in the formation of depositional placers in longitudinal gravel bars. The flume is of heavy aluminium construction supporting plexiglass sides along one section which allows for visual observation of fluvial and sediment interactions. It is 5 metres long, 45 centimetres wide, and 40 centimetres deep in the plexiglass portion, and somewhat narrower in all other sections. Water velocity is regulated by means of a belt and pulley system connecting an electric motor to a paddle wheel. The slope of the flume was fixed. The flume was modified for this project by installing five pressure taps along the bottom of the plexiglass portion that were used to measure the slope of the hydraulic gradient. Water velocity generated within the flume was measured by means of an Ott propeller-type current meter. The propeller was positioned in the centre of the flume and at 0.4 the flow depth (see Middleton and Southard, 1984).

Three sizes of quartz sand (density 2.65 g/cm^3) were used in the flume: fine (2.59 Phi, 0.17 mm); medium (1.84 Phi, 0.28 mm); and coarse (0.97 Phi, 0.51 mm). The sand was separated into these three sizes so that the sorting of the sand during the experimental runs would be minimised, but the sorting of heavy minerals based on density would be highlighted. Well rounded clasts were sorted into cobbles (82 cm^2, long axis times short axis), large pebbles (32 cm^2), and small pebbles (11 cm^2). These clasts were used to construct open framework gravel bars in the flume during each run. Three sizes of pyroxene grains (density 3.5 g/cm^3) were also used in the flume: fine

(2.43 Phi, 0.19 mm); medium (1.91 Phi, 0.27 mm); and coarse (1.18 Phi, 0.44 mm). Magnetite grains (density 5.5 g/cm^3; 2.1 Phi, 0.23 mm) were first removed from the original sand, prior to initial sieving, and redistributed in order to obtain concentrations of five percent in each of the three sand fractions. Lead grains (density 11.2 g/cm^3; mean grain size 2.3 Phi, 0.20 mm) and lead pellets (density 11.2 g/cm^3; mean grain size -0.58 Phi, 1.50 mm) were also added to each of the three sand fractions. The detrital lead was commercial purchased to ensure that a constant grain size was used during each experimental run. The lead to sand ratio was approximately ten percent. In addition, detrital pyroxene (density 3.5 g/cm^3) accounted for roughly 30 percent of the sediments used in flume experimentation.

In total, 27 experimental flume runs were systematically conducted with one variable changed following the completion of each run. Variables altered were: flow velocity, depth of flow, sand grain size, and clast size contained in the the gravel bar. Each run started with all sand positioned upstream of the gravel bar. The bar was completely free of sediment prior to each run so that any sediment found trapped in the gravel bar would be directly attributed to a known set of variables. The thickness of the gravel bars constructed ranged from two clasts (cobbles), to six clasts (pebbles). Following bar construction, the flume was filled with either 9 (fast and medium velocity runs) or 15 (slow velocity runs) centimetres of water, depending on the velocities required. The duration of each experiment ranged from ten minutes (fast and medium velocity runs) to five hours (slow velocity runs).

During each run, velocity measurements were recorded at six preselected sites. Depth of flow, from the water's surface to the sediment interface, was recorded at the same locations as the velocity measurements. The slope of the energy gradient line (Middleton and Southard's, 1984, energy slope) was recorded by measuring the difference in the hydrostatic head of the water between the five pressure taps. Sediment movement was also described and recorded during each run.

Following the completion of a run, the water was drained from the flume, thereby exposing the gravel bar and sediments which were further described and subsequently photographed and sampled. The sampling of sediments took place at two sites, one near the bar head, the other near the bar tail. At each site, two samples of sediments were collected; one from the surface, the other from the matrix. After sampling, the flume was set up for the next run with a change in one variable.

Following the completion of all flume experimentation, the 108 samples of sediment collected were then analysed. Samples were first dried and magnetite was then

separated out using a hand magnet. The magnetite fraction was subsequently degaussed to eliminate any residual magnetic attraction. Following this procedure, all samples underwent heavy liquid separation using Bromoform (density 2.8 g/cm^3). This was conducted to separate quartz sand from the remaining heavy minerals. The heavy fraction obtained from heavy liquid separations was then passed through a magnetic separator. This procedure separated detrital lead from pyroxene grains. This was followed by dry sieving (at 0.25 Phi intervals) 108 quartz sand, 108 magnetite, and 108 pyroxene samples. The lead samples were only weighed as the grain size was constant and sample sizes were, on average, too small to make sieving viable. Weighing of all samples was to the fourth decimal place but for the sake of brevity, all values have been rounded off to two significant figures.

Settling velocities of the detrital minerals used in this study were calculated using a modified version of Figure 3 from Tourtelot (1968) where curves for pyroxene, magnetite, and lead were added to the graph. Shear velocity was calculated from shear stress values provided in Appendix 4. Rouse Z values were computed using the formula given in Equation 6.21 in Middleton and Southard (1984) where Rouse Z equals settling velocity divided by Beta times von Karman's constant times shear velocity.

All graphs were drawn using the MacIntosh Computer programme Cricketgraph. An IBM PC computer programme was designed and used to determine each sample's mean grain size and standard deviation using moment measure analysis. The pyroxene portion of the heavy mineral grains was analysed using X-Ray Defraction and Scanning Electron Microscopy with Energy Dispersive Spectrometry. The pyroxene was found to be predominantly Fe-rich with a specific density of 3.5 g/cm^3.

CHAPTER 2: A REVIEW OF BRAIDED RIVER FLUVIAL SEDIMENTOLOGY AND ALLUVIAL PLACER FORMATION

2.1: Coarse-Grained Braided Fluvial Systems:

Of the four types of channel patterns: meandering, straight, anastomosed, and braided, this paper will investigate only braided rivers. For a detailed account of meandering, straight, and anastomosed river systems, the reader is referred to Leopold and Wolman (1957), Smith (1973), and Miall (1977).

Braided rivers are extremely complex natural systems that typically develop on alluvial fans and proglacial outwash plains (or Sandur, Church,1972, terminology). Braided river systems have been the focus of much research and have received a great deal of attention in the literature, especially over the last 20 years (see Williams and Rust, 1969; Smith, 1970,1985; Rust, 1972a; McDonald and Banerjee, 1971; Church, 1972; Gustavson, 1974; Boothroyd and Ashley, 1975; Hein and Walker, 1977; Miall, 1977, 1984; Schumm, 1977; Boothroyd and Nummedal, 1978; Rust and Koster, 1984; and Smith and Smith, 1984).

The exact reason that causes a river to become braided is a topic of much debate, however, it is generally agreed that the primary factors responsible for the development of a braided river include: large diurnal and seasonal fluctuation in discharge, a substantial and continuous supply of coarse alluvium, a sudden increase in slope, aggradation, high discharge velocities, bed roughness, and the presence of predominantly unconsolidated and unstable river banks owing to a pronounced lack of vegetation (see Leopold and Wolman, 1957; Smith, 1970; Smith, 1972, 1973; Miall, 1977; and Smith and Smith, 1984).

Braided rivers possess complex channel morphologies and are characterised by an endless series of channels that are occupied at various levels of discharge. Williams and Rust (1969) recognised four topographic levels associated with braided river systems. Level 1 river channels are those that contain the greatest fluvial activity at all discharges, contain virtually no vegetation, and are the primary route of sediment transport. At lower discharges, many channel bars become subaerially exposed causing the river to further braid. Level 2 river channels are those normally occupied during high discharge events and often there is a sparse vegetative cover present. These channels are generally referred to as chute channels. Level 3 channels have little continuous water movement and normally transport water as a result of overbank flooding during high discharge events. This level is typically characterised by a good vegetative cover. Level

4 represents the highest level on the braid plain and all channels are abandoned. This level contains a permanent cover of vegetation, especially trees (see Williams and Rust, 1969, for a complete discussion). This study is primarily concerned with levels 1 through 3.

Braided rivers contain multiple channels whose geometry is typically characterised by a high width to depth ratio. Such channel geometries are more efficient at moving large quantities of coarse detrital sediments than channels with low width to depth ratios (see Miall, 1977). In river channels with high width to depth ratios, the movement of sediments by bed load processes predominates with saltation and suspended load making up a relatively small percentage of the overall amount of sediment in transport. Bed load transport will be the primary means of sediment movement that this paper will focus on. For a complete discussion of saltation and suspended load sediment transport, the reader is referred to Middleton and Southard (1984), and Smith (1985).

The majority of detritus moved in bed load occurs only during a very short period of time over the course of a year. Only during high discharge events are coarse materials, such as large cobbles and boulders, transported down the river system. Smith (1985) describes the transport of sediments in bed load as sporadic, moving in short bursts during the highest flows in a given season. Hammer and Smith (1983) describe bed load sediment transport increasing at an exponential rate with river discharge.

Because the majority of coarse alluvial sediments are transported in bed load during high discharge events, as discharge is reduced, so is the river's ability to continue transporting this material down slope. With a reduction in discharge, the largest sediments in bed load stop moving first and are deposited on the river bed (see Middleton and Southard, 1984). As larger sized clasts become fixed to the river bed, the river is then forced to diverge, flowing around and over these clasts. This produces lower energy areas immediately downstream of these sites and results in the deposition and accumulation of finer clasts and sediments. This process is accentuated during waning flow and eventually leads to the formation of gravel bars within the river channel (see Smith, 1970). With a continued reduction in discharge, the gravel bar emerges above river level, causing the river to further diverge.

Bars that form in braided systems have been extensively described by Gustavson, 1974; Boothroyd and Ashley (1975); Miall (1977), and Smith (1985). Bars commonly associated with these systems are longitudinal, transverse, linguoid, point bars, side bars, and lateral bars (see Miall, 1977, Figure 3). A full discussion of all

these bar types is beyond the scope of this paper, however, longitudinal bars will be examined in more detail.

Leopold and Wolman (1957) provide a full account of the processes resulting in the development of longitudinal bars in alluvial sediments. Miall (1977) describes longitudinal bars as: "...diamond- or lozenge-shaped in plan...elongated parallel to flow direction...bounded by active channels on both sides and may, as a result, have partially eroded margins" (p. 12). Smith (1985) describes longitudinal bars as: "...long, narrow, convex upward, and generally symmetrical..." (p. 103). However, Boothroyd and Ashley (1975) distinguish between upper, mid, and lower fan longitudinal gravel bars. This distinction is based on the following criteria: slope, mean maximum clast size, position with respect to channels, morphology, sedimentary structures and fabric, and time of initial movement (see Boothroyd and Ashley, 1975, Table 1).

Longitudinal bars are typically composed of massive coarse-grained alluvium and are clast supported with minor lenses of finer grained sand and gravel. The clast supported deposits (McDonald and Banerjee's Stable Framework Gravel) of longitudinal bars often contain finer sediments that infiltrate open pore spaces between clasts during waning flows (McDonald and Banerjee, 1971; Rust and Koster, 1984; Frostick et al, 1984). This process typically results in a graded matrix (Frostick et al, 1984). While these bars are submerged during maximum discharge events, they are subjected to extremely turbulent flow conditions, during which time, they are modified by both erosional and depositional processes. Such processes result in the upstream head of the bar being continually reworked producing a well sorted and coarser grained deposit. A significant decrease in velocity over the length of the bar results in a corresponding decrease in the size of sediment being transported. This process produces a grading effect over the length of the bar. A typical longitudinal bar will therefore have a coarser head than tail.

The gravel fabric on the surface of many longitudinal bars often display morphologic features including series of regularly spaced linear ridges orientated perpendicular to the mean direction of flow. These ridges are composed of pebbles, cobbles, or boulders (see Smith, 1985, Figure 3-13). These regularly spaced ridges are known as transverse ribs and are thought to form on the surface of subaqueous gravel bars in response to the presence of hydraulic jumps. Transverse ribs can be useful in determining the mean palaeocurrent direction of river deposits. For a thorough discussion of transverse ribs, the reader is referred to McDonald and Banerjee (1971), Gustavson (1974), Boothroyd and Ashley (1975), Koster (1978), and Smith, (1985).

The surfaces of many longitudinal bars are often intersected by chute channels that form during waning flows. Chute channels (Williams and Rust's Level 2) cut across longitudinal bars as a result of decreasing river discharge and often contain finer grained sediments that may, for example, form ripple or dune fields in channels (see Williams and Rust, 1969). Such channels often result in finer grained lenticular units characterised by small to medium scale sedimentary features such as ripple lamination or trough cross-stratification (Miall, 1977) that become embedded in coarse-grained bar successions. In addition, abandoned chute channels often contain isolated pools of standing water that allow fine silts and muds to settle out of suspension producing mud drapes over coarser grained chute channel deposits. Such mud deposits may also develop desiccation cracks (Miall, 1977) as a result of subaerial exposure and may subsequently become infilled with aeolian sediments. Where chute channels rejoin main river channels, chute channel deltas often form as a result of the downstream migration of ripples or dunes.

Along the sides and tails of longitudinal bars, well sorted accumulations of sand are often deposited. Such deposits are referred to as bar edge and bar tail sand wedges and are thought to form in response to a reduction in energy at these sites (see Rust, 1972a, Figure 4). Such sediment accumulations often have little preservation potential as they are generally eroded away during subsequent high discharge events.

Finally, clast size has been documented in several papers to decrease exponentially as a function of channel gradient (see Boothroyd and Ashley, 1975; Boothroyd and Nummedal, 1978; and Smith, 1985). Boothroyd and Nummedal (1978) aptly displayed this relationship with selected glacial outwash fans from Alaska and Iceland. They showed that clast size and gradient were interdependent and decreased in a "...predictable manner from proximal to distal environments" (p. 650) (see also Boothroyd and Nummedal, 1978, Figure 6b). Smith (1985) discusses how the coarsest gravels move sporadically for short distances only during the highest discharge events but finer sediments are able to be transported almost continually at lower discharges that occur most often. This process results in the separation of coarse gravels from fine sediments. This manner of selective sorting is the dominant process operating in coarse-grained braided fluvial systems to separate coarse gravels from finer sediments. The mechanical action of breaking down coarse sediments into finer sediments, although operating congruently, has only a minor affect on the overall selective sorting process (Smith, 1985).

2.2: Alluvial Placer Formation in Fluvial Environments

Alluvial placer deposits are formed by the preferential accumulation of heavy minerals by a variety of hydraulic processes operating within a fluvial environment.

Placer deposits are known to have formed in response to four different processes: aeolian, elluvial, littoral, and alluvial. However, a detailed discussion of aeolian, elluvial, and littoral placer deposits is beyond the scope of this paper. For a detailed discussion of these types of placer deposits, the reader is referred to Bateman (1951), Park and MacDiarmid (1964), Schumm (1977), Slingerland (1977), and Gladwell and Hale (1981).

Schumm (1977) discusses the various types of alluvial placers that can develop in fluvial environments. He identifies six areas in which placers have been discovered: 1) bedrock terraces; 2) alluvial terraces; 3) channel lags; 4) floodplains, point bars; 5) lags in valley fill; and 6) bedrock (see Schumm, 1977, Figure 6-28).

Bedrock and alluvial terrace placers represent deposits that were deposited early in the history of a river and may have developed through a combination of alluvial and colluvial sedimentary processes. Depending on the source of sediments, placers have been discovered high above active river channels. Such areas should be considered potential for placer development, especially where local tectonic activity has resulted in the relatively rapid uplift of sediment source areas producing an increase in the rate of downcutting of the river channel. On a much larger scale, Henley and Adams (1979) related the formation of gold placers to regional uplift that can be related to changes in the relative plate motions of the earth's crust. For an indepth discussion of the interaction and role of basin dynamics, tectonics, and channel processes leading to the formation of placer deposits, the reader is referred to Adams, Zimpfer, and McLane (1979).

Channel and floodplain placers are intimately related to former river channels and their morphologic features such as sand and gravel bars, bends, pools, and changes in channel width (see Crampton, 1937). High heavy mineral concentrations are typically found in the upstream portion of point bars or mid channel bars. The lateral and/or downstream migration of meandering channels across and down floodplains can result in placer deposits being formed throughout the floodplain. Abandoned channel meanders such as oxbow lakes are therefore also likely areas for placer deposits. Such features will often contain remnant channel features such as point bars that may contain heavy mineral accumulations. Placer occurrences may also form as a result of the reworking of sediments previously deposited under different basin and hydrologic parameters. A placer deposit forming in response to current hydrologic conditions may therefore simply

represent the reworking of heavy mineral rich sediments previously deposited by a totally different set of environmental conditions.

Valley fill placers are associated with sediments that were deposited in the past. Schumm (1977) considers changes in baselevel, tectonic activity, and climate, as being fundamental in altering rates of denudation which in turn, affects the location of placer deposits in valley fill facies successions.

Finally, bedrock placer deposits form directly on bedrock channel bottoms, or in the sediments lying on the valley floor (Tuck, 1968). Raeburn and Milner (1927) discuss the possibility of encountering "false bottoms" in valley floor successions where the river channel itself, or former channel sediments, are found overlaying thick mudflow or volcanic ash layers. Encountering such a layer often results in exploration activities ceasing, when in fact, a placer deposit may lie directly below this "false bottom".

Cheney and Patton (1967) suggest that bedrock placers, often found under thick layers of sediments, originated during exceptionally large flood events as a result of the process of channel scouring. Heavy minerals are deposited in the deepest parts of the channel and subsequently buried with the return to normal discharges following the flood event. Gunn (1968) suggests that as a river flows over previously deposited channel sediments, the sediments are agitated by turbulence which results in the gradual downward movement of heavier detrital sediments. Similarly, Kolesov (1975) discusses how the lower portions of bedrock placer deposits often contain higher concentrations of gold resulting in a graded placer deposit. He suggests that the settling of gold into the interstices of channel deposits is highly dependent upon pore space with large pore openings allowing more gold to settle deeper in the open framework deposit.

Tuck (1968) explains that high concentrations of gold in fluvial deposits lying directly on bedrock are the result of a significant period of erosion where the river is predominantly downcutting. He likens bedrock placer development to that of a large scale sluice box used in heavy mineral recovery from fluvial sediments. Once heavy minerals have reached bedrock level, they will remain there and collect in the many crevasses and scours along the channel bottom. He further explains that once a river has reached bedrock, it often begins to erode laterally, resulting in the placer deposit being spread horizontally across the bedrock.

Krook (1968) explains how a change in climate can result in the transition from vertical to lateral erosion and aggradation. He discusses how the presence of abundant vegetative cover results in a significant decrease in the size of sediments being eroded

and therefore transported in fluvial systems. He further suggests that in more arid climates, where there is a pronounced lack of dense vegetation, increased mechanical weathering and erosion results in wider valleys with coarser fluvial deposits. More humid climatic conditions typically leads to more vegetation resulting in a corresponding decrease in the size of sediments being eroded due to an increasing dominance in chemical weathering.

In a more recent paper, Mosley and Schumm (1977) explained how stream junctions are probable locations for bedrock placers to occur. Their study indicated that heavy mineral concentrations were increased in fluvial sediments that experienced a significant amount of reworking due to turbulence and that such conditions were typically associated with tributary stream junctions. They explained that at stream junctions, bedrock scour depths were found to be greatest and that "...placer minerals are known to be deposited preferentially in and around depressions in the bedrock surface..." (p. 694). As a result, Mosley and Schumm (1977) suggest that stream junctions are probable sites of heavy mineral accumulation and therefore promising areas for prospecting. Smith and Beukes' (1983) findings concur with those of Mosley and Schumm's (1977), in that converging flows resulted in significant heavy mineral enrichment in fluvial sediments at these locations.

However, the above theories of placer formation can be collectively referred to as "erosional placer deposits". As has already been shown, erosional placer deposits form through the reworking of previously sedimented detritus that results in the separation of lighter minerals from heavier minerals by the preferential transport of the lights. This study will be investigating the occurrence and processes leading to the formation of "depositional placer accumulations".

There has been very little written in the literature specifically on the formation of depositional placer accumulations. This is the case, even though at Elliot Lake, and selective deposits in the Witwatersrand and Jacobina, large economic accumulations of heavy minerals form the matrix in palaeo-longitudinal gravel bars. The processes resulting in the deposition and subsequent accumulation of heavy minerals in coarse-grained longitudinal gravel bars are complex due to the highly turbulent nature of these environments.

CHAPTER 3: THE NORTH SASKATCHEWAN RIVER SYSTEM

3.1: Discussion

The North Saskatchewan River, set in a highly mountainous terrain, is typical of most proglacial fluvial systems. Such systems have received much attention in the literature (see Williams and Rust, 1969; Church, 1972; Boothroyd and Ashley, 1975; Church and Gilbert, 1975; Boothroyd and Nummedal, 1978; Reading, 1978; Hammer and Smith, 1983; Miall, 1984; and Smith, 1985). The Saskatchewan Glacier acts as the primary source of water to the North Saskatchewan River (see Figure 2). It is a large valley glacier that is roughly ten kilometres in length and averages one kilometre in width. It descends approximately 1000 metres from the Columbia Icefields, at an elevation of 2800 metres above sea level, to its snout, at an elevation of 1800 metres. The Columbia Icefields cover 120 square miles (300 square kilometres) (Smith, 1972) and are situated on the continental divide on the British Columbia/Alberta border and Banff/Jasper National Park boundary. For a full description of the Saskatchewan Glacier, the reader is referred to Meier (1960a).

High alpine glacial fed drainage systems are controlled by a variety of processes. The production of meltwater from a glacier plays an integral role. It represents the main product of ablation and is responsible for the removal of huge volumes of sediment. Meltwater is principally derived from two areas: the surface of the glacier, and from basal/internal sources. Shreve (1972) noted that surface meltwater production exceeds that of basal and internal by at least one order of magnitude.

Surface meltwater runoff is regulated by diurnal controls that normally result in peak discharges by late afternoon, depending on local climatic conditions, and seasonal controls that result in steadily increasing discharges throughout the summer (see Burton, 1986). Basal meltwater production however, fluctuates less markedly and is normally responsible for maintaining base flows throughout the year. Such hydrologic regimes have pronounced effects on the proglacial fluvial environment.

The melting of snow and ice on the surface of a glacier occurs largely as a result of its exposure to solar radiation. Freshly fallen snow, typical of early summer conditions, reflects the majority of solar radiation back into the atmosphere. As a result, the maximum daily temperature that directly controls surface meltwater production early in the season resulting in significant diurnal fluctuations in discharge. However, as snow cover becomes depleted and more ice becomes exposed, less solar radiation is reflected back into the atmosphere which results in a significant increase in ablation rates

Figure 2: Profile view of the terminus of the Saskatchewan Glacier, proglacial lake, and source of the North Saskatchewan River.

(Sugden and John, 1976). This process accounts for the large seasonal variations in discharge that are characteristic of glacially controlled fluvial systems. It is throughout this period of high discharge that the majority of glaciofluvial sediments are transported and channel morphology significantly modified.

The second major source of meltwater is derived from basal and internal sources. The production of meltwater from these sources is dependent on the heat produced by basal and internal movements of the glacier. Melting may also result from the frictional heat released by the flow of meltwater, geothermal heat, or from relatively warm surface water flowing down to the base of the glacier (Shreve, 1972). However, the total amount of meltwater produced by these processes is relatively insignificant in comparison. The contribution of basal and internal meltwater to the overall flow regime is relatively minor and is somewhat analogous to that of groundwater discharge in non-glacierised drainage basins.

Derikx and Loijens (1970) estimate that 70 percent of the annual North Saskatchewan River discharge occurs over three months (June, July, and August). As a result, most channel modification and sediment movement occurs during this relatively short period of time.

Studies have documented fluctuations in meltwater discharged from glaciers ranging from seconds to days (see Sugden and John, 1976; Smith, 1985). These fluctuations are the result of sudden releases (or bursts) of water that have pooled in subglacial, englacial, or supraglacial depressions, and ice-dammed lakes (Smith, 1985). Such catastrophic releases, or outbursts, are known as Jokulhlaups and often result in huge volumes of sediment being eroded and subsequently deposited in proglacial outwash plains. This can result in the formation of a variety of features such as huge trench-shaped channels, large coarse-grained alluvial fans (Kehew and Lord, 1987), and large fluvial bedforms and presents a possible alternate mode of alluvial placer formation (see Fralick and Miall, 1987).

Immediately downriver of the Saskatchewan Glacier, a relatively large proglacial lake has formed (see Figure 2). This lake is similarly affected by diurnal and seasonal fluctuations in discharge. It also acts as a sediment trap where both fine- and coarse-grained sediments are deposited.

Downriver of the lake, the North Saskatchewan River is similar to most glaciofluvial braided systems and displays morphologic channel features typically associated with this environment. It is unvegetated and contains a vast supply of coarse unconsolidated alluvial sediments. These two features, together with a relatively steep

slope and large diurnal and seasonal fluctuations in meltwater discharge, are largely responsible for the extensive braided channel network that has developed in this section of the river.

Smith, (1972, 1973) interpreted a section of the North Saskatchewan as an anastomosed river system and provides criteria on which to distinguish between braided and anastomosed channel patterns. The North Saskatchewan River changes from braided to anastomosed only once it has been joined by the Alexandra River, a large tributary river system. This junction occurs approximately two kilometres downriver of the longitudinal bar sampled at Site 4 of this study (see Figure 1). Smith attributes this sudden change to an abundance of vegetation within the river's floodplain that acts to stabilise coarse alluvial river banks, making them less susceptible to erosion. The North Saskatchewan River becomes braided again immediately down river of the junction with the Howse River, another large braided river system (see Figure 1). Due to the substantial supply of coarse alluvium delivered to the North Saskatchewan by the Howse River and a lack of vegetation in the floodplain, the river once again becomes highly braided.

Four longitudinal gravel bars were randomly selected for study in the upper 21 kilometres of the North Saskatchewan River. The fifth bar selected was located some 15 kilometres downriver of the North Saskatchewan/Howse River junction.

The study area was visited in June of 1987. Discharges at that time were relatively low and only small diurnal fluctuations were observed. However, the study area was revisited one month later and discharge had increased significantly. As a result of this increase, many of the longitudinal bars previously sampled had been substantially modified.

The magnetite content in sediment samples from this river system is somewhat limited owing to the source terrain and ranged from 0.0003 to 0.0335 weight percent. The magnetite in this area of the Cordillera is derived primarily from volcanic ash layers that originated from the Mazama, St. Helens Y, and Bridge River volcanic units (Brewster and Barnett, 1979).

3.2: Description of Longitudinal Bars

3.2.1: Site 1

The longitudinal bar sampled at Site 1 was located approximately one kilometre downriver of the Saskatchewan Glacier. The river at this location is typical of most

proximal upper fans and is restricted primarily to one main channel. This bar is coarse-grained, low relief, and has formed in the centre of the channel resulting in the river diverging (see Figure 3). Boothroyd and Ashley (1975) describe longitudinal bars that form in upper fans as follows: "The longitudinal bars of the upper fan are diamond-shaped in plan with a slightly higher central axis and little to no slipface development on their downstream margins. They occur mainly in interstream areas between incised erosional channels and are rarely subject to flooding. These bars appear to consist of a thin sheet of coarse, poorly-sorted, well-imbricated gravel with the coarsest material concentrated along the central axis" (p. 202). The bar at Site 1 matches this description.

The first bar selected was approximately 75 metres long and 25 metres in width. A total of 13 samples were obtained from sediments that accumulated between clasts (matrix) and in fine-grained lenses on the upper surface (sand). A wide variety of morphologic features were encountered and subsequently sampled.

The bar exhibited a significant decrease in clast size over its length from bar head (large boulders) to bar tail (small cobbles) (see Table 1). At the bar head, the boulders were well imbricated and found to contain very coarse, poorly to moderately poorly sorted matrix, while at the bar tail, the cobbles contained very coarse and poorly sorted matrix.

Matrix sediments were also sampled in several other areas over the bar. Large cobbles that accumulated on the bar top, contained very coarse and poorly sorted matrix sediments. Both active and inactive chute channels had developed diagonally across the bar and each displayed a series of transverse ribs along its upper surface (see Figure 3). The inactive chute channel sampled contained boulder sized clasts on an erosive channel floor. Matrix that accumulated between these clasts were moderately poorly sorted and medium grained. On the bar top, next to the above abandoned chute channel, pebble sized clasts were deposited immediately downriver of an erosive scour and contained very coarse and moderately sorted matrix.

A laterally extensive accretionary lobe that had been in the process of prograding down over the surface of the bar while submerged during higher discharge, was also sampled. Three samples were obtained from the lobe, one from each of the top, fore, and toesets. The topset was predominantly composed of large cobbles with very coarse and poorly sorted matrix. The foreset contained small cobbles with very coarse and moderately poorly sorted sediments. However, the toeset was composed of very fine grained and well sorted sand. Clasts were noticeably absent from the toeset deposit.

Figure 3: Photomosaic of the longitudinal bar studied at Site 1 on the North Saskatchewan River.

a) View of bar head and chute channels looking upstream. Flow is from left to right.

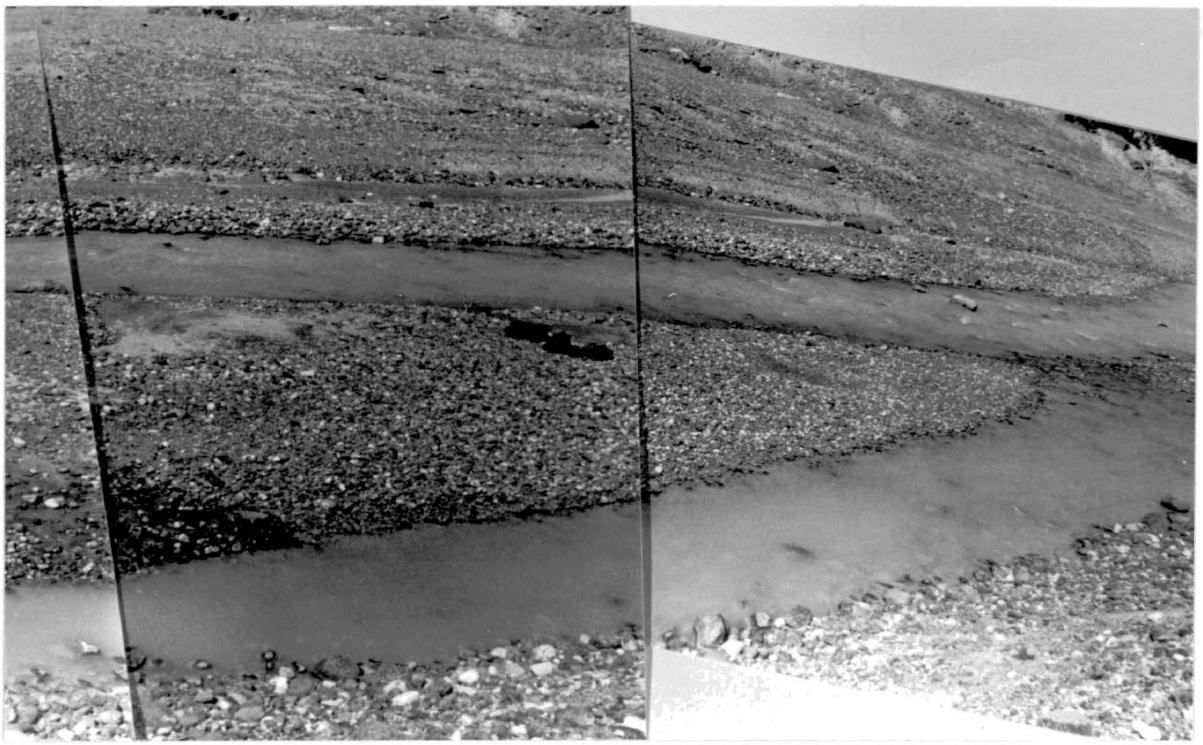

b) View of bar tail looking downsteam. Flow is from left to right. The back packs on the bar tail give an indication of scale.

Table 1. Data from sediment analysis of samples collected from Site 1 on the North Saskatchewan River.

Sample Number	Sample Site Description	Sediment Type	Mean Quartz		Sorting of Quartz		Percent Magnetite	Percent Mud	Clast Size (cm2)
1	Bar head	Matrix	(VC)	-0.37	(PS)	2.32	0.0117	N/A	237
11	Bar head	Matrix	(VC)	-0.28	(MPS)	1.88	0.0021	17.07	359
7	Bar top	Matrix	(VC)	-0.50	(MPS)	1.66	0.0027	15.73	81
13	Bar tail	Matrix	(VC)	-0.67	(PS)	2.01	0.0030	19.13	41
4	Chute channel	Matrix	(M)	1.26	(MPS)	1.61	0.0053	23.79	186
8	Accretionary lobe (top)	Matrix	(VC)	-0.29	(PS)	2.11	0.0041	15.71	81
9	Accretionary lobe (fore)	Matrix	(VC)	-0.40	(MPS)	1.78	0.0020	6.24	44
6	Sand lens next to scour	Matrix	(VC)	-0.05	(MPS)	1.83	0.0045	11.51	29
10	Accretionary lobe (toe)	Sand	(VF)	3.20	(WS)	0.56	0.0106	69.80	0
2	Mud-rich lens	Sand	(VF)	3.25	(WS)	0.57	0.0174	72.64	0
3	Bar edge sand wedge	Sand	(VF)	3.08	(WS)	0.68	0.0169	61.84	0
12	Low velocity zone	Sand	(C)	0.97	(MWS)	1.17	0.0007	0.87	0
5	Bar tail sand wedge	Sand	(F)	2.02	(MWS)	1.11	0.0129	9.90	0

Grain Size Legend		Sorting Legend	
VF	Very Fine-Grained	VWS	Very Well Sorted
F	Fine-Grained	WS	Well Sorted
M	Medium-Grained	MWS	Moderately Well Sorted
C	Coarse-Grained	MPS	Moderately Poorly Sorted
VC	Very Coarse-Grained	PS	Poorly Sorted
G	Granule	VPS	Very Poorly Sorted

This sand deposit likely formed due to flow separation over the lobe that resulted in a loss of flow competence and the deposition of suspended sediments. The accretionary lobe that migrated over this sand lens represents bed load transport processes.

Several sand lenses were also sampled over the bar surface (see Table 1). Near the bar head, two samples were obtained from a relatively thick sand wedge that had developed on the side of the bar. The first sample was collected from surficial sediments and was well sorted and very fine-grained with a high mud content. The second sample obtained from this sand wedge was collected approximately five centimetres below that of the first sample and was similarly composed of well sorted and very fine-grained sand. The mud content of this sample was substantial, but somewhat less than that found in the previous sample.

A low velocity zone, immediately downriver of a large boulder, accumulated fine sands on the bar top (see Figure 3). This deposit was composed of moderately well sorted coarse-grained sands. The final sample obtained from this bar was from a bar tail sand wedge. This relatively thick sand deposit accumulated at the downriver edge of the bar tail and was composed of moderately well sorted fine-grained sands.

The magnetite content of the sediments collected from this bar ranged from 0.0007 to 0.0169 weight percent. The highest percentages of magnetite obtained from matrix samples were generally associated with poorly to moderately poorly sorted, very coarse-grained matrix. However, the highest percentages of magnetite obtained from sand samples were found in well sorted, very fine-grained sand (see Table 1).

3.2.2: Site 2

The area sampled at Site 2 was located approximately five kilometres downriver of the Saskatchewan Glacier (see Figure 1). At this site, the river channel system was 50 metres wide, decreasing to 30 metres, and confined between a steep erosional embankment on the right, and the Banff/Jasper Highway on the left (see Figure 4).

At the time of sampling, the majority of river flow was restricted to one main channel next to the highway containing several in-channel longitudinal bars. The gravel flats located between the river channel and erosional embankment contained several longitudinal bars that were intersected by numerous abandoned chute channels normally occupied during higher discharges later in the summer (Level 2). A total of 12 samples were obtained from both active and currently inactive areas of this river channel system. The site was briefly revisited one month later after initial sampling and with significantly increased discharges, the river had divided into two main channels with many of the

Figure 4: The longitudinal bar system studied at Site 2 on the North Saskatchewan River.

a) View of bar system looking upstream. Flow is from right to left.

b) View of bar system looking downsteam. Flow is from right to left.

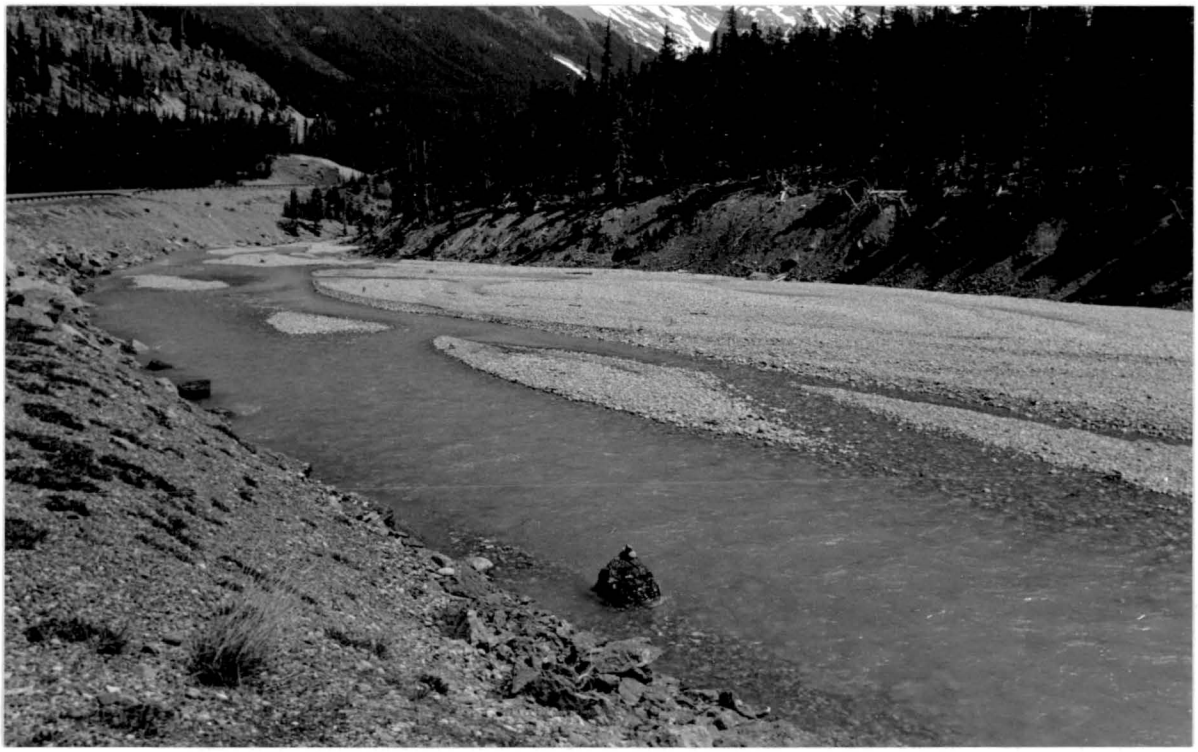

previously abandoned chute channels now active.

A 150 metre section of the bar system was examined in detail. Longitudinal bars at this site exhibited significant decreases in clast size from bar head (large cobbles) to bar tail (small cobbles) (see Table 2). Samples obtained from the bar head contained matrix that was very coarse-grained and moderately well to poorly sorted. At the bar tail, the matrix was similarly very coarse-grained and moderately well sorted.

A bar top was composed of medium sized cobbles with matrix that was granule sized and moderately well sorted. An inactive chute channel was found to contain large cobbles on an erosive channel floor with moderately poorly sorted granule sized matrix. A prograding accretionary gravel lobe in the process of cutting off the mouth of an abandoned chute channel (see Figure 5) was sampled and composed of medium to large cobbles and moderately well sorted granule sized matrix. Figure 6 depicts a longitudinal bar with water from the main river channel seeping into the gravel framework at the upstream portion of the bar and subsequently emerging towards the bar tail (see Section 6.2 for a complete discussion).

Large cobbles that had accumulated in a deep scour trough, next to a very large boulder, contained poorly sorted, coarse-grained matrix. A second sample was collected approximately one metre downriver of this boulder from between clasts that were pebble sized. The sediment sample was composed of very poorly sorted, coarse-grained matrix. However, a finer grained deposit that formed in the low velocity zone directly downriver of this boulder contained well sorted fine-grained sands. This sample site also contained the highest percentage of magnetite obtained in samples collected from the North Saskatchewan River system.

Sediments forming an active chute channel delta as a result of the infilling of the mouth of an abandoned chute channel, were found to contain well sorted, coarse-grained sands. Sediments sampled from a bar edge sand wedge deposit were moderately well sorted, fine grained sands. A bar tail sand wedge that formed at the downriver edge of the bar, was composed of well sorted, medium-grained sands.

The percentage of magnetite obtained in samples from this site ranged from 0.0007 to 0.0335 weight percent. The highest percentages of magnetite were generally found in very poorly sorted, coarse-grained sediments deposited proximal to the large boulder encountered at this site. However, relatively high values were also obtained in those areas that contained the highest concentrations of mud (see Table 2).

Table 2. Data from sediment analysis of samples collected from Site 2 on the North Saskatchewan River.

Sample Number	Sample Site Description	Sediment Type	Mean Quartz		Sorting of Quartz		Percent Magnetite	Percent Mud	Clast Size (cm2)
1	Bar head	Matrix	(VC)	-0.25	(MPS)	1.74	0.0059	3.23	73
5	Bar head	Matrix	(VC)	-0.97	(MWS)	1.47	0.0015	2.76	139
2	Bar top	Matrix	(G)	-1.15	(MWS)	1.59	0.0028	2.50	48
6	Bar tail	Matrix	(VC)	-0.50	(MWS)	1.32	0.0003	5.14	38
4	Chute channel	Matrix	(G)	-1.13	(MPS)	1.51	0.0022	5.96	109
8	Low velocity zone	Matrix	(C)	0.97	(VPS)	2.50	0.0230	15.20	25
10	High velocity zone	Matrix	(C)	0.17	(PS)	2.03	0.0114	9.34	95
12	Accretionary lobe	Matrix	(G)	-1.24	(MWS)	1.25	0.0007	1.32	66
11	Chute channel delta	Sand	(C)	0.91	(WS)	0.91	0.0030	N/A	0
3	Bar edge sand wedge	Sand	(F)	2.03	(MWS)	1.07	0.0196	5.33	0
7	Bar tail sand wedge	Sand	(M)	1.02	(WS)	0.63	0.0024	0.03	0
9	Low velocity zone	Sand	(F)	2.38	(WS)	0.69	0.0335	17.09	0

Grain Size Legend		Sorting Legend	
VF	Very Fine-Grained	VWS	Very Well Sorted
F	Fine-Grained	WS	Well Sorted
M	Medium-Grained	MWS	Moderately Well Sorted
C	Coarse-Grained	MPS	Moderately Poorly Sorted
VC	Very Coarse-Grained	PS	Poorly Sorted
G	Granule	VPS	Very Poorly Sorted

Figure 5: A prograding gravel lobe in the process of cutting off an abandoned chute channel at Site 2 on the North Saskatchewan River. Flow is from right to left. The back pack in the lower right corner gives an indication of scale.

Figure 6: Water seepage and matrix flushing process operating on a longitudinal bar at Site 2 on the North Saskatchewan River. Flow is from top to bottom. The back pack along the left margin gives an indication of scale.

3.2.3: Site 3

This sample site was located approximately 13 kilometres downriver of the Saskatchewan Glacier (see Figure 1). The river channel system is about 100 metres wide and a 150 metre section was examined in detail. The bar is of low relief and exhibits numerous abandoned chute channels and fine-grained lenses over its upper surface (see Figure 7).

A total of 22 sediment samples were collected from this site (see Table 3). Clast sizes varied from bar head (small cobbles) to bar tail (pebbles). Samples from the bar head contained poorly sorted, very coarse-grained matrix whereas at the bar tail, samples were composed of moderately poorly sorted, granule sized matrix. Four samples were collected over the bar top between clasts ranging in size from medium cobbles to pebbles. Matrix sediments were all very coarse-grained and predominantly moderately poorly sorted. Three matrix samples were collected from among medium sized cobbles that had accumulated on the floor of abandoned chute channels. Each sample was composed of moderately poorly sorted, very coarse-grained matrix sediments (see Table 3).

A prograding accretionary gravel lobe that was in the process of cutting off the mouth of an abandoned chute channel was sampled (see Figure 5). Clasts were predominantly small cobble sized and found to contain moderately poorly sorted, very coarse-grained matrix sediments. However, this gravel lobe was prograding over a previously formed fine grained chute channel deposit that was composed of well sorted, medium-grained sands.

Three additional samples were obtained from abandoned chute channel fill deposits (sands). Samples contained well to moderately well sorted, coarse- to medium-grained sands (see Table 3). A one by five metre bar composed entirely of sand, formed in the mouth of an abandoned chute channel (see Figure 8) and displayed dune bedforms throughout its length. The side of the bar closest to the river bank was covered by a mud drape. Sands collected from this bar were well sorted and medium-grained. The final four samples from this site were obtained from bar edge sand wedge deposits. These sand wedges were composed predominantly of well to moderately well sorted, medium- to fine-grained sands.

The percentage of magnetite obtained in samples from this site ranged from 0.0004 to 0.0208 weight percent. The highest percentage was found in poorly sorted, very coarse-grained matrix sediments obtained from a bar top sample (see Table 3).

Figure 7: The longitudinal bar system studied at Site 3 on the North Saskatchewan River. Flow is from right to left.The 2 lane highway in the bottom right corner gives an indication of scale.

Table 3. Data from sediment analysis of samples collected from Site 3 on the North Saskatchewan River.

Sample Number	Sample Site Description	Sediment Type	Mean Quartz		Sorting of Quartz		Percent Magnetite	Percent Mud	Clast Size (cm2)
1	Bar head	Matrix	(VC)	-0.55	(PS)	2.08	0.0052	11.59	23
8	Bar top	Matrix	(VC)	-0.80	(MPS)	1.82	0.0020	2.86	10
12	Bar top	Matrix	(VC)	-0.62	(MPS)	1.89	0.0053	4.04	25
14	Bar top	Matrix	(VC)	-0.26	(PS)	2.47	0.0208	11.38	33
16	Bar top	Matrix	(VC)	-0.60	(MWS)	1.48	0.0006	2.58	46
15	Bar tail	Matrix	(G)	-1.00	(MPS)	1.73	0.0010	3.18	12
7	Chute channel	Matrix	(VC)	-0.83	(MPS)	1.67	0.0014	2.97	43
9	Chute channel	Matrix	(VC)	-0.82	(MPS)	1.83	0.0023	7.48	34
10	Chute channel	Matrix	(VC)	-0.77	(MPS)	1.84	0.0032	9.49	59
22	Accretionary lobe	Matrix	(VC)	-0.85	(MPS)	1.80	0.0058	5.26	27
5	Accretionary lobe	Matrix	(VC)	-0.53	(MPS)	1.77	0.0023	5.89	27
6	Bar top	Sand	(M)	1.46	(WS)	0.94	0.0091	13.00	0
4	Chute channel	Sand	(M)	1.86	(WS)	0.65	0.0050	18.29	0
18	Chute channel	Sand	(C)	0.46	(MWS)	1.05	0.0004	N/A	0
19	Chute channel	Sand	(C)	0.60	(WS)	0.68	0.0004	0.21	0
20	Chute channel	Sand	(M)	1.59	(WS)	0.57	0.0023	0.83	0
17	Chute channel	Sand	(G)	-1.04	(MPS)	1.58	0.0010	2.44	0
2	Scroll bar	Sand	(M)	1.05	(WS)	0.58	0.0009	0.36	0
11	Bar edge sand wedge	Sand	(M)	1.80	(WS)	0.78	0.0056	2.42	0
13	Bar edge sand wedge	Sand	(M)	1.62	(MWS)	1.34	0.0039	2.23	0
21	Bar edge sand wedge	Sand	(F)	2.18	(WS)	0.59	0.0064	2.70	0
3	Bar edge sand wedge	Sand	(M)	1.58	(MWS)	1.02	0.0095	17.66	0

Grain Size Legend		Sorting Legend	
VF	Very Fine-Grained	VWS	Very Well Sorted
F	Fine-Grained	WS	Well Sorted
M	Medium-Grained	MWS	Moderately Well Sorted
C	Coarse-Grained	MPS	Moderately Poorly Sorted
VC	Very Coarse-Grained	PS	Poorly Sorted
G	Granule	VPS	Very Poorly Sorted

Figure 8: An abandoned chute channel and finer grained sandy lens at Site 3 on the North Saskatchewan River. Flow is from top to bottom. River width is approximately 5 metres.

3.2.4: Site 4

The fourth bar sampled was located 21 kilometres downriver of the Saskatchewan Glacier (see Figure 1). The river channel system was approximately 85 metres wide and confined between steep erosional embankments (see Figure 9). The bar was composed of a series of overlapping longitudinal bars and contained numerous abandoned chute channels and sand lenses. At the time of sampling, discharge was relatively low and confined predominantly to one main channel (see Figure 9). However, the bar was revisited one month later and it was observed that the channel system had been substantially modified during this time. Many of the low lying areas of the bar containing sand lenses and abandoned chute channels were now submerged (see Figure 10). The bar had experienced a significant amount of erosion; in addition, the main channel had also switched, virtually abandoning the main channel occupied only one month previous (compare Figures 9 and 10).

A total of five samples were obtained form this bar; three of matrix and two of sand sediments (see Table 4). A sample collected from a bar head contained poorly sorted, very coarse-grained matrix sediments deposited between small cobble sized clasts. A sample obtained from a bar top was composed of very poorly sorted, very coarse-grained matrix sediments that had accumulated between pebble sized clasts. No bar tail matrix sample was collected at this site. An accreting gravel lobe was sampled and found to be composed of pebble sized clasts with poorly sorted, granule sized matrix.

Two samples of sand were obtained from this site; one from a bar tail sand wedge, the other from a dunefield radiating from a deep erosive scour in the active river channel. The bar tail sand wedge was composed of well sorted, medium-grained sands; the dunefield was very well sorted and similarly medium-grained.

The magnetite content of these samples ranged from 0.0022 to 0.0063 weight percent. The highest percentage was obtained from sediments that were very poorly sorted and very coarse-grained that were collected from the bar top (see Table 4).

3.2.5: Site 5

The fifth bar sampled was located 55 kilometres downriver of the Saskatchewan Glacier (see Figure 1). The bar selected was approximately 40 metres long and 15 metres wide (see Figure 11).

A total of six samples were obtained from this bar; three of matrix and three of sand. Clast sizes decreased from bar head and bar top (medium cobbles) to bar tail

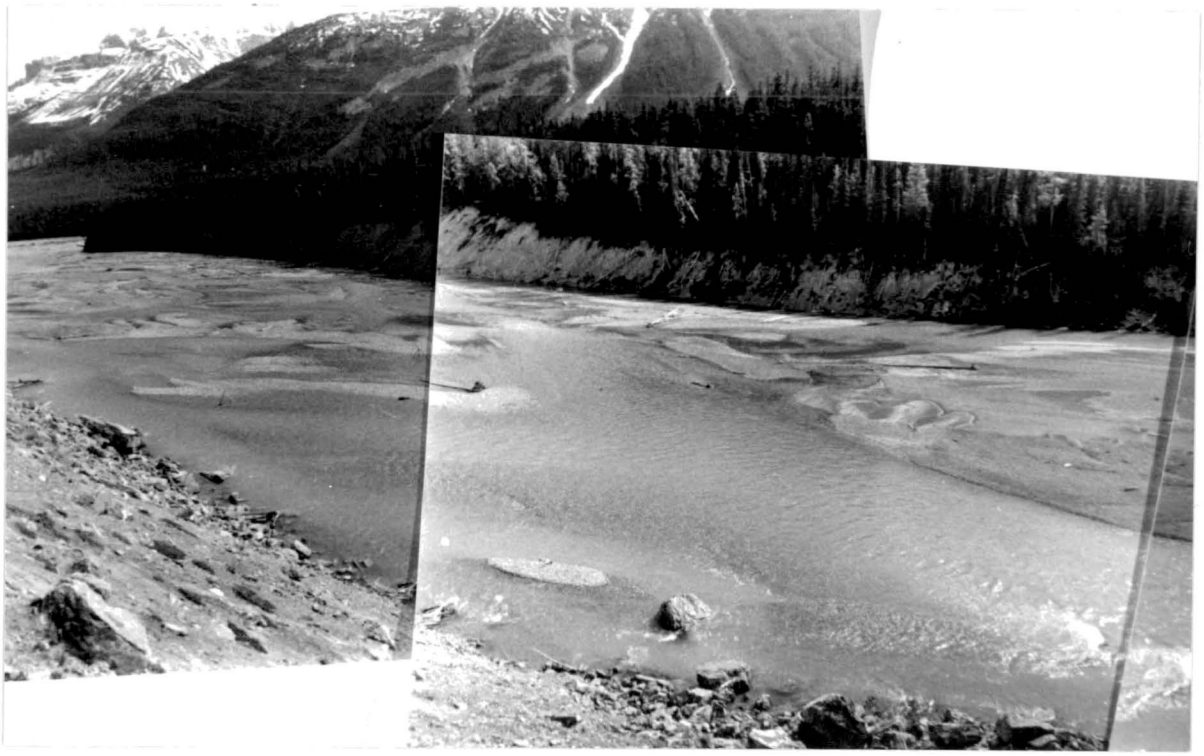

Figure 9: Photomosaic of the longitudinal bar system studied at Site 4 on the North Saskatchewan River. The width of the entire channel is approximately 80 metres.

a) View of bar tail area. Flow is from right to left.

b) View of bar head area looking upsteam. Flow is from right to left.

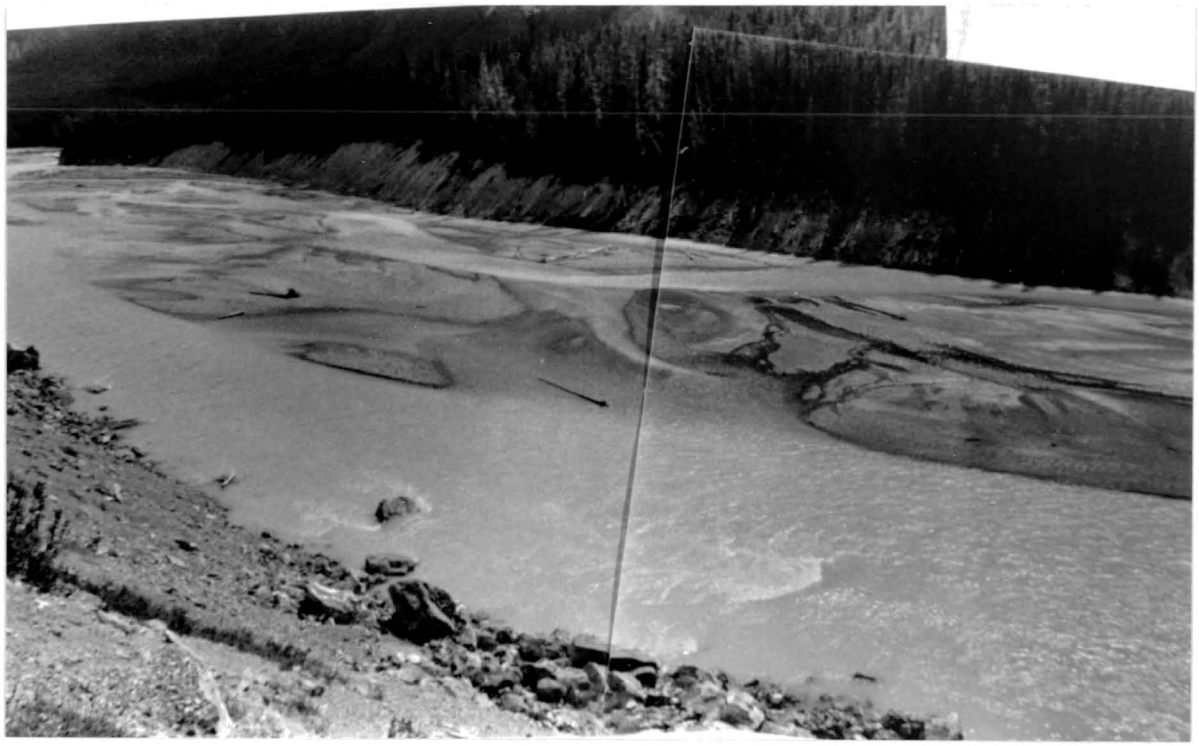

Figure 10: Photomosaic of the longitudinal bar system studied at Site 4 on the North Saskatchewan River approximately 1 month later than Figure 9 during increased river discharge.

a) View of bar tail area. Flow is from right to left.

b) View of bar head area looking upsteam. Flow is from right to left.

Table 4. Data from sediment analysis of samples collected from Site 4 on the North Saskatchewan River.

Sample Number	Sample Site Description	Sediment Type	Mean Quartz		Sorting of Quartz		Percent Magnetite	Percent Mud	Clast Size (cm2)
1	Bar head	Matrix	(VC)	-0.51	(PS)	2.31	0.0033	1.51	31
5	Bar top	Matrix	(VC)	-0.33	(VPS)	2.50	0.0063	5.53	19
3	Accretionary lobe	Matrix	(VC)	-1.03	(PS)	2.27	0.0044	6.62	0
4	Bar tail sand wedge	Sand	(M)	1.41	(WS)	0.70	0.0022	0.80	0
2	Dunefield radiating from pool	Sand	(M)	1.95	(VWS)	0.48	0.0034	0.33	0

Grain Size Legend		Sorting Legend	
VF	Very Fine-Grained	VWS	Very Well Sorted
F	Fine-Grained	WS	Well Sorted
M	Medium-Grained	MWS	Moderately Well Sorted
C	Coarse-Grained	MPS	Moderately Poorly Sorted
VC	Very Coarse-Grained	PS	Poorly Sorted
G	Granule	VPS	Very Poorly Sorted

Figure 11: The longitudinal bar system studied at Site 5 on the North Saskatchewan River. The bar length is approximately 60 metres.

a) View of bar tail. Flow is from right to left.

b) View of bar head looking upsteam. Flow is from right to left.

(pebbles). Matrix sediments obtained from the bar head, top, and tail, were all moderately poorly sorted and very coarse-grained. The three sand samples were obtained from a combination of bar edge and bar tail sand wedges. Although deposited in different areas of the bar, each sand wedge contained of well sorted and fine-grained sands.

The percentage of magnetite recovered from this bar ranged from 0.0021 to 0.0219 weight percent. The highest percentage came from a bar tail sand wedge composed of well sorted, fine-grained sands (see Table 5).

3.3: Comparison of Bars

In this section, similarities and differences in surficial sediment and matrix of the bars studied will be discussed. In general, the grain size and sorting characteristics of matrix and sand samples exhibited very little dependency to increased distance away from the glacier (see Figures 12a to 12d). Moreover, the percentage of magnetite similarly demonstrated little relationship to distance (see Figures 12e and 12f). However, both clast size and mud content in matrix and sand samples exhibited an inverse relationship, with an increase in distance resulting in an exponential decline in both these variables (see Figure 13).

Matrix samples obtained from bar head, bar top, and bar tail areas from all five bars were composed of poorly to moderately poorly sorted, very coarse-grained sediments (see Tables 1 through 5). Chute channels were also sampled in the first three bars. The first contained moderately poorly sorted, medium-grained matrix sampled from between boulder sized clasts. A second chute channel, located at Site 2, contained sediments that were similarly moderately poorly sorted but somewhat coarser grained matrix in the granule size range that accumulated between large cobbles. Three samples were obtained from chute channels at Site 3 and all contained moderately poorly sorted, very coarse-grained matrix sediments that had accumulated between medium sized cobble clasts. Although the first chute channel was somewhat finer grained than that sampled downriver, matrix obtained from the second and third bars exhibited a decrease in grain size with no change in sorting.

Several accretionary lobes were also sampled but showed no trends between bars. Matrix sediments were generally poorly to moderately poorly sorted, very coarse to granule grain size. Clast size ranged from large cobble to pebble size.

Sediments which accumulated in sand lens deposits were much finer grained than those of matrix sediments. The chute channel sand fill deposits sampled on the

Table 5. Data from sediment analysis of samples collected from Site 5 on the North Saskatchewan River.

Sample Number	Sample Site Description	Sediment Type	Mean Quartz		Sorting of Quartz		Percent Magnetite	Percent Mud	Clast Size (cm2)
1	Bar head	Matrix	(VC)	-0.91	(MPS)	1.74	0.0021	0.49	43
2	Bar top	Matrix	(VC)	-0.77	(MPS)	1.74	0.0023	2.31	42
4	Bar tail	Matrix	(VC)	-0.51	(MPS)	1.70	0.0047	1.27	28
3	Bar edge sand wedge	Sand	(F)	2.18	(WS)	0.51	0.0086	1.34	0
5	Bar tail sand wedge	Sand	(F)	2.19	(WS)	0.65	0.0062	3.23	0
6	Bar tail sand wedge	Sand	(F)	2.17	(WS)	0.54	0.0219	1.85	0

Grain Size Legend		Sorting Legend	
VF	Very Fine-Grained	VWS	Very Well Sorted
F	Fine-Grained	WS	Well Sorted
M	Medium-Grained	MWS	Moderately Well Sorted
C	Coarse-Grained	MPS	Moderately Poorly Sorted
VC	Very Coarse-Grained	PS	Poorly Sorted
G	Granule	VPS	Very Poorly Sorted

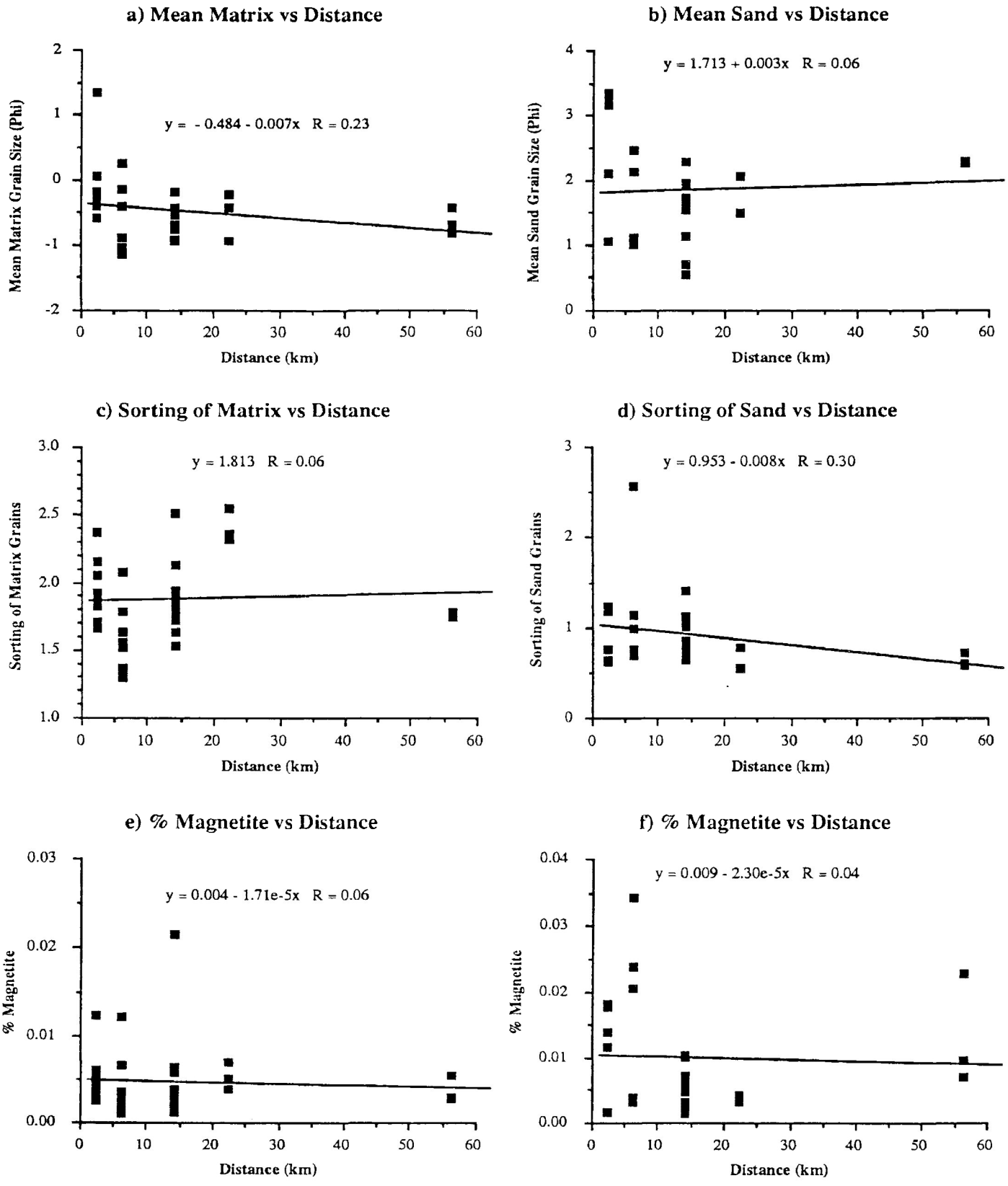

Figure 12. Scatter diagrams of the mean, sorting, and percentage of magnetite versus distance derived from matrix and surficial sediments sampled on the North Saskatchewan River.

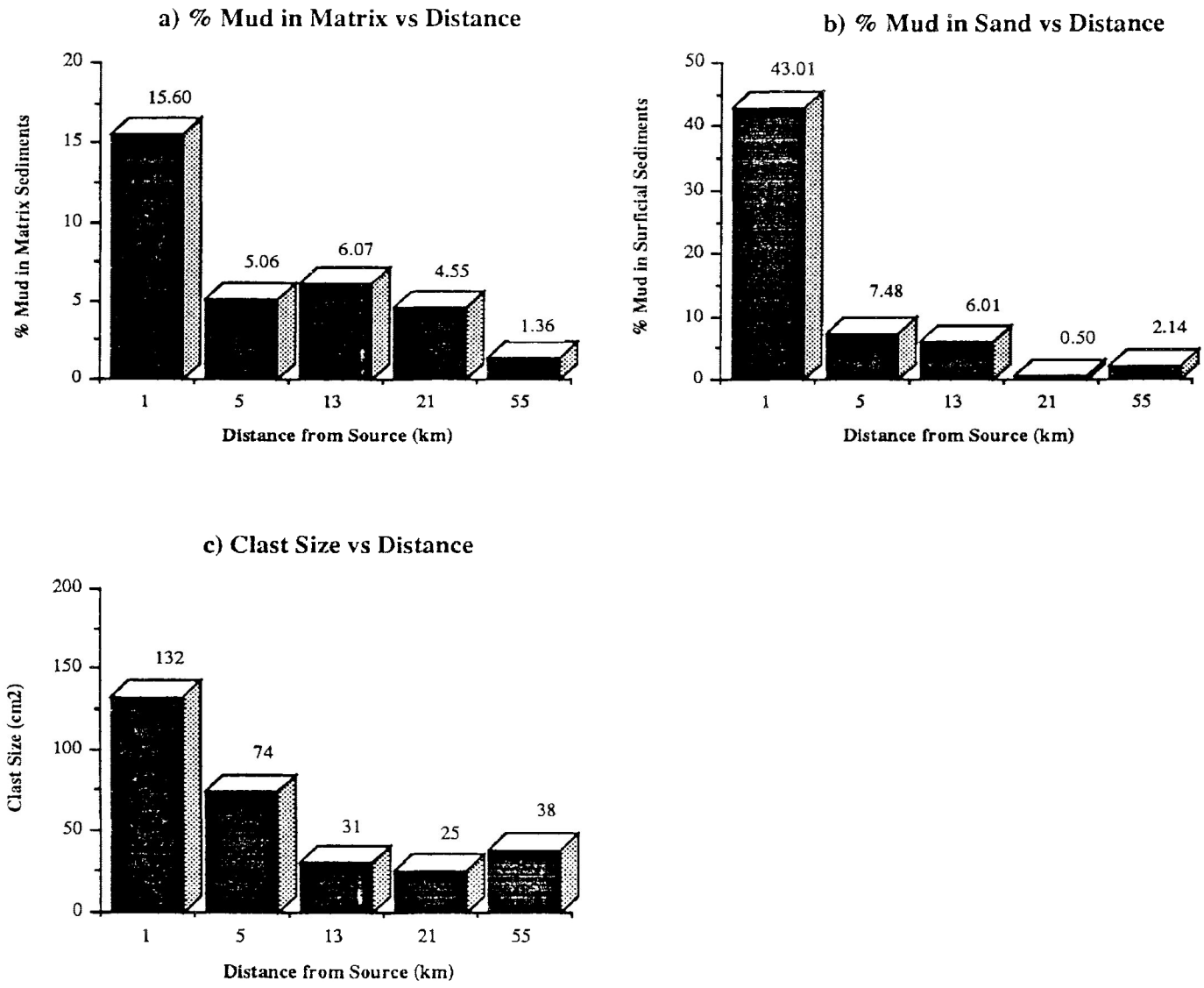

Figure 13. Bar graphs showing a decrease in the average percentage of mud in river sediments and the decrease in the average clast size away from the source of the North Saskatchewan River.

third bar were well to moderately well sorted, medium- to coarse-grained. These sands were better sorted and finer grained than the matrix sediments sampled from between clasts in the floor of these chute channels. Several bar edge sand wedges were sampled on four of the bars and were composed mostly of well to moderately well sorted, medium- to very fine-grained sands. Bar tail sand wedges were similarly sampled on four of the bars and were also found to contain well to moderately well sorted, medium- to fine-grained sands. Both bar edge and bar tail sand wedges appear to be composed of sands with similar grain size and sorting characteristics. A chute channel delta sampled on the second bar was composed of well sorted coarse-grained sands, somewhat coarser grained than chute channel fill deposits. The sand wedge sampled on the third bar was composed of well sorted, medium-grained sand and is similar to the well sorted, medium-grained sands deposited on the bar top of the same bar.

The percentage of magnetite contained in the samples collected from this river system demonstrated little relationship with distance (see Figures 12e and 12f). However, magnetite content does appear to increase in poorly sorted and finer grained matrix sediments (see Figures 14a and 14c). Although not as significant, a similar trend exists with respect to sand deposits (see Figures 14b and 14d).

As previously discussed, the mud content in both matrix and sand sediment samples exponentially declined away from the Saskatchewan Glacier (see Figures 13a and 13b). The average mud content in matrix samples declines from 15.60 (Bar 1) to 1.36 (Bar 5) weight percent. Similarly, the average mud content in sand samples declined from 43.01 (Bar 1) to 2.14 (Bar 5) weight percent.

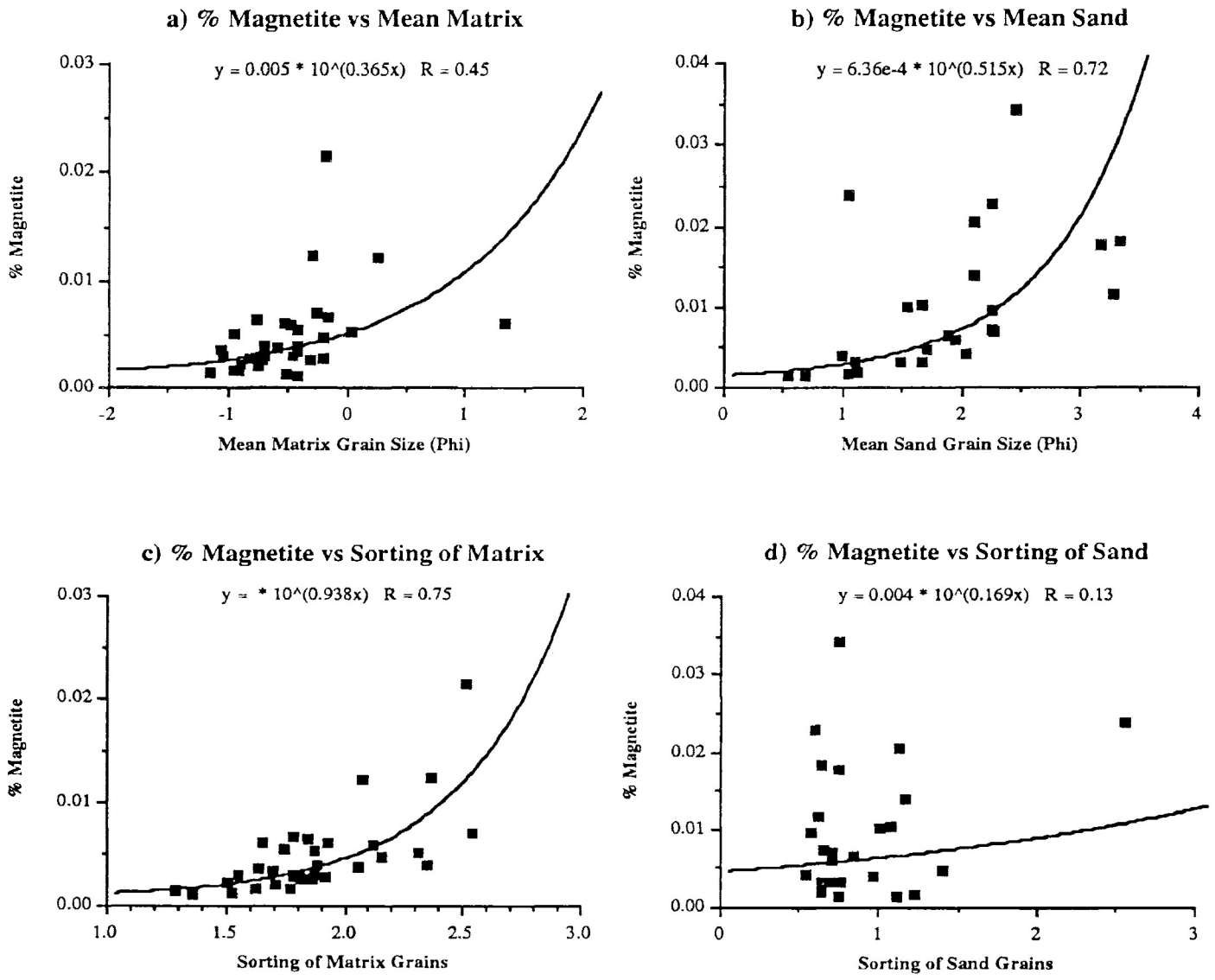

Figure 14. Scatter diagrams of the percentage of magnetite versus its average grain size and sorting derived from matrix and surficial sediments sampled on the North Saskatchewan River.

CHAPTER 4: NORTHERN ONTARIO RIVERS STUDIED

4.1: Drainage Basin Processes

The rivers studied in Northern Ontario receive water from a variety of sources that contribute to maintain river discharge throughout the year. Because of the absence of glaciers in this area, river discharge is governed by other processes including spring runoff, storm events, overland flow, throughflow, groundwater, infiltration rates, and vegetation.

Each year, the study area receives a significant amount of snowfall which, when melted in the spring, produces a substantial supply of runoff. As snow cover is depleted, the amount of runoff is similarly reduced. Throughout this period, a small diurnal fluctuation in discharge occurs, especially on warm spring days where increased melting rates result in corresponding increases in river discharge. For a relatively short period of time each year, river discharge in watersheds situated in temperate continental areas may somewhat resemble glacial discharge patterns, similar to that which was observed on the North Saskatchewan River in Alberta. Substantial quantities of alluvial sediments are transported during this annual period of peak discharge. Gravel bars are also typically submerged at this time and are subsequently modified. As peak flows following spring runoff subside, gravel bars emerge and generally lay dormant for the remainder of the year, during which time, they are subject to modification by subaerial processes.

Once spring runoff has passed, river discharge is controlled by the processes previously mentioned. Vegetation acts to regulate discharge by reducing surface compaction, thereby affecting rates of infiltration. Vegetation also controls overland flow velocities. Where vegetation is noticeably absent, or where rainfall intensity exceeds infiltration rates, surface waters quickly flow overland into the river system resulting in higher peak discharges and coarser grained sediments being transported. Therefore, in areas of little to no vegetation, sediments are largely unconsolidated, and significantly higher rates of aggradation can be expected. This is a possible explanation for the presence of thick sedimentary sequences deposited during the Proterozoic prior to the development of vegetation. However, in areas of abundant vegetation, erosional rates are significantly reduced resulting in finer grained sediments being eroded and subsequently transported by the fluvial system, thereby reducing the likelihood of coarse-grained bar formation and alluvial placer development.

The process of throughflow is an important element in river discharge. Water accumulating on the surface of the ground may eventually infiltrate the soil, depending on compaction. Movement continues until some relatively impervious layer is encountered, at which level, the water may flow laterally down slope, towards the river channel. Throughflow flows much more slowly than that of overland flow because subsurface water must travel through an infinite number of soil pore spaces which results in significantly slower water movement rates. Water passing through the soil as throughflow will generally reach the river channel sometime after peak surface discharge has left the system thereby reducing the likelihood of extreme discharge events.

Water movement in the upper soil horizons is much faster than that encountered deep below the surface and is generally referred to as base or groundwater flow. Groundwater discharge into a river system represents a natural regulating process which ensures minimum baseflows in river channels during summer and winter low flow periods. This process is also particularly important during prolonged dry periods in maintaining minimum baseflows. Groundwater discharge can therefore be distinguished by its constancy of flow throughout most of the year with other discharge events simply superimposed on top of normal groundwater discharge levels.

The processes outlined above operate congruently and acts to reduce the effects of severe storm events by buffering their intensity and lessening their severity. This reduces the likelihood of "flashfloods", typical of ephemeral rivers, that have the potential of moving large quantities of sediment during relatively short periods of time. A consequence of these processes is that most bar modification and sedimentation occur during peak spring discharges and during infrequent, and sometimes catastrophic storm events. A thorough discussion of watershed drainage basin processes is beyond the scope of this paper. For a full description of these, and other processes affecting runoff, the reader is referred to Gregory and Walling (1973), and Dunne and Leopold (1978).

A total of 61 samples of fluvial sediments were collected from four coarse-grained longitudinal bars in Northern Ontario; one bar from each of the Jackpine and Mississagi Rivers, and two from the Agawa River (see Figure 1). As previously described in Chapter 1, each of the rivers selected in this study displayed classic longitudinal gravel bars. Each river system contained large quantities of coarse-grained alluvium made available from locally abundant supplies of glacial drift deposited over the area during the last ice advance/retreat cycle. A variety of minerals are transported in

each river system, depending on local source terrain. Sediments were found to contain relatively higher percentages of magnetite than those sampled from the North Saskatchewan river system. The percentage of magnetite in the samples analysed from the four bars ranged from 0.0711 to 9.8397 weight percent, as compared to those values obtained in sediments from the North Saskatchewan (0.0003 to 0.0335 weight percent).

Data obtained from each bar is presented in the form of eleven scatter diagrams which show the relationship between specific variables. On each scatter diagram, a best fitting regression line and equation have been calculated along with the correlation of the line. A combination of linear and exponential regression lines have been fitted to the various graphs.

4.2: Description of Rivers Studied

4.2.1: The Jackpine River

The longitudinal bar examined on the Jackpine River is approximately 75 metres long and 40 metres wide; some vegetation was present on this bar (see Figure 15). In total, 16 samples of matrix and sand were obtained (see Table 6).

The bar exhibited a significant decrease in clast size from bar head (large boulders), to bar top and tail (medium to small cobbles) (see Figure 15). An analysis of matrix samples obtained from the bar showed a decrease in sorting over the length of the bar; the average grain size of the matrix sediments exhibited little change.

Sand samples collected from a low velocity zone immediately downriver of a very large boulder were found to progressively coarsen with depth, changing from medium- to coarse-grained. The sand was well sorted overall but better sorted at the surface than at depth. Magnetite grains
were somewhat finer grained (medium grain size) and showed a similar coarsening with depth. However, magnetite was better sorted at depth than at the surface. Two other low velocity zones that were sampled displayed similar grain size characteristics to those previously discussed.

Sand samples were collected from an erosive scour on the bar top; one from along the upper outer edge, the other from the bottom of the scour. Both the sand and magnetite fractions of the two samples were well sorted and coarse-grained. Surficial sediments were also collected from a relatively large sand wedge. Sands became somewhat finer grained (coarse to medium) and better sorted (moderately well to well) in

Figure 15: The longitudinal bar studied on the Jackpine River. Flow is from bottom right to top left. The bar is approximately 30 metres in width.

Table 6. Data from sediment analysis of samples collected from the Jackpine River.

Sample Number	Sample Site Description	Sediment Type	Mean Quartz		Sorting of Quartz		Mean Magnetite		Sorting of Magnetite		Percent Magnetite	Clast Size (cm2)
1	Bar head (surface)	Matrix	(C)	0.31	(MWS)	1.36	(VC)	-0.13	(MWS)	1.06	0.89	631
2	Bar head (below surface)	Matrix	(VC)	-0.69	(MWS)	1.42	(VC)	-0.69	(WS)	0.95	1.34	631
3	Bar head (surface)	Matrix	(VC)	-0.07	(MWS)	1.47	(VC)	-0.50	(MWS)	1.20	1.07	631
7	Bar top (surface)	Matrix	(VC)	-0.59	(MPS)	1.53	(VC)	-0.33	(MWS)	1.15	1.78	29
12	Bar top (surface)	Matrix	(VC)	-0.26	(MPS)	1.53	(VC)	-0.31	(MWS)	1.21	1.74	58
16	Bar tail (surface)	Matrix	(VC)	-0.79	(MPS)	1.57	(VC)	-0.52	(MWS)	1.19	0.87	52
4	Low vel zone (surface)	Sand	(M)	1.36	(WS)	0.73	(M)	1.42	(WS)	0.84	0.21	1288
5	Low vel zone (below surface)	Sand	(M)	1.20	(WS)	0.80	(M)	1.22	(WS)	0.81	0.18	1288
6	Low vel zone (below surface)	Sand	(C)	0.91	(WS)	0.92	(M)	1.22	(WS)	0.76	0.07	1288
8	Low vel zone (surface)	Sand	(M)	1.39	(WS)	0.88	(M)	1.02	(MWS)	1.03	0.34	529
9	Low vel zone (surface)	Sand	(M)	1.68	(WS)	0.73	(M)	1.50	(WS)	0.93	0.16	3600
10	Outer edge of scour	Sand	(C)	0.59	(WS)	0.90	(C)	0.59	(WS)	0.69	0.39	0
11	Bottom of scour	Sand	(C)	0.56	(WS)	0.86	(C)	0.39	(WS)	0.66	0.23	0
13	Sand wedge	Sand	(C)	0.07	(MWS)	1.33	(VC)	-0.01	(MWS)	1.07	0.36	0
14	Sand wedge	Sand	(M)	1.17	(WS)	0.76	(M)	1.01	(WS)	0.89	0.36	0
15	Sand wedge	Sand	(M)	1.07	(WS)	0.99	(C)	0.52	(WS)	0.95	0.38	0

Grain Size Legend		Sorting Legend	
VF	Very Fine-Grained	VWS	Very Well Sorted
F	Fine-Grained	WS	Well Sorted
M	Medium-Grained	MWS	Moderately Well Sorted
C	Coarse-Grained	MPS	Moderately Poorly Sorted
VC	Very Coarse-Grained	PS	Poorly Sorted
G	Granule	VPS	Very Poorly Sorted

a downriver direction. Magnetite grains changed from very coarse to medium to coarse. Sorting improved somewhat, changing from moderately well to well sorted.

Figure 16 illustrates the interaction of mean grain size and sorting of quartz and magnetite in sediments deposited on this bar. Figure 16a plots the mean grain size of quartz sand against that of magnetite. This data set displays a significant positive trend indicating that in any given site on the bar, coarse magnetite grains will be deposited with coarse quartz grains. A similar positive trend occurs in Figure 16b; where magnetite grains are poorly sorted, quartz grains are similarly poorly sorted. Figures 16c and 16d indicate that higher percentages of magnetite are found in samples containing coarse magnetite and quartz sediments. Similarly, Figures 16e and 16f show that magnetite content is higher in poorly sorted sediments. As sorting improves, the percentage of magnetite is significantly reduced.

Figure 17 illustrates how clast size affects average grain size, sorting, and magnetite content in matrix sediments. Figures 17a and 17b suggest that with an increase in clast size, quartz and magnetite matrix sediments become finer grained. Because clast sizes are typically larger at the head of the bar than those found at the tail, matrix sediments deposited at the bar head will generally be finer grained than those accumulating at the bar tail. Figures 17c and 17d suggest that with an increase in clast size, magnetite and quartz grains become better sorted. Figure 17e shows that larger clasts are generally associated with matrix sediments containing lower percentages of magnetite.

The data obtained from the Jackpine River indicates that magnetite content increases in poorly sorted, very coarse-grained sediments. The highest percentage of magnetite obtained from this bar was found in two bar top matrix samples that accumulated between small to medium sized cobbles. Both quartz and magnetite grains at these two sites were moderately poorly sorted and very coarse-grained (see Table 6). On this bar, the highest percentages of magnetite are found in matrix sediments, not sand deposits.

4.2.2: The Agawa River: Site 1

This longitudinal bar is located approximately 100 metres upriver from the Highway 17 bridge. The bar is 60 metres long and 30 metres wide; there was no vegetation present (see Figure 18). A total of 18 samples of matrix and sand sediments were obtained from this bar (see Table 7). The clasts on the bar were well imbricated

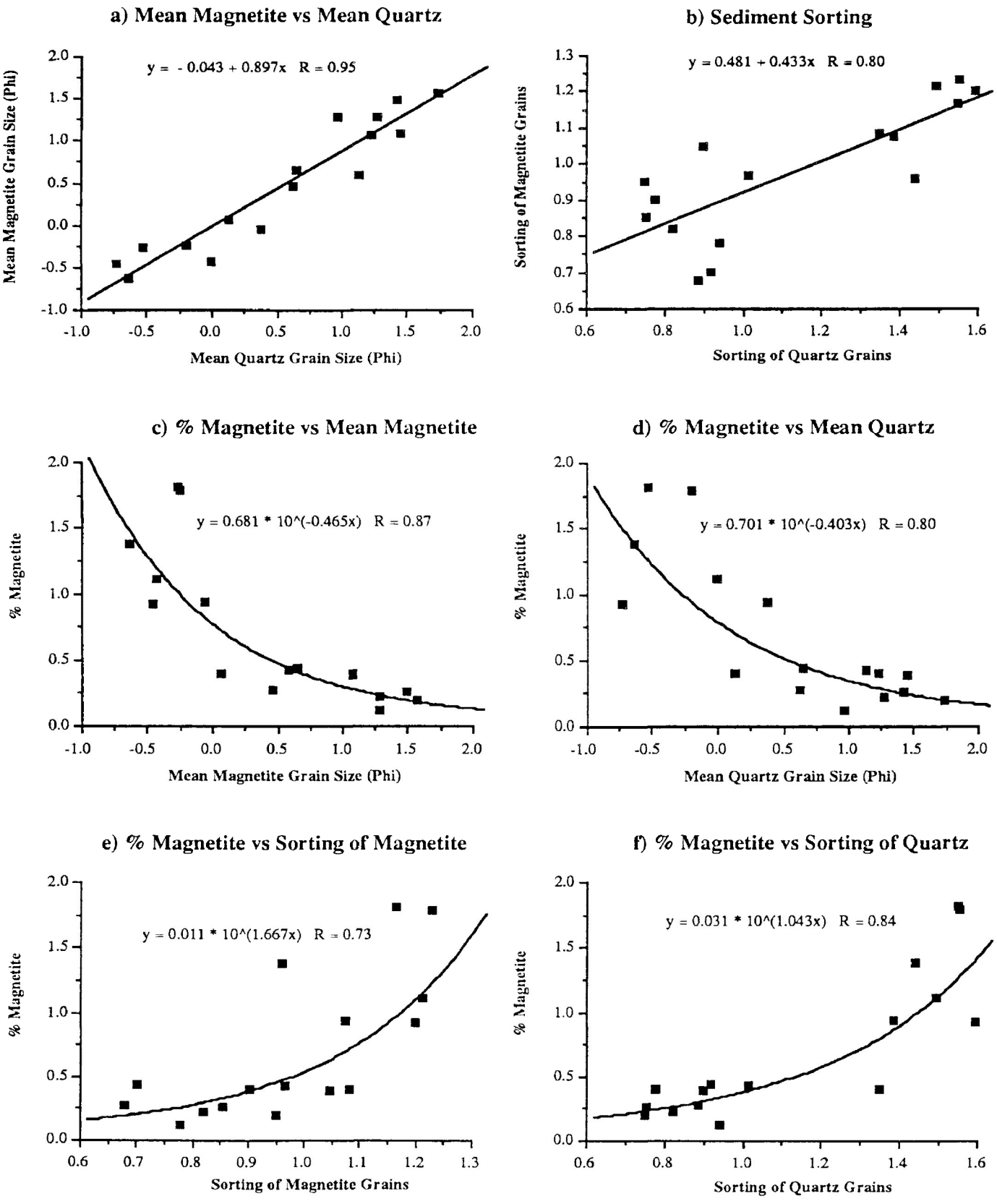

Figure 16. Scatter diagrams of variables derived from sediments sampled on the Jackpine River.

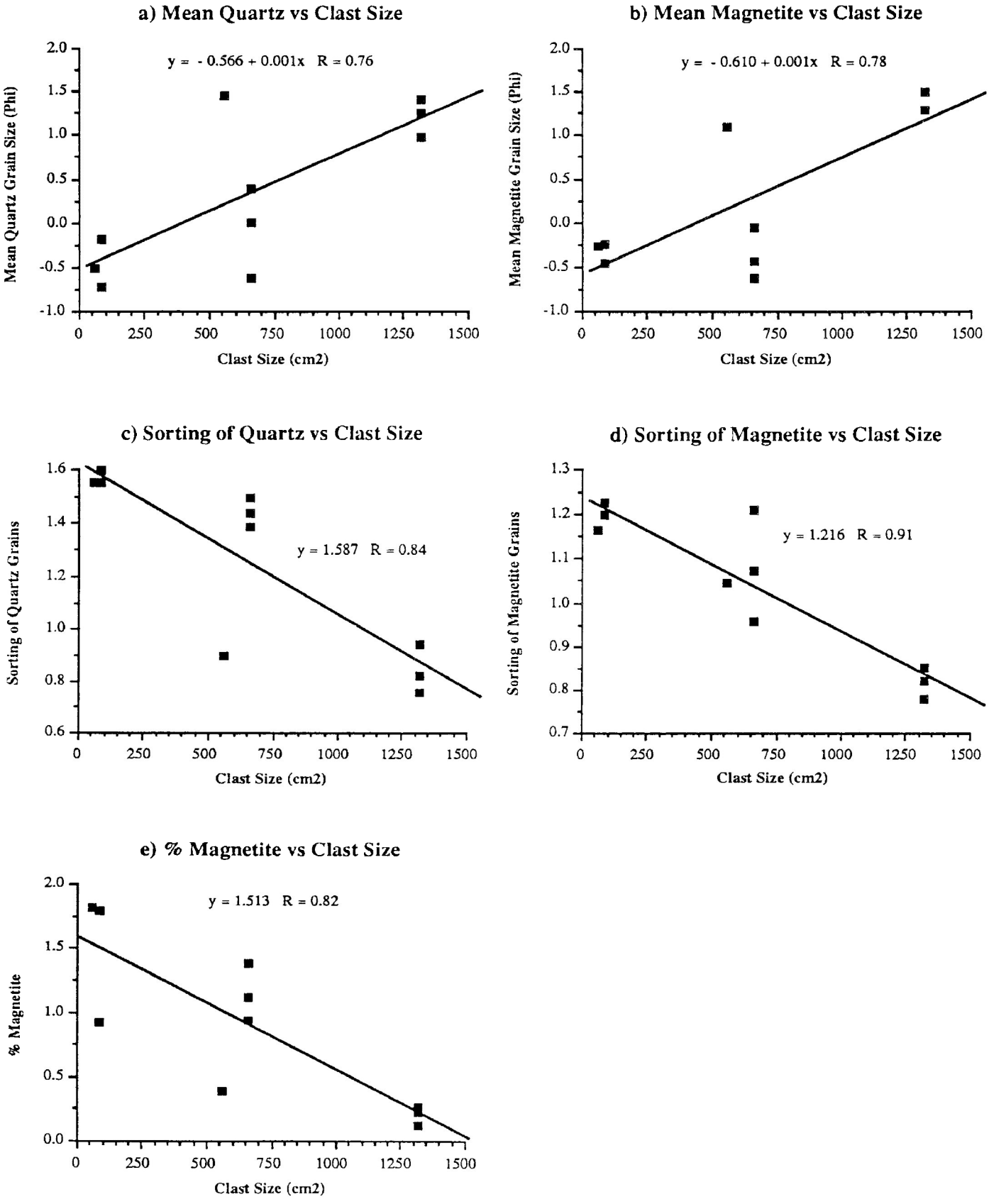

Figure 17. Scatter diagrams of variables derived from sediments sampled on the Jackpine River in relation to clast size.

Figure 18: The longitudinal bar studied at Site 1 on the Agawa River. Flow is from bottom to top. The bridge gives an indication of scale.

Table 7. Data from sediment analysis of samples collected from Site 1 on the Agawa River.

Sample Number	Sample Site Description	Sediment Type	Mean Quartz	Sorting of Quartz	Mean Magnetite	Sorting of Magnetite	Percent Magnetite	Clast Size (cm2)
1	Bar head (surface)	Matrix	(VC) -0.80	(MWS) 1.36	(VC) -0.09	(MWS) 1.11	2.14	155
2	Bar head (surface)	Matrix	(VC) -0.06	(MWS) 1.09	(C) 0.33	(WS) 0.86	1.49	276
16	Bar tail	Matrix	(VC) -0.78	(MWS) 1.43	(VC) -0.29	(MWS) 1.19	3.26	70
17	Bar tail	Matrix	(C) 0.00	(MWS) 1.44	(C) 0.87	(WS) 0.96	3.10	45
18	Bar tail	Matrix	(C) 0.10	(MWS) 1.34	(C) 0.96	(WS) 0.83	3.10	45
3	Upriver of large clast (surface)	Sand	(C) 0.08	(WS) 0.72	(C) 0.39	(WS) 0.62	2.79	189
4	Upriver of large clast (below)	Sand	(VC) -0.57	(MWS) 1.15	(C) 0.06	(WS) 0.82	1.97	189
5	Behind large clast (surface)	Sand	(VC) -0.18	(WS) 0.72	(C) 0.24	(WS) 0.62	1.72	0
6	Bar edge sand wedge (surface)	Sand	(VC) -0.21	(WS) 0.52	(C) 0.01	(WS) 0.53	0.84	0
7	Bar edge sand wedge (below)	Sand	(C) 0.10	(WS) 0.60	(C) 0.33	(WS) 0.55	0.86	0
8	Bar edge sand wedge (next to clasts)	Sand	(VC) -0.01	(WS) 0.73	(C) 0.25	(WS) 0.87	1.98	0
9	Between 2 large clasts (surface)	Sand	(VC) -0.94	(MWS) 1.34	(VC) -0.50	(MWS) 1.00	3.73	247
10	Old bar edge sand wedge (surface)	Sand	(VC) -0.23	(WS) 0.64	(C) 0.10	(WS) 0.54	2.22	0
11	Old bar edge sand wedge (below)	Sand	(C) 0.47	(WS) 0.73	(C) 0.63	(WS) 0.58	1.97	0
12	Bar edge sand wedge (surface)	Sand	(C) 0.04	(WS) 0.81	(C) 0.22	(WS) 0.65	1.03	0
13	Bar edge sand wedge (below)	Sand	(VC) -0.59	(MWS) 1.36	(C) 0.36	(WS) 0.90	1.86	0
14	Sand Lens, upriver of large clast	Sand	(C) 0.42	(VWS) 0.49	(C) 0.58	(VWS) 0.44	1.22	197
15	Sand shadow upriver of large clast	Sand	(C) 0.47	(WS) 0.62	(C) 0.57	(WS) 0.51	1.60	405

Grain Size Legend		Sorting Legend	
VF	Very Fine-Grained	VWS	Very Well Sorted
F	Fine-Grained	WS	Well Sorted
M	Medium-Grained	MWS	Moderately Well Sorted
C	Coarse-Grained	MPS	Moderately Poorly Sorted
VC	Very Coarse-Grained	PS	Poorly Sorted
G	Granule	VPS	Very Poorly Sorted

and ranged in size from boulders (bar head) to medium cobbles (bar tail). Matrix samples displayed similar grain size and sorting characteristics at these sites (see Table 7). The quartz and magnetite fractions obtained from sand samples collected from around a relatively large boulder on the bar top were generally well sorted and coarse-grained. They showed little variation with depth.

Quartz and magnetite sediments collected from a bar edge sand wedge were generally well sorted and coarse-grained. They showed little deviation between the various wedges whether sampled from the surface or within the sand wedge. Quartz and magnetite grains were also collected from between two large boulders and found to be moderately well sorted and very coarse-grained. Samples obtained from sand deposits that formed upriver of large boulders were well to very well sorted and coarse-grained.

Figure 19 illustrates the interaction of mean grain size and sorting of quartz and magnetite in sediments deposited on this bar. Figure 19a plots the mean grain size of quartz sand against that of magnetite. This data set displays a similar positive trend as that obtained from the Jackpine River (see Figure 16a) indicating that in any given site on the bar, coarse magnetite grains will be deposited with coarse quartz grains. Figure 19b also shows a significant positive trend indicating that where magnetite grains are poorly sorted, quartz grains are similarly poorly sorted and visa versa. Figures 19c and 19d show very little relationship between the percentage of magnetite and the average grain size of sediments. However, Figures 19e and 19f show that magnetite content improves somewhat in poorly sorted sediments. As matrix sediments become better sorted, the percentage of magnetite is reduced.

Figure 20 illustrates how clast size affects average grain size, sorting, and magnetite content in matrix sediments. Figures 20a and 20b show no correlation between clast size and average quartz and magnetite grain size on this bar. Figures 20c and 20d similarly show little relationship between clast size and the sorting of quartz and magnetite sediments. Figure 20e suggests that as clast size decreases, the magnetite content in matrix sediments will increase.

Similar to those results obtained from the bar sampled on the Jackpine River (Figures 16 and 17), the percentage of magnetite tends to increase in coarser and more poorly sorted sediments deposited between smaller sized clasts. Magnetite content was however highest (3.73 weight percent) on this bar in moderately well sorted, very coarse-grained sediments that accumulated between two relatively large boulders. Bar tail matrix samples, collected from between medium sized cobbles, also contained

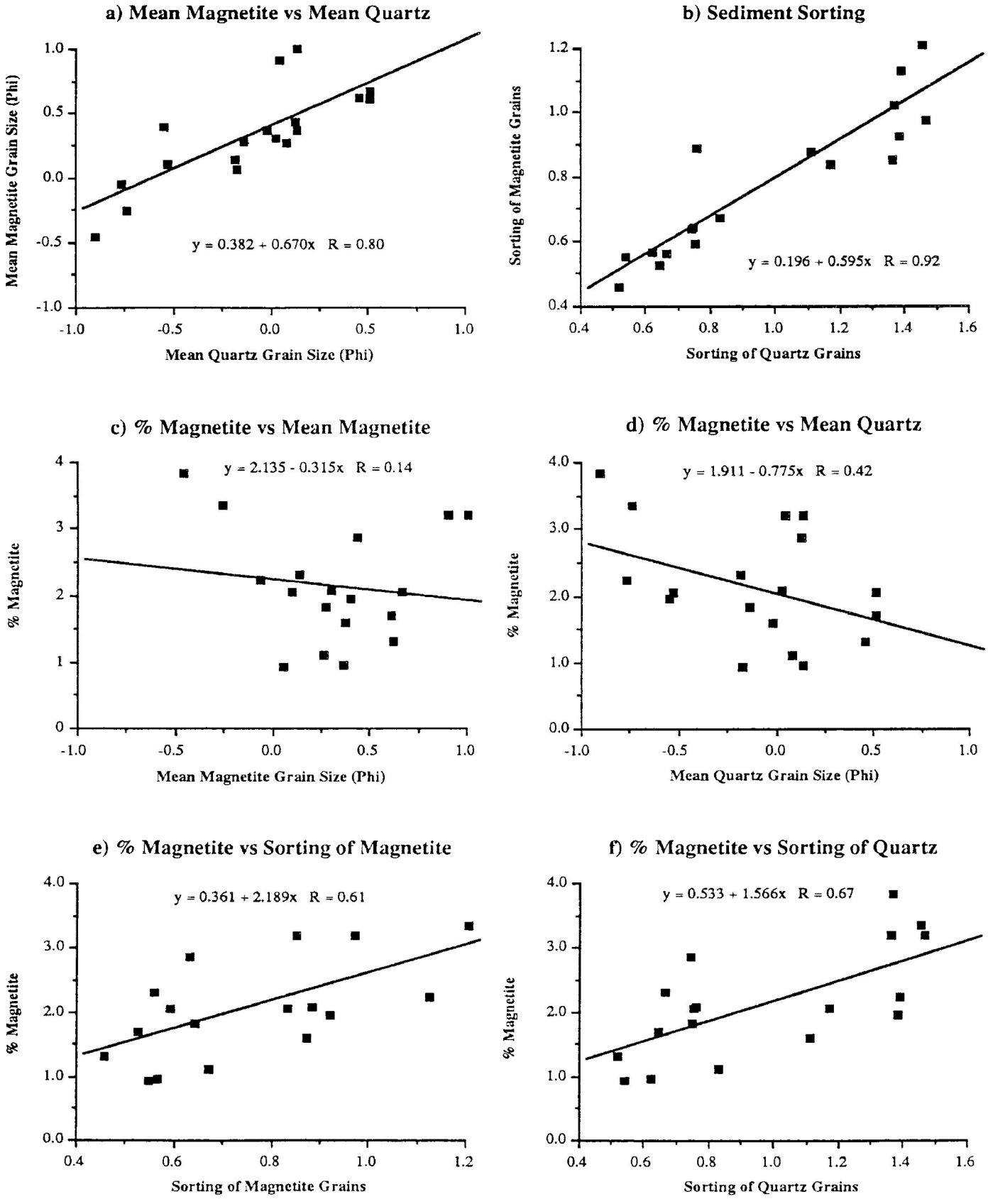

Figure 19. Scatter diagrams of variables derived from sediments sampled at Site 1 on the Agawa River.

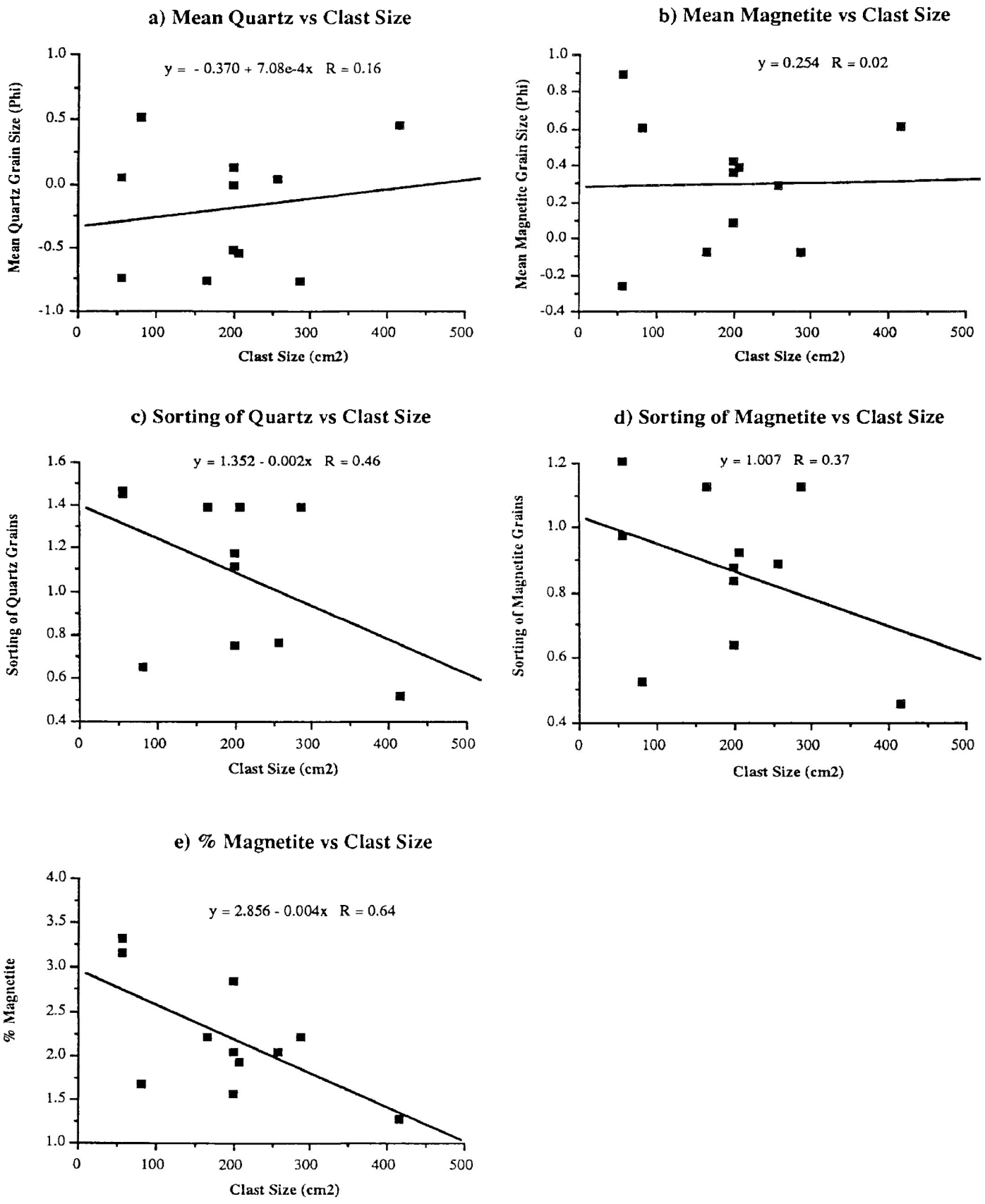

Figure 20. Scatter diagrams of variables derived from sediments sampled at Site 1 on the Agawa River in relation to clast size.

relatively high percentages of magnetite (averaging 3.15 weight percent) and were also moderately well sorted and coarse- to very coarse-grained (see Table 7). In this bar, the highest percentage of magnetite was found in matrix sediments, with slightly lower percentages in sand deposits.

4.2.3: The Agawa River: Site 2

The longitudinal bar examined at this site is located five kilometres upriver of the previously described bar. The bar is approximately 80 metres long and 30 metres wide; some vegetation was present (see Figure 21). A total of 15 samples of matrix and sand sediments were obtained from this bar (see Table 8).

The bar exhibited a substantial decrease in clast size from bar head (large boulders) to bar top and bar tail (medium cobbles). Matrix samples displayed similar grain size and sorting characteristics at these sites (see Table 8). Sediments were predominantly moderately poorly sorted and coarse-grained.

Several sand samples were obtained from the large bar edge sand wedge deposit found on this bar (see Figure 21b). Analysis indicates that quartz and magnetite sediments generally become better sorted and finer grained with increasing distance away from the edge of the river. There was little change in sediment characteristics with depth (see Table 8).

Figure 22 illustrates the interaction of mean grain size and sorting of quartz and magnetite in sediments deposited on this bar. Figure 22a plots the mean grain size of quartz against that of magnetite. This data set displays a similar significant positive trend as the previous two bars (Figures 16a and 19a) indicating that in any given site on the bar, coarse magnetite grains will be deposited with coarse quartz grains. Figure 22b also shows a similar significant positive trend indicating that where magnetite grains are poorly sorted, quartz grains will be similarly poorly sorted. Figures 22c and 22d suggest that higher percentages of magnetite may be found in samples containing coarse magnetite and quartz sediments. Similarly, Figures 22e and 22f suggest that as sorting improves, the percentage of magnetite in bar sediments may decrease.

Figure 23 illustrates that there is no correlation between clast size and mean grain size, sorting, and the percentage of magnetite, and mean grain size and sorting of quartz on this bar.

The data obtained from Site 2 of the Agawa River indicates that the percentage of magnetite increases in coarser and more poorly sorted sediments as a result of

Figure 21: The longitudinal bar studied at Site 2 on the Agawa River. The channel is approximately 80 metres in width.

a) View of bar head from upstream. Flow is from bottom to top.

b) View of bar tail with bar tail sand wedge. Flow is from left to right.

Table 8. Data from sediment analysis of samples collected from Site 2 on the Agawa River.

Sample Number	Sample Site Description	Sediment Type	Mean Quartz		Sorting of Quartz		Mean Magnetite		Sorting of Magnetite		Percent Magnetite	Clast Size (cm2)
14	Bar head	Matrix	(C)	0.03	(MPS)	1.58	(VC)	-0.18	(MWS)	1.29	1.74	864
13	Bar head	Matrix	(VC)	-0.99	(MPS)	1.79	(VC)	-0.49	(MWS)	1.42	0.23	0
12	Near bar head	Matrix	(C)	0.24	(MWS)	1.48	(VC)	-0.12	(MWS)	1.20	0.39	303
10	Bar top	Matrix	(C)	0.21	(MPS)	1.62	(VC)	-0.31	(MWS)	1.25	0.16	223
6	Bar tail	Matrix	(M)	1.50	(WS)	0.61	(M)	1.56	(WS)	0.58	0.07	47
3	Bar tail (next to river)	Matrix	(VC)	-0.59	(MWS)	1.46	(VC)	-0.27	(MWS)	1.24	1.07	50
15	Bar edge sand wedge	Sand	(M)	1.72	(WS)	0.59	(M)	1.57	(WS)	0.63	0.36	0
9	Sand shadow	Sand	(M)	1.82	(WS)	0.74	(M)	1.70	(WS)	0.82	0.34	560
7	Bar tail	Sand	(C)	0.54	(WS)	0.69	(C)	0.40	(WS)	0.61	1.78	0
1	Bar tail sand wedge	Sand	(M)	1.01	(VWS)	0.42	(C)	0.98	(VWS)	0.45	0.89	0
2	bar tail sand wedge (below)	Sand	(C)	0.45	(WS)	0.89	(C)	0.39	(WS)	0.80	1.34	0
4	Bar tail sand wedge (higher up)	Sand	(VC)	-0.05	(VWS)	0.45	(VC)	-0.04	(VWS)	0.41	0.21	0
5	Bar tail sand wedge (higher up)	Sand	(M)	1.51	(VWS)	0.49	(M)	1.39	(WS)	0.50	0.18	0

Grain Size Legend		Sorting Legend	
VF	Very Fine-Grained	VWS	Very Well Sorted
F	Fine-Grained	WS	Well Sorted
M	Medium-Grained	MWS	Moderately Well Sorted
C	Coarse-Grained	MPS	Moderately Poorly Sorted
VC	Very Coarse-Grained	PS	Poorly Sorted
G	Granule	VPS	Very Poorly Sorted

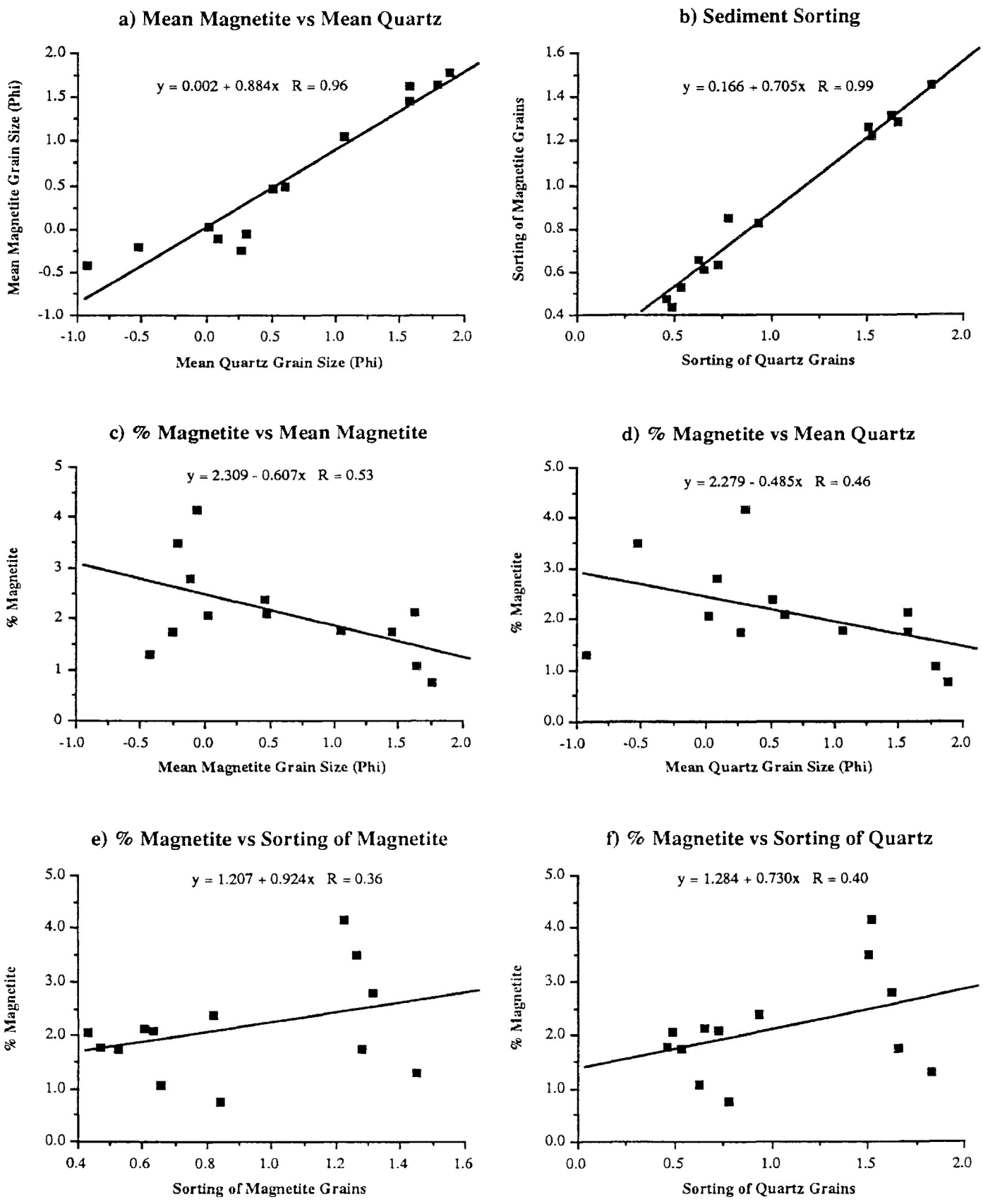

Figure 22. Scatter diagrams of variables derived from sediments sampled at Site 2 on the Agawa River.

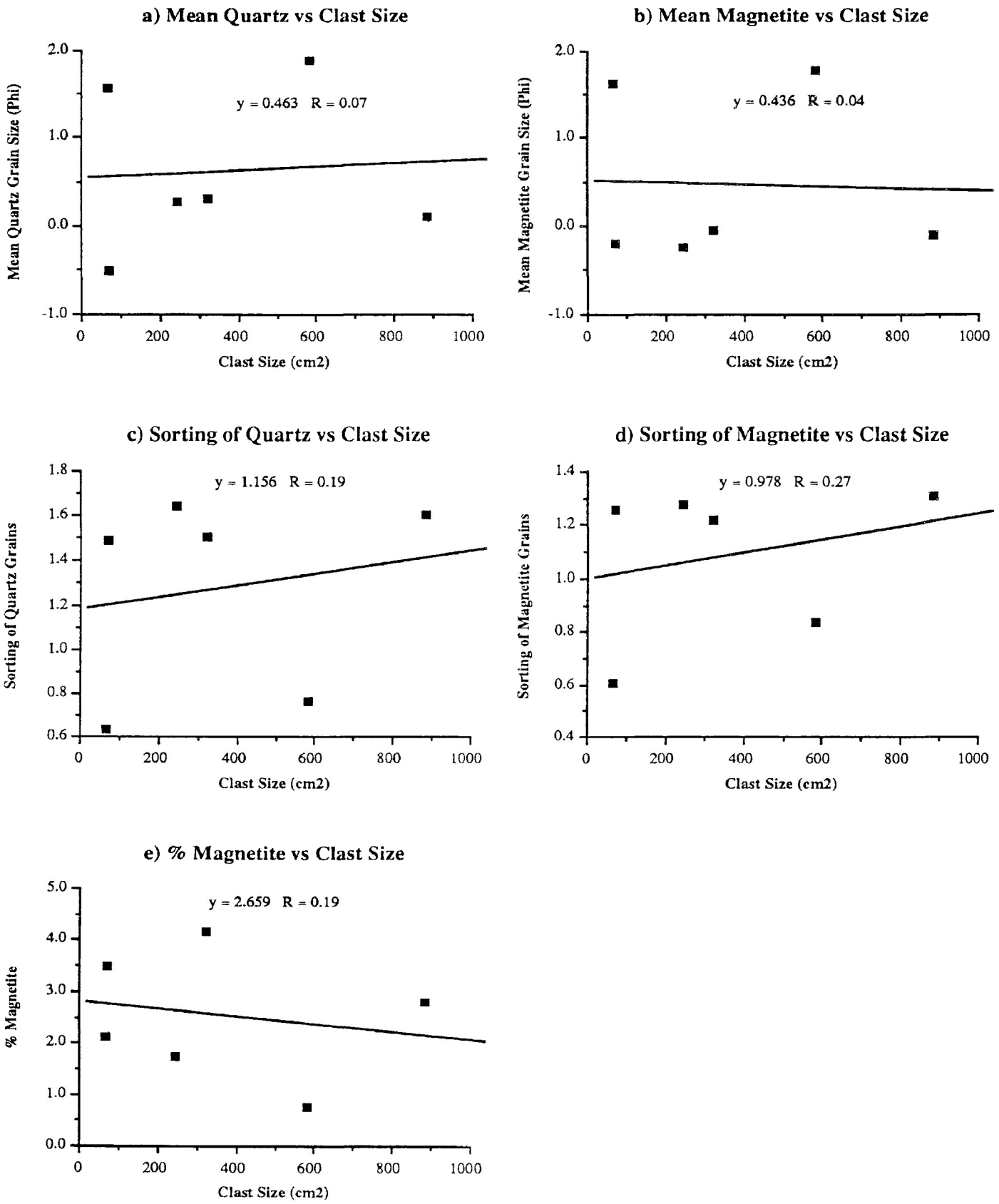

Figure 23. Scatter diagrams of variables derived from sediments sampled at Site 2 on the Agawa River in relation to clast size.

processes operating independently of clast size.

The highest concentration of magnetite was found in a sand deposit near the tail of the bar and was composed of well sorted, coarse-grained quartz and magnetite grains (see Table 8). In this bar, magnetite content doesn't appear to preferentially concentrate in either matrix or sand deposits but is relatively evenly distributed between both these two types of deposits.

4.2.4: The Mississagi River

The longitudinal bar examined on the Mississagi River was approximately 30 metres long and 10 metres wide; no vegetation was present (see Figure 24). A total of 12 samples of matrix and sand sediments were obtained (see Table 9).

The clasts were well imbricated and exhibited a slight decrease in size from bar head (medium boulders) to bar tail (large cobbles). The sorting of matrix sediments improved somewhat over the length of the bar and became slightly coarser grained. With depth, matrix sediments became better sorted but coarser grained (see Table 9).

Matrix samples were obtained from under and around clasts at the bar head, top, and tail. All samples were moderately well sorted but exhibited a decrease in mean grain size down the bar from very coarse- (bar head and top) to medium-grained (bar tail). An abandoned chute channel floor, composed of small boulders, contained quartz matrix sediments that were moderately well sorted and very coarse-grained. However, the magnetite fraction of the sample was better sorted than that of the quartz.

The majority of sand deposits sampled on the bar were composed of moderately well sorted and very coarse-grained quartz sediments obtained from a variety of settings (see Table 9). The magnetite fraction of these samples were all well sorted and similarly very coarse-grained. Surficial sands collected downriver of a large boulder near the bar tail were composed of quartz and magnetite sediments that were moderately poorly sorted and coarse-grained.

Figure 25 illustrates the interaction of mean grain size and sorting characteristics of quartz and magnetite in sediments deposited on this bar. Figure 25a plots the mean grain size of quartz against that of magnetite. This data set displays a similar significant trend as the previous three bars (Figures 16a, 19a, and 22a) indicating that throughout the bar, coarse magnetite grains will be deposited with coarse quartz grains. Figure 25b also exhibits a positive trend, although not as significant as the previous bars sampled (see Figures 16b, 19b, and 22b). This trend suggests that where magnetite grains are

Figure 24: The longitudinal bar studied on the Mississagi River (bar on left). The river channel is approximatey 125 metres in width.

a) Profile view of bar. Flow is from right to left.

b) View of bar looking upsteam. Flow is from top to bottom.

Table 9. Data from sediment analysis of samples collected from the Mississagi River.

Sample Number	Sample Site Description	Sediment Type	Mean Quartz		Sorting of Quartz		Mean Magnetite		Sorting of Magnetite		Percent Magnetite	Clast Size (cm2)
1	Bar head	Matrix	(VC)	-0.59	(MPS)	1.71	(G)	-0.10	(MWS)	1.10	4.02	173
2	Bar head (below)	Matrix	(VC)	-1.31	(MWS)	1.43	(G)	-1.20	(WS)	0.92	4.18	173
4	Under and around large clast	Matrix	(VC)	-0.82	(MWS)	1.31	(M)	1.20	(MWS)	1.00	5.48	280
7	Abandoned chute channel	Matrix	(VC)	-0.49	(MPS)	1.76	(VC)	-0.97	(MWS)	1.26	3.21	153
9	Bar top	Matrix	(VC)	-0.30	(MWS)	1.41	(VC)	-0.56	(MWS)	1.14	4.28	0
10	Bar tail	Matrix	(VC)	-0.91	(MWS)	1.47	(VC)	-0.99	(WS)	0.99	5.24	105
12	Bar tail (under large clast)	Sand	(M)	1.10	(MWS)	1.21	(M)	0.57	(MWS)	1.17	1.01	693
3	Downriver of large clast	Sand	(VC)	-0.65	(MWS)	1.05	(VC)	-0.81	(WS)	0.79	9.84	0
5	Low velocity zone behind clast	Sand	(VC)	-0.38	(MWS)	1.31	(VC)	-0.64	(WS)	0.94	5.49	280
6	Bar edge sand wedge	Sand	(VC)	-0.24	(MWS)	1.39	(VC)	-0.59	(WS)	0.87	6.77	0
8	Bar edge sand wedge (near tail)	Sand	(VC)	-0.64	(MWS)	1.36	(VC)	-1.13	(MWS)	1.10	5.91	0
11	Downriver of large clast	Sand	(C)	0.46	(MPS)	1.52	(C)	0.01	(MPS)	1.51	2.89	693

Grain Size Legend		Sorting Legend	
VF	Very Fine-Grained	VWS	Very Well Sorted
F	Fine-Grained	WS	Well Sorted
M	Medium-Grained	MWS	Moderately Well Sorted
C	Coarse-Grained	MPS	Moderately Poorly Sorted
VC	Very Coarse-Grained	PS	Poorly Sorted
G	Granule	VPS	Very Poorly Sorted

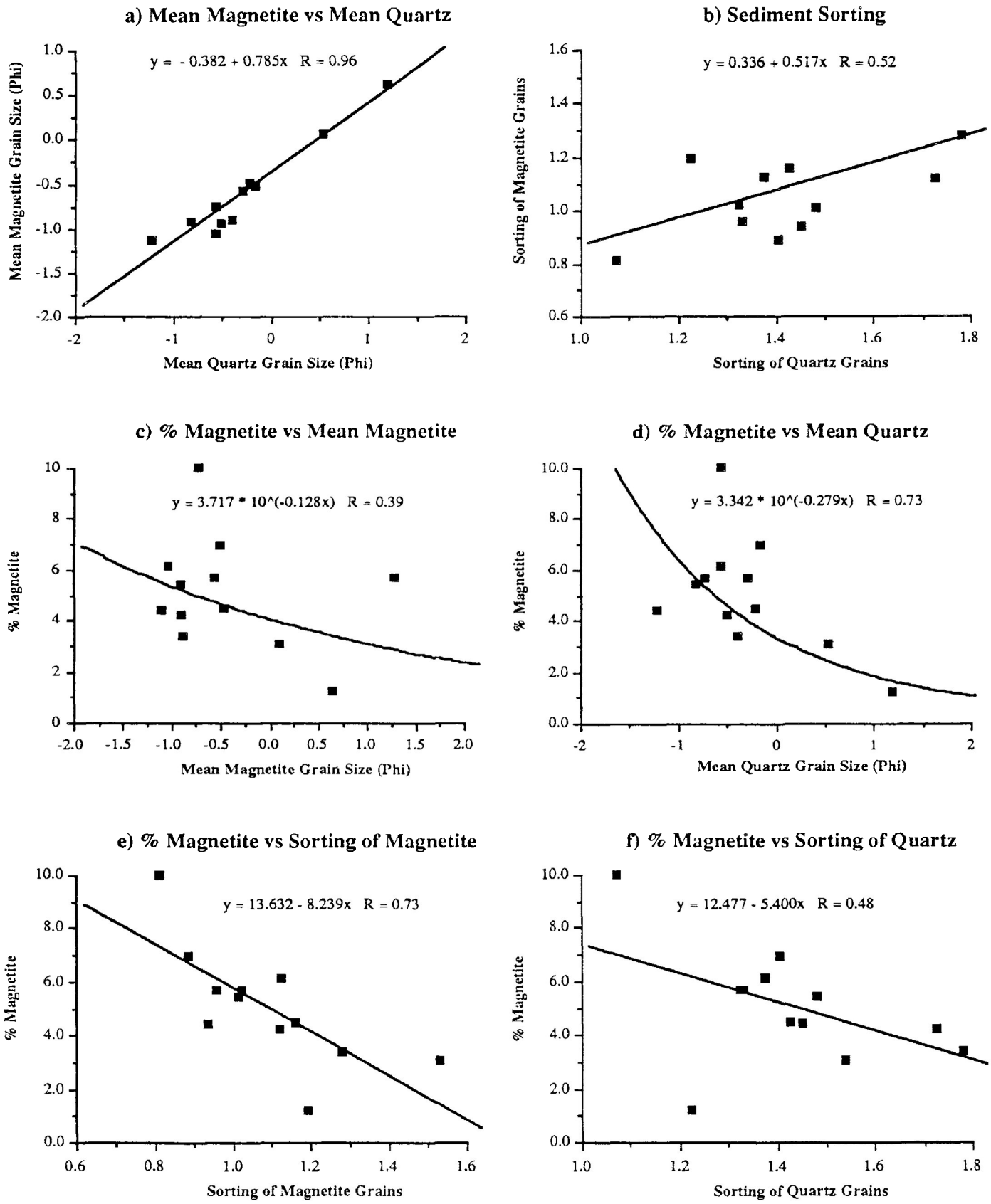

Figure 25. Scatter diagrams of variables derived from sediments sampled on the Mississagi River.

poorly sorted, quartz grains may be similarly poorly sorted. Figures 25c and 25d show that magnetite content increases in those areas of the bar that accumulate coarse magnetite and quartz sediments. However, Figures 25e and 25f show trends opposite those results previously obtained (see Figures 16e, 16f, 19e, 19f, 22e, and 22f). The results from the Mississagi bar indicate that as sorting improves, the percentage of magnetite in matrix sediments also increases.

Figure 26 illustrates how clast size affects average grain size, sorting, and magnetite content of matrix sediments. Figures 26a and 26b suggest that with an increase in clast size, quartz and magnetite matrix sediments become finer grained. Because clast sizes are generally larger at the bar head, matrix sediments deposited at this location will generally be finer grained than those that accumulate at the bar tail. Figures 26c and 26d suggest that there is little relationship between clast size and sediment sorting on this bar. Figure 26e shows that larger clasts are generally associated with matrix sediments containing lower concentrations of magnetite. This suggests that the downriver portion of the bar, typically containing the smaller clasts, will invariably have the highest percentage of magnetite.

The highest percentage of magnetite (9.84 weight percent) was obtained in a moderately well sorted and very coarse-grained sand lens deposited in a low velocity zone downriver of a large boulder. A second sand deposit that contained a high percentage of magnetite (6.77 weight percent) was obtained from a bar edge sand wedge composed of moderately well sorted, very coarse-grained quartz grains. Magnetite grains in both these two deposits were well sorted and very coarse-grained. Figures 25 and 26 suggest that the percentage of magnetite will increase in poorly sorted, coarse-grained sediments deposited in those areas of the bar where the smallest clasts accumulate. The highest percentages of magnetite are found in the sand deposits, not in the matrix sediments.

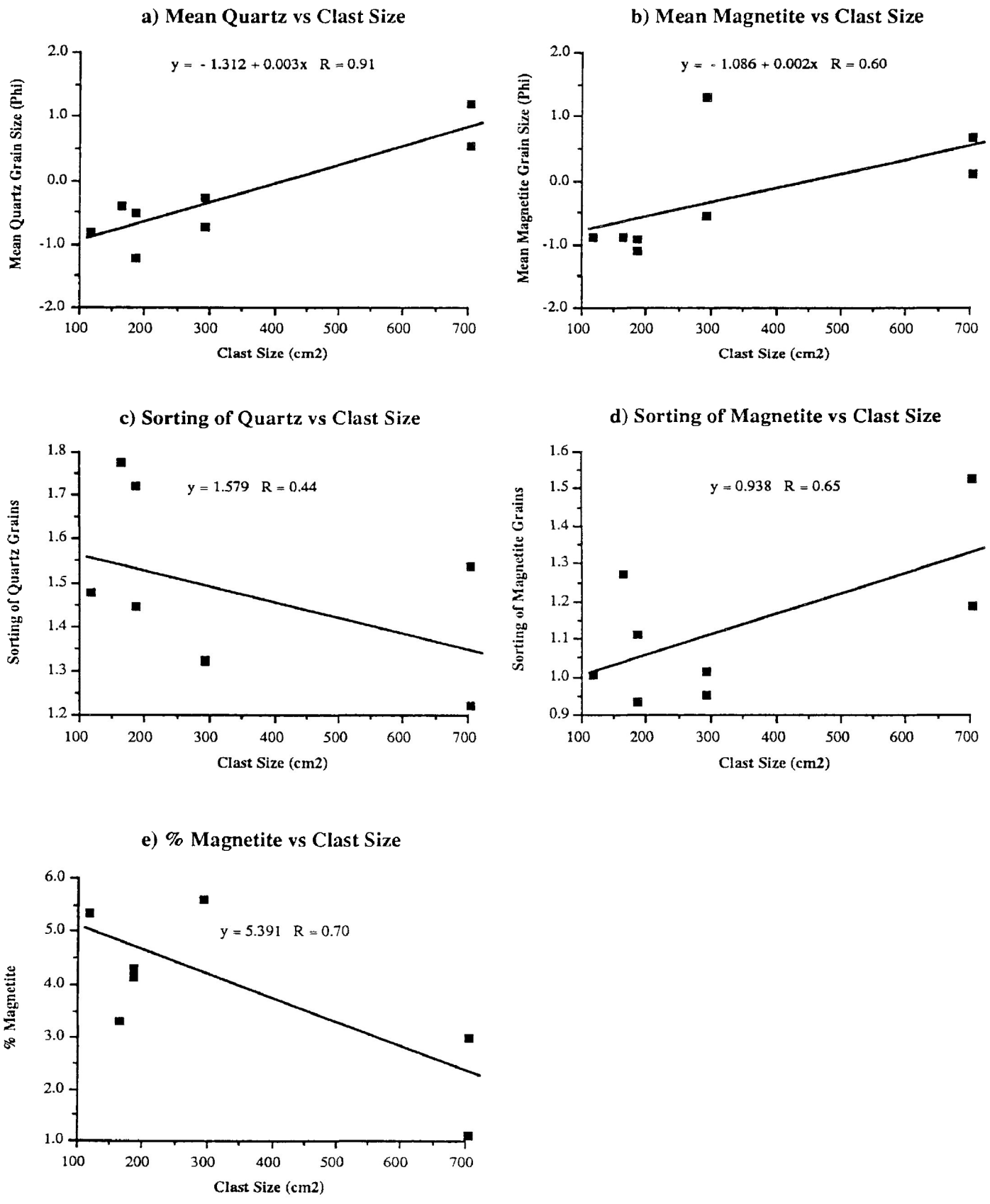

Figure 26. Scatter diagrams of variables derived from sediments sampled on the Mississagi River in relation to clast size.

CHAPTER 5: LABORATORY FLUME EXPERIMENTATION

5.1: Description

A total of 27 experimental runs were systematically conducted in a sediment-water recirculating laboratory flume to assess the processes responsible for the formation of depositional placer accumulations in coarse-grained braided river systems. Variables measured during each run included flow velocity, depth of flow, slope of the water's surface, and water temperature (see Figure 27). This data augmented controlled variables such as sediment grain size and clast size (see Appendix 1). The information was subsequently utilised to determine the parameters operating during each run including the slope of the energy gradient, Froude Number, and bed shear stress.

5.2: Discussion

The 27 experimental runs were divided into slow, medium, and fast velocities. The fastest and slowest velocity runs from each of these divisions were selected for further discussion (see Appendix 3).

Figure 28 illustrates that depth of flow measurements produced relatively similar results, regardless of the velocities attained. The runs showed only slight changes in depth over the length of the flume upstream of the bar. However, immediately upstream of the bar, a slight increase in depth occurred in most runs followed by a relative decrease in depth over the bar in a downstream direction. At the bar tail, all runs experienced a sudden significant increase in depth. This increase in depth is generally attributable to the presence of a hydraulic jump at this location.

Figure 29 shows that during the slowest runs (runs 19 and 17), velocity generally decreased over the length of the flume, especially over the gravel bar. The slowest medium velocity run (run 4) showed no increase over the length of the flume upstream of the bar. However, immediately in front of the bar head, the velocity slowed somewhat and then suddenly increased. At the end of the bar, a sudden decrease in velocity occurred. The fastest medium (run 23) and fastest overall runs (runs 24 and 22) produced similar results whereby velocity increased slightly down the flume, followed by a slight to moderate decrease immediately upstream of the bar, an increase in velocity over the bar, and a sharp decrease immediately after the bar at the site of a hydraulic jump.

Froude numbers were calculated from the data obtained from these runs and once plotted, produced graphs understandably similar to the velocity graphs (compare

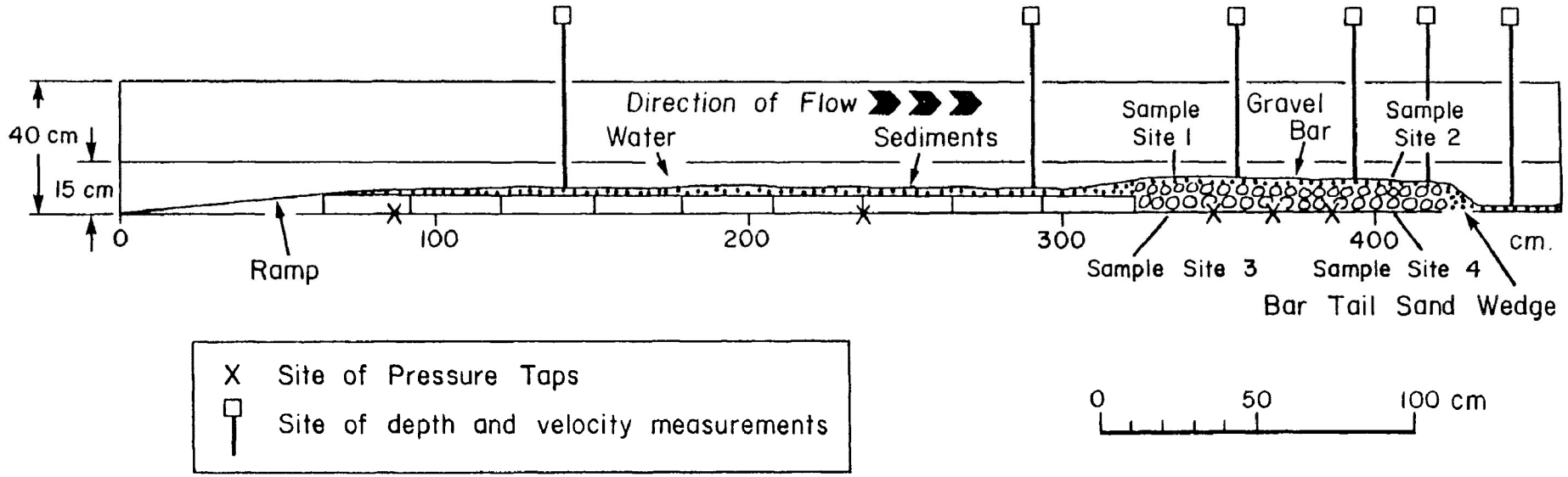

Figure 27. Diagram of laboratory flume setup.

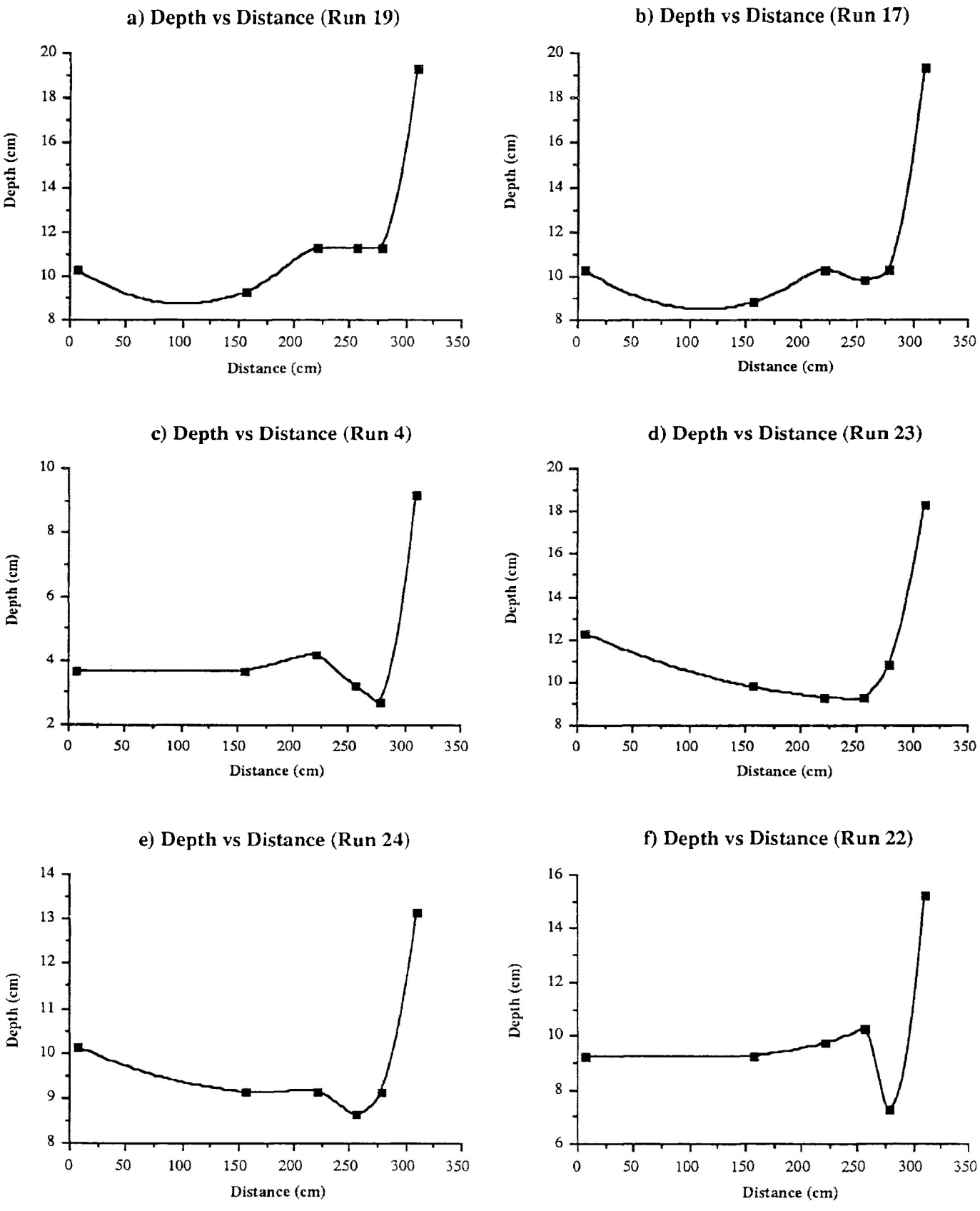

Figure 28. Scatter diagrams of the change in depth of water over the length of the flume.

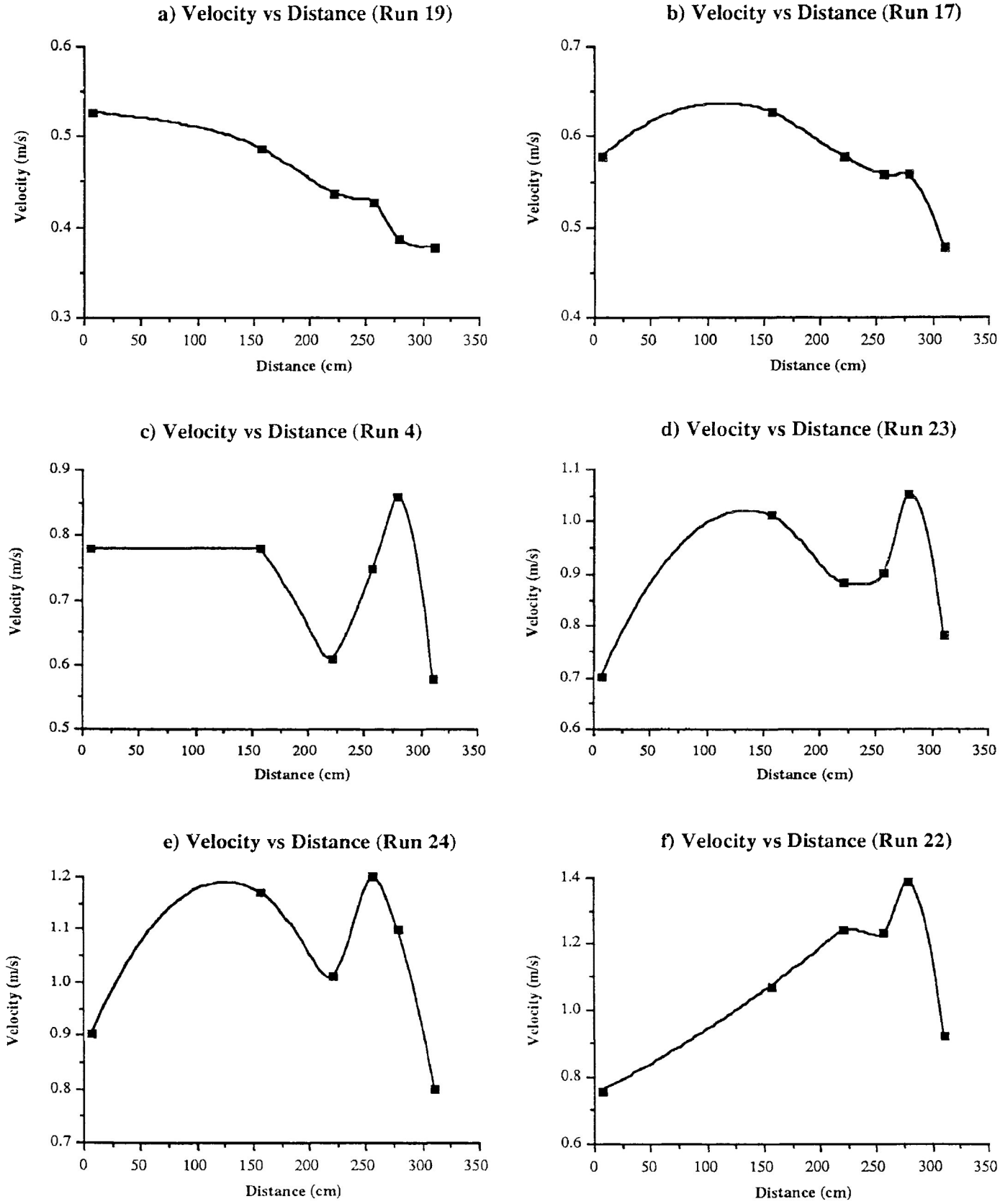

Figure 29. Scatter diagrams of the change in water velocity over the length of the flume.

Figures 29 and 30). The development of a hydraulic jump at the bar tail, a substantial increase in depth, coupled with a sudden decrease in velocity, typically resulted in a change from supercritical to subcritical flow over a very short distance. With this sudden change, a significant loss of energy occurred at this site.

The third variable measured during the experimental runs was the slope of the energy gradient. A comparison of Figures 31 and 32 with Figure 28 indicates that both slope and bed shear stress generally increase with increasing depth.

5.3: Sediment Movement During Experimental Runs:

A full range of velocities (0.41 to 1.27 m/s) were attained during the experimental runs. At the velocities reached, the fine-grained and some medium-grained runs clearly demonstrated density segregation (see Figure 33). However, coarse-grained runs showed little to no correlation with the independent variables used at the velocities obtained.

Prior to each run, a relatively homogeneous mixture of detrital sediments composed of quartz, pyroxene, magnetite, lead grains, and lead pellets, were evenly distributed upstream of the bar. Immediately following the start of each run, segregation due to grain density differences quickly began (see Figure 33). During the finer grained runs, lighter quartz grains on the upper surface became immediately entrained during higher velocity runs, leaving behind a progressively enriched heavy mineral (predominantly lead) lag deposit. Following the removal of the majority of lighter grains, a relatively thick, heavy mineral rich layer, composed predominantly of magnetite, lead grains, and lead pellets blanketed the channel bottom, which in turn, prevented further erosion of underlying lighter grains not yet removed. Most heavy mineral transport occurred only once the channel bottom had become thickly armoured by a heavy mineral rich lag deposit. Figure 34 shows the bed configuration during the initiation of heavy mineral transport on a heavily armoured channel bed. The transport of heavy minerals was typically in the form of isolated, low amplitude, dune-like features that left trailing lead streaks as the bedform advanced down the flume (see Figure 35). These bedforms resemble the parabolic sand dunes typically associated with aeolian environments.

It became apparent that two different depositional processes were operating during the experimental runs. The first depositional process operating in the flume which resulted in the deposition of sediments within the bar was that of suspension rain-out. During this process, grains that were winnowed away from further upstream

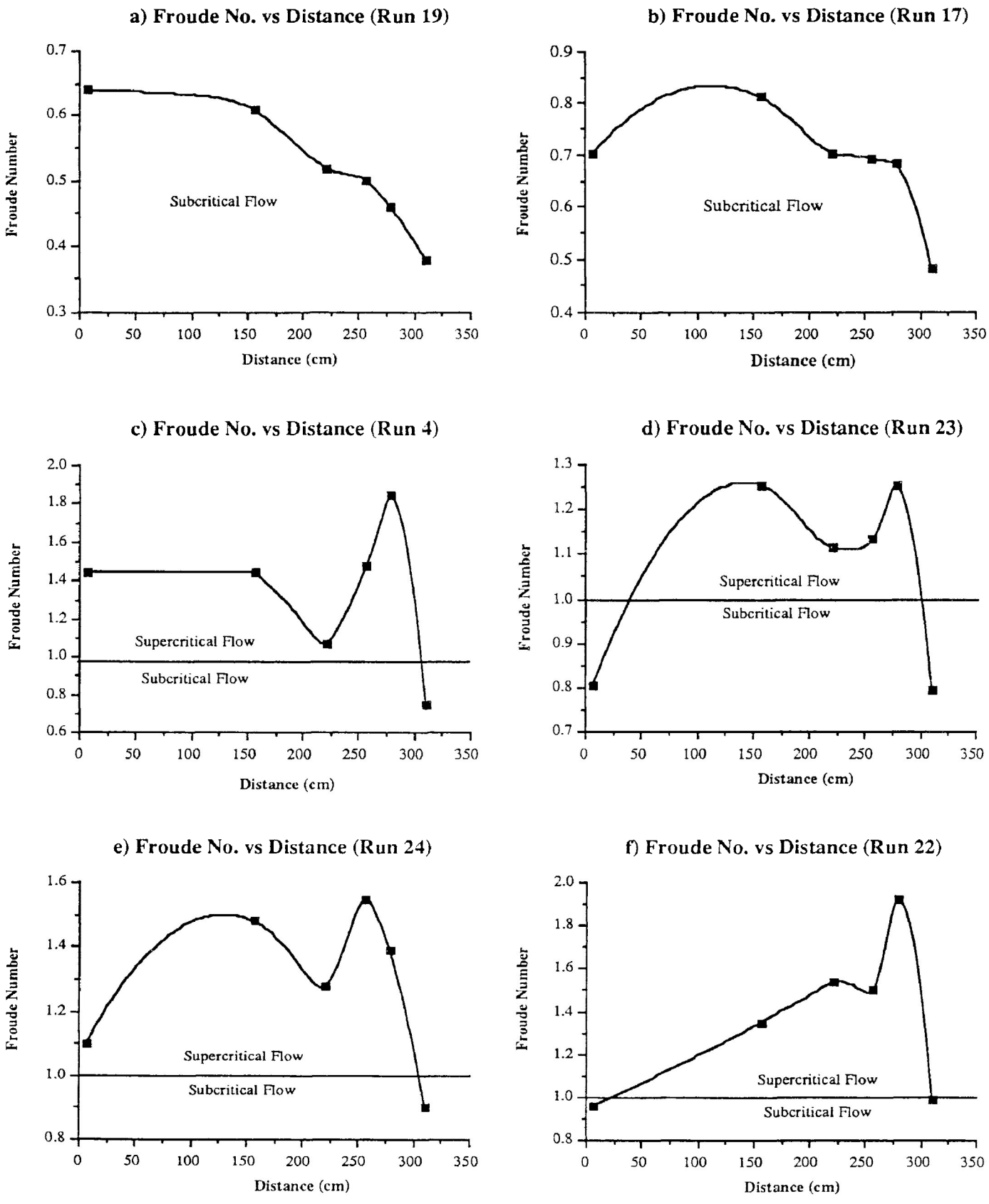

Figure 30. Scatter diagrams of the change in Froude Number over the length of the flume.

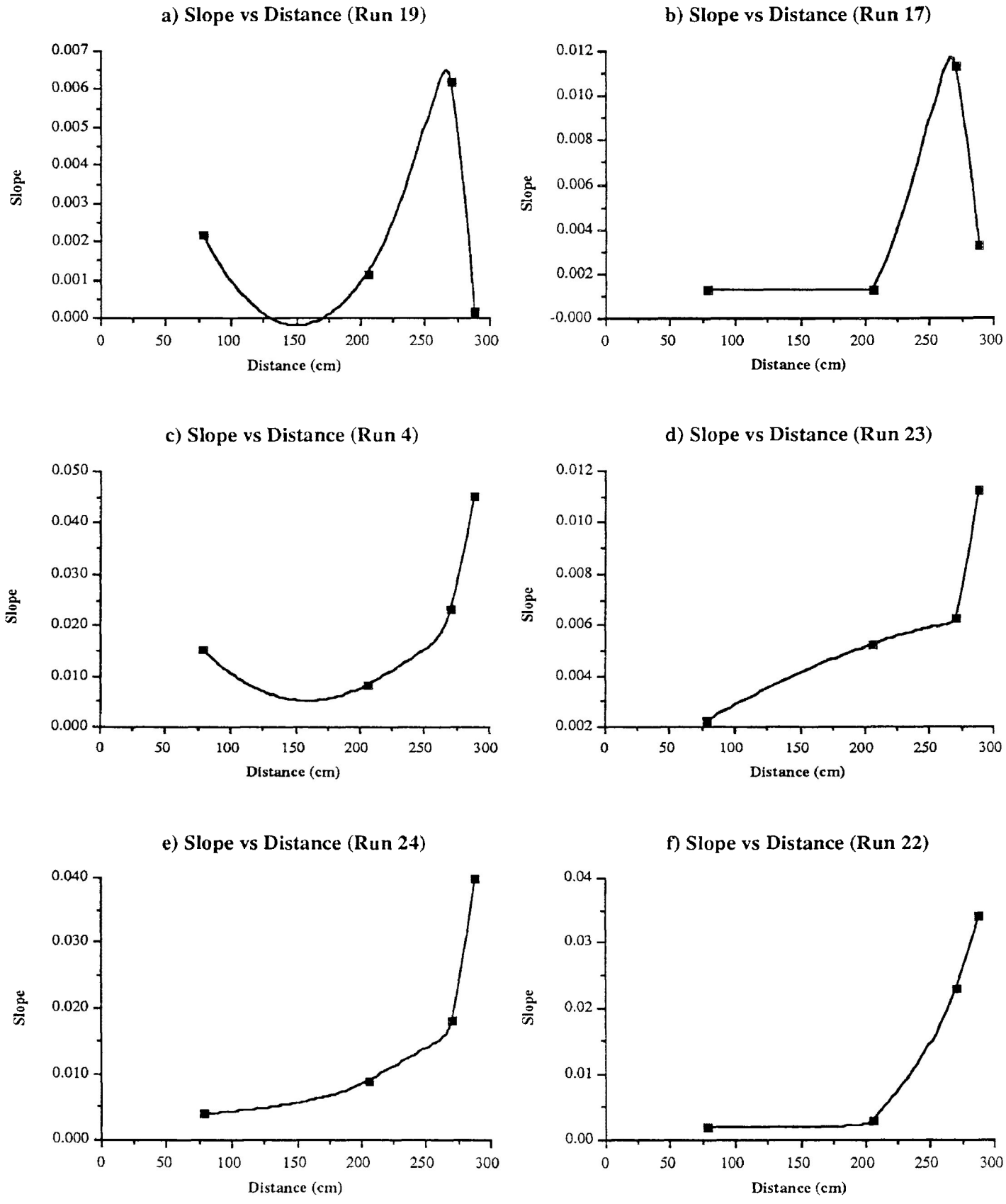

Figure 31. Scatter diagrams of the change in slope over the length of the flume.

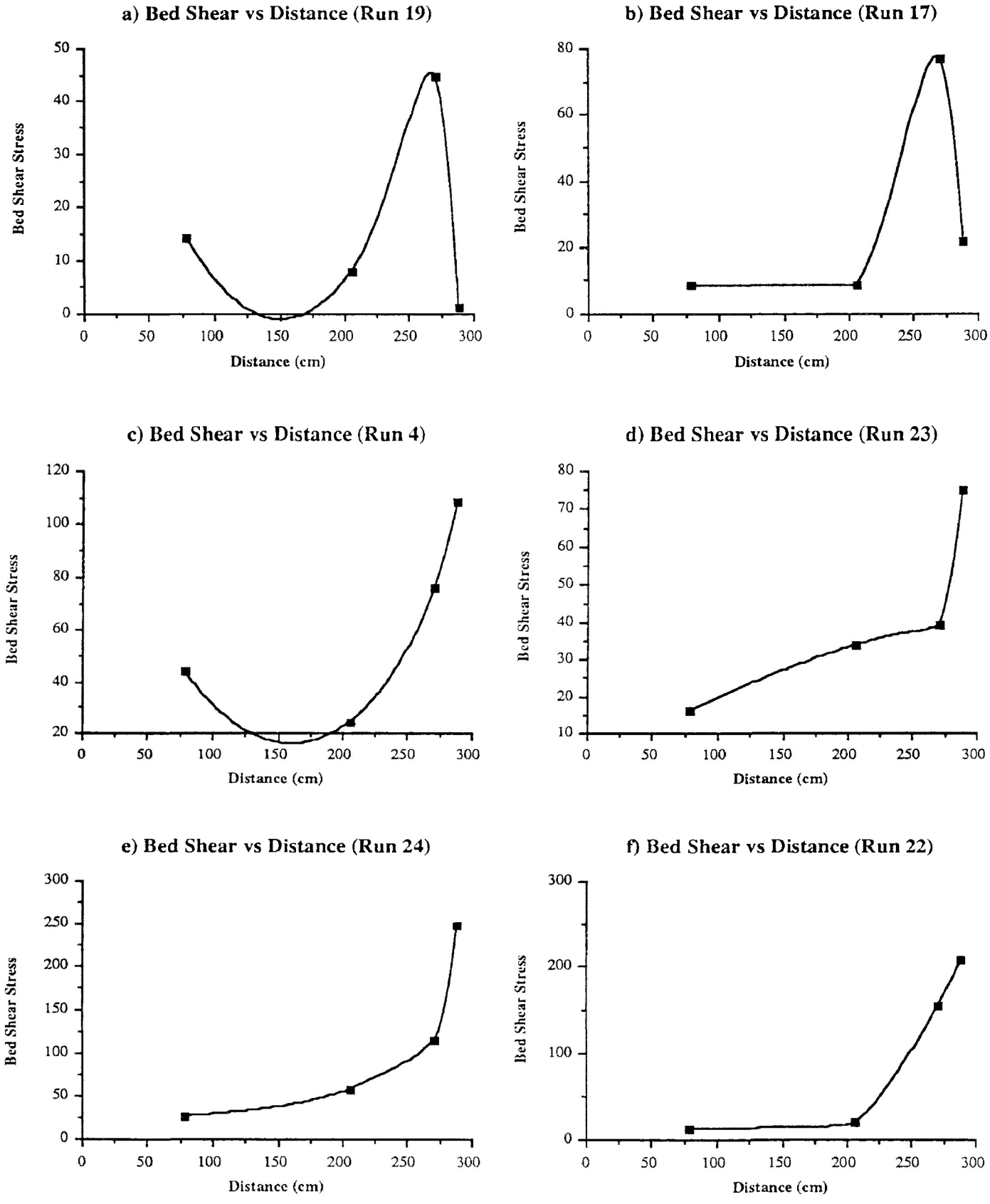

Figure 32. Scatter diagrams of the change in bed shear stress over the length of the flume.

Figure 33: Heavy mineral concentration (lighter coloured material) developed on the stoss side of lunate and linguoid dunes in the flume. Flow is from right to left.

Figure 34: Bed configuration during the initiation of heavy mineral transport (lighter coloured material) on a heavily armoured channel bed in the flume. Flow is from right to left.

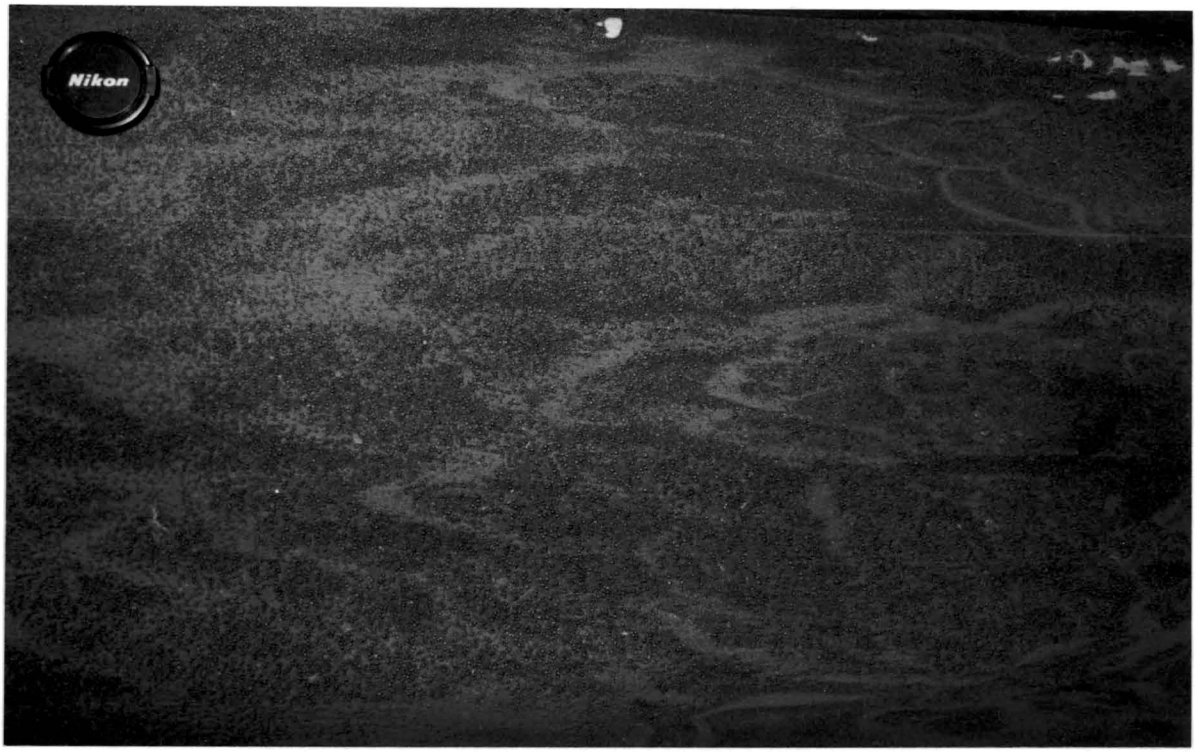

Figure 35: Low amplitude detrital lead bedforms (lighter coloured material) with trailing lead streaks in the flume. Flow is from right to left.

were deposited between clasts due to a loss in flow competence within the fluid in contact with the clasts. Once separated from the main flow, individual grains would simply settle out, filtering their way down to the base of the open framework gravel bar (see Figure 36). This was the dominant process operating during higher velocity runs.

The second depositional process occurred as a result of traction and saltation bed load transport and will be referred to as micro-delta progradation. This process resulted in the deposition of sediment by an advancing avalanche face where entrained grains were transported very close to the sediment/water interface. Grains were swept over the crest of the prograding avalanche face and either rolled or slumped to the base of the slope at the angle of repose. This process typically resulted in the eventual filling of the bar as the bedform migrated down the flume. Once the bar had been completely filled, a continuation of this process often resulted in the formation of a bar tail sand wedge (see Figure 37). Micro-delta development was found to generally predominate during most low velocity runs.

A combination of the two previously described processes occurred during several of the runs. Grains travelling in suspension would settle out immediately downstream of the advancing avalanche face due to the suspension rain-out process previously discussed. These grains would then blanket the base of the bar, often filling the open framework gravel somewhat before eventually being buried by the prograding micro-delta avalanche face (see Figure 37). Grains were also observed flowing through the bar and accumulating in low velocity zones behind clasts or immediately downstream of the bar. Lower velocity runs generally resulted in very low concentrations of heavy minerals accumulating within the bar as the erosive energy necessary to transport them from further upstream was generally not present under these conditions. The majority of heavy minerals sampled from the bar following such a run were generally retrieved amongst surficial sediments. However, during higher velocity runs, although the processes outlined above were operating which segregated lighter grains from heavier grains, a larger portion of heavy mineral grains were able to be transported down the flume and subsequently deposited in the bar, both as surficial sediments and as matrix.

The average grain size of the quartz sand used in the flume during a particular run appeared to exhibit some control over the amount of heavy minerals deposited in both open framework gravels and surficial sediments. Table 10 shows the average percentage of heavy minerals which accumulated in surficial and matrix sediments during the runs and is separated into fine-, medium-, and coarse-grained runs.

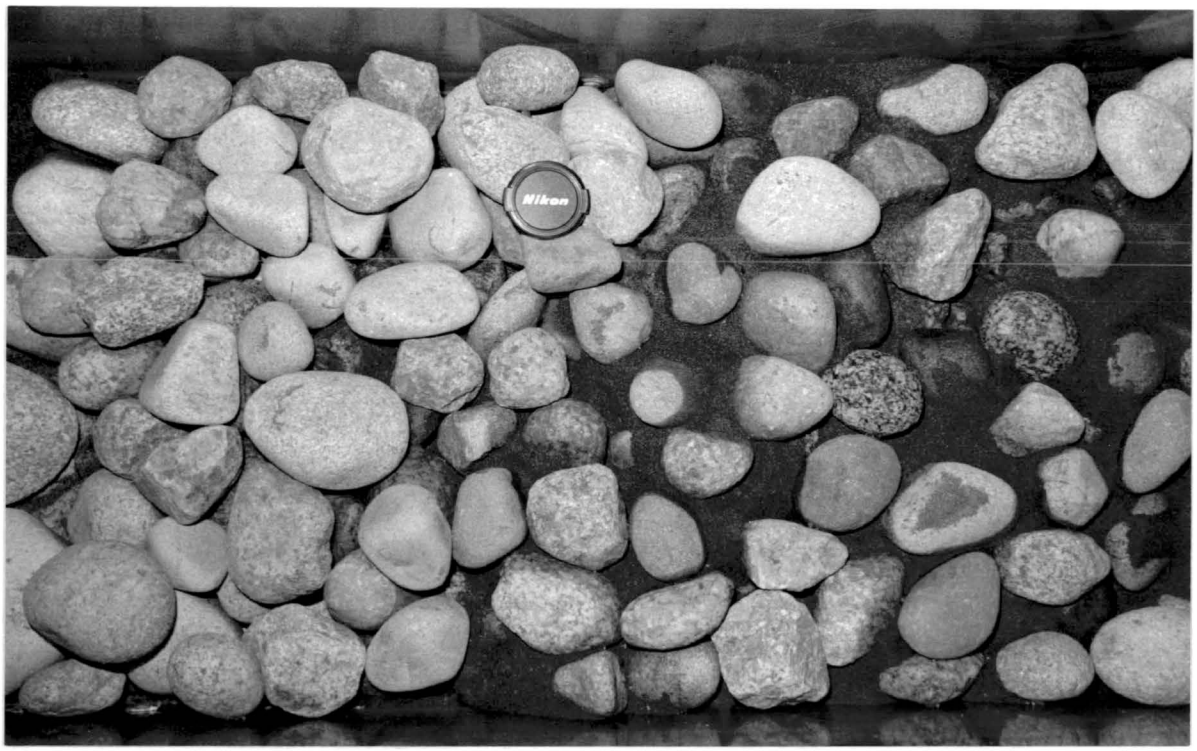

Figure 36: Gravel bar following an experimental run with the majority of sediments deposited from suspension rain out. Flow is from right to left.

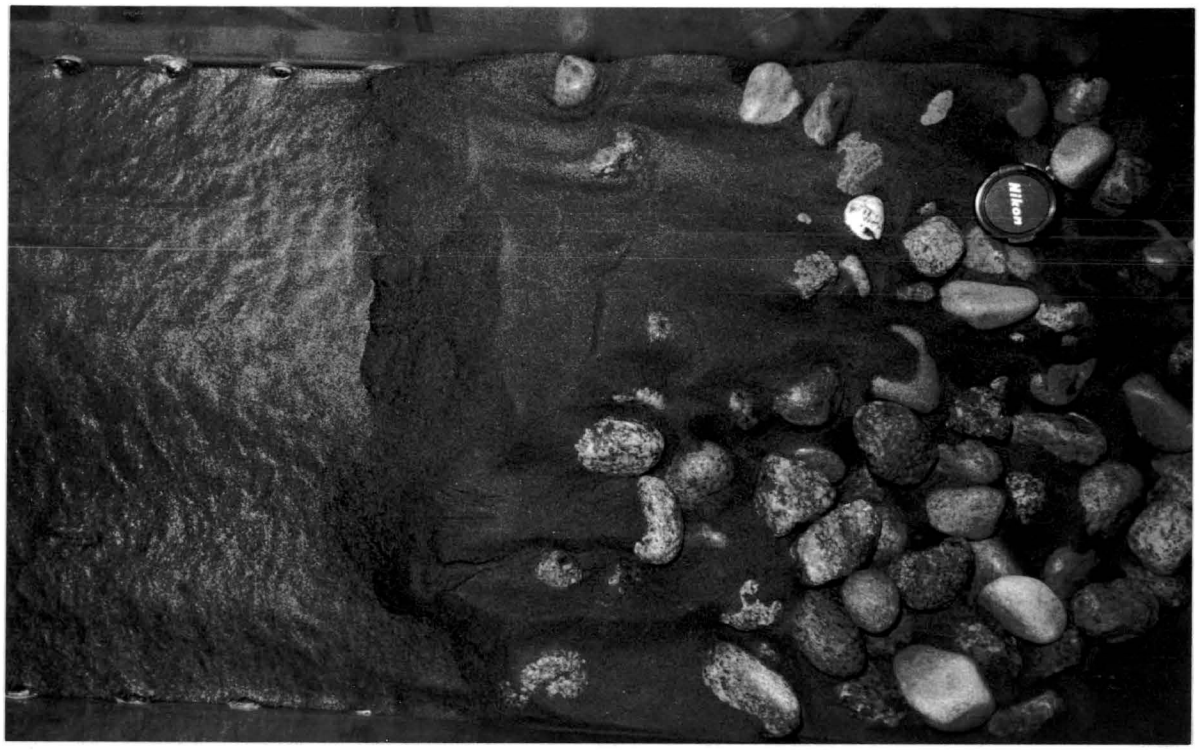

Figure 37: Photograph of tail section of gravel bar following an experimental run showing an avalanche face prograding over a previously sedimented suspension rain out deposit in the flume. Flow is from right to left.

Table 10: The percentage of heavy minerals that accumulated during flume experimentation.

SAMPLE	% Pyroxene After Run	% Pyroxene Enriched (+) Depleted (-)	% Magnetite After Run	% Magnetite Enriched (+) Depleted (-)	% Lead Grains After Run	% Lead Grains Enriched (+) Depleted (-)
Surficial Fine	46.77	+09.70	8.68	+4.56	17.33	+06.56
Surficial Medium	46.17	+16.88	8.72	+3.65	15.82	+09.12
Surficial Coarse	17.09	- 01.64	8.19	+3.01	23.75	+12.41
Matrix Fine	41.26	+04.19	3.38	- 0.74	2.44	- 08.33
Matrix Medium	29.74	+00.45	4.62	- 0.45	0.41	- 06.29
Matrix Coarse	12.10	- 06.63	3.90	- 1.28	0.55	- 10.79

It is evident from the values outlined above that the percentage of heavy minerals also varies significantly between surficial and matrix sands, regardless of the grain size present. The average pyroxene content was 35.93% in surficial sands but only 27.70% in matrix sands. The magnetite content was 8.52% in surficial sands but only 3.97% in matrix sands. The average lead grain content was 18.90% in surficial sands but only 1.58% in matrix sands. These figures clearly indicate that the highest percentage of heavy minerals are associated with surficial sediments and not matrix sediments. Data also indicates that the difference between the average heavy mineral content found in surficial sediments compared to that found in matrix sediments will increase with increasing density. This suggests that denser detritus are more likely to be deposited amongst surficial sediments than matrix, whereas less dense detritus are more likely to be vertically distributed throughout the bar.

It is also apparent that clast size exerts some control over the amount and type of heavy minerals deposited. The average content of detrital lead deposited amongst surficial sands is 64% higher in gravel bars constructed of small sized pebbles than those bars constructed of larger sized cobbles. This trend becomes somewhat more pronounced with matrix sediments. The average content of detrital lead grains accumulating as matrix between small clasts is 76% higher than those deposited as matrix between larger clasts (one data set anomaly removed). However, the results obtained from the analysis of magnetite and pyroxene detrital grains suggests that this trend is only true for the denser lead grains. The amount of magnetite and pyroxene deposited in the gravel bar showed very little correlation with clast size. The average content deposited in both surficial and matrix sediments was virtually identical in small pebble bars to that of large cobble bars.

Of the 27 experimental runs conducted, only eight were found to have accumulated lead pellets in the bar. The highest concentration of lead pellets was found

to have accumulated in surficial sediments during the fastest velocity runs in gravel bars constructed of small pebble sized clasts. A very small percentage was also found deposited amongst matrix sediments during these particular runs. Results suggest that there is very little correlation with sand grain size, however, clast size and velocity do appear to have been the two major controls on lead pellet movement and subsequent deposition.

5.4: Discussion of Graphs Produced from Experimental Data.

A total of 126 scatter diagrams have been produced from the data obtained from the experimental runs which depict the interrelationships of a variety of controlled factors used in the flume. The graphs have been divided by site of deposition, i.e. either surface sediments or as matrix. The graphs have also been further separated by grain size, i.e. fine, medium, and coarse sand. Each graph also contains either a best fitting linear or exponential curve with correlation coefficients plotted.

By plotting the various heavy minerals against one another, several interesting relationships were identified. The percentage of both magnetite and pyroxene showed varying positive correlations suggesting that as the percentage of one heavy mineral increased, a corresponding increase occurred with the other (see Appendix 2, page 108). The percentage of lead was also plotted against the percentage of pyroxene. These graphs generally suggest that there exists a negative relationship in that as the percentage of lead increases, the percentage of pyroxene decreases amongst surficial sediments, however, matrix samples show no correlation (see Appendix 2, page 109). The percentage of lead was also plotted against the percentage of magnetite. Most graphs demonstrated little correlation between these two variables, however, fine and medium surficial data show that a similar negative relationship exists whereby the percentage of lead increased with decreasing magnetite content (see Appendix 2, page 110). The data also show that in surficial sediments, velocity exerts some control over average grain size and the sorting of fine- and medium-grained quartz sediments. There is little relationship between these variables in matrix sediments.

The remaining graphs in Appendix 2 (pages 111 to 128) describe various relationships between pyroxene, magnetite, and lead against several controlled parameters during flume experimentation. Each is broken down by grain size and by site of deposition, i.e. surficial or matrix sediments. Coarse sediments demonstrated no correlation with the controlled parameters as the energy required to effectively transport these sediments in suspension was not fully reached. However, several interesting

relationships became apparent during the fine- and some medium-grained experimental runs. The remaining discussion will, as a result, focus primarily on the graphs produced from the finer grained runs.

An examination of graphs plotting the percentage of pyroxene, magnetite, and lead grains against velocity (see Appendix 2, pages 113, 119, and 125) reveals there was little relationship between these parameters. However, the percentage of pyroxene and magnetite in fine-grained surficial sediments decreased with increasing velocity (see Appendix 2, graphs 113a and 119a) whereas the percentage of pyroxene actually increased in medium-grained matrix sediments under increasing velocities. The percentage of lead which accumulated amongst surficial and matrix sediments showed a reversal of these trends by demonstrating a slight increase during increased flow velocities (see Appendix 2, graphs 125a and 125b). However, an examination of the flume data in Appendix 1 reveals that the highest velocity runs, in combination with gravel bars composed of pebble-sized clasts, produced the highest concentrations of lead. Clast size therefore also appears to influence the amount of heavy minerals being deposited in gravel bars.

The percentage of pyroxene and magnetite deposited was found to decrease in poorly sorted, finer grained surficial and matrix sediments (see Appendix 2, pages 115, 116, 121, and 122. However, the percentage of lead deposited increased slightly in more poorly sorted fine-grained sediments (see Appendix 2, page 127).

CHAPTER 6: CONCLUSIONS

6.1: Discussion of Matrix Infiltration Processes - a literature review Two processes can operate to form matrix in gravelly longitudinal bars: 1) matrix sedimentation during active periods of bar growth, or 2) matrix infiltration after an open framework bar has formed. Most work to date has concentrated on the latter. There have been a number of papers written over recent years pertaining to the process of sediment infiltration into coarse alluvial gravels (see Cary, 1951; Einstein, 1968; Minter and Toens, 1970; Dyer, 1970; Meehan and Swanston, 1977; Beschta and Jackson, 1979; Carling, 1984; Frostick et al, 1984; Slingerland and Smith, 1986; etc.). Much of this research has centred around studying how the process of fine sediment infiltration into open framework gravels directly affects stream habitat with respect to the natural spawning beds of fish (Einstein, 1968; Meehan and Swanston, 1977; Beschta and Jackson, 1979; and Carling, 1984).

The effect of an increase in the amount of fine sediment transported by a fluvial system as a result of man induced changes in the upper watershed through logging, placer mining, or urbanisation typically results in increased deposition in open framework gravels. The filling or clogging of open pore spaces in gravel reaches of rivers as a result of disturbances upstream directly affects the spawning potential of the river downstream. This accounts for the amount of research that has centred on fluvial sedimentation processes and how it adversely affects the natural spawning beds of fish in the gravel reaches of modern river systems.

Einstein (1968) noted that an increase in the deposition of fine-grained sediments results in the clogging of pore spaces in gravel bars. Once clogged, a river's ability to remove or flush out these sediments by water percolating through pore spaces in the bar is significantly reduced. He also explained how silt sized particles being transported in suspension over a gravel bed typically results in the clogging of open framework gravels from their base upwards. However, the upper most layer of gravel often remains relatively free of sediment due to the higher turbulence associated with this level. Einstein (1968) hypothesised this process of sediment infiltration and matrix formation as follows:

> The main point of a possible theory for this process of deposition is the assumption of a surface or plane of demarcation somewhere near the surface of the bed with the following characteristics: 1) Particles above this plane are a part of the suspended load and are not affected by the bed (therefore, they are governed by the laws of suspension); and

> 2) there is no exchange of fluid or water through this plane; particles can only settle through it and will do so if they are in a particular location just above the surface of the bed. Once they have started to settle through this plane they cannot be affected by turbulence any more, they are caught and must settle out. (p.1200).

This process helps to explain how matrix formation is dependent upon the size of the material in transport. A change in the energy in the river system, typical of flood or waning flows, results in the development of a graded matrix deposit as sediments accumulate in gravel traps on the river bed. Carling (1984) states: "Turbulent resuspension of sediment prevented deposition in a surface layer of gravel of thickness approximately equal to the mean grain size of the gravel" (p. 263). This supports a similar view held by Einstein (1968). However, Dyer (1970) explains how during extremely turbulent flows, water will penetrate the pore spaces of gravel beds, flushing out most finer grained sediments previously deposited. He also states that this process is particularly true while the gravel is still in transport and not yet sedimented to the river bed. During less turbulent flows, finer grained sediments are more likely to infiltrate the open pore spaces contained in the gravel bar (p. 619). Cary (1951) further suggests that open framework gravels are kept free of sand by vortex action produced by the turbulence created over the gravel bar.

Meehan and Swanston (1977) studied the relationship between fine sediment accumulation rates with that of gravel shape and stream discharge. They also examined the effect of gravel shape and how it affected the survival of salmon eggs. They suggest that gravel shape influences short term sediment accumulation in gravel beds (p.16). They concluded: "At very low flows...round gravels tend to accumulate more fine sediments than angular gravels. This relationship is reversed as flow rates increase...and angular gravels tend to accumulate more sediment." (p.16).

Beschta and Jackson (1979) also examined the intrusion of fine sediment into gravel beds. Using flume experimentation, they observed how sediment generally became entrapped in the pores found in the upper 10 centimetres of a gravel bar. This layer of sediment subsequently acted as a barrier which restricted further infiltration into the framework of the bar during later flow events. Beschta and Jackson (1979) state: "An analysis of flow variables showed that flow conditions...significantly affected intrusion amounts, possibly by influencing the rate and depth of formation of the sand seal" (p. 204). Further experiments using finer grained sediments produced an increase in the overall depth of infiltration into the gravel. Based on these results, they suggest: "...particle size, and not hydraulic variables, may have a more important influence on the

total amount of intrusion" (Beschta and Jackson, 1979, p.204).

Frostick et al (1984) attribute the infiltration of fine sediments into coarse alluvial gravels to several factors. These include "...the rate of supply and the size characteristics of potential matrix sediment, the size and shape of the framework pores, and the cross-sectional morphology of the channel and its affect on stream flow. The interaction of these variables dictates a complex pattern of matrix development and helps to explain the wide range of gravel fabrics..." (p. 964). They also suggest that fine matrix sediments are derived from both bed load and suspended load.

Fraser (1935) discusses how the forces necessary to transport coarse gravel in a river will also be able to transport large volumes of finer grained sediments through a combination of bed load, saltation, and suspension. He points out however that despite a river having the potential to move a large range of clast and sediment sizes, it is rare to find a situation where the river has sedimented this range of material at the same time. He further states:

> "Small changes in velocity will thus result in great variations in the size of material moved. A 7 per cent increase in velocity would increase the size of particles moved by 50 per cent; a 12.25 increase in velocity, 100 per cent; and a 30.75 per cent increase, 400 per cent. In a gravel which varies from pebbles 10 inches (25.4 cm) in diameter to sand...1 mm in diameter, the actual variation is 250 times or 25,000 per cent. Accordingly, the velocity in a stream carrying such pebbles would necessarily be decreased 60 per cent before the 1 mm sand could be deposited" (p. 987).

Sudden reductions in velocity necessary to deposit such a large range of detritus typically occurs on beaches and on floodplains, but as Fraser (1935) points out: "...it seems unlikely that such violent changes in the current velocity always occur when coarse material is deposited" (p. 987). As a result, he suggests that gravel and finer grained sediments are rarely deposited at the same time. Therefore, gravel bars would be expected to accumulate on the channel bottom virtually free of all finer grained sediments which would later settle into the voids found in the open framework gravels by subsequent infiltration during waning flows. This infiltration process would typically result in a graded matrix deposit (see Fraser, 1935, for a complete discussion).

6.2: Discussion of Field Data

In the natural systems examined in this study, matrix material associated with finer grained gravels was found to contain coarser grained and more poorly sorted

sediments than matrix associated with larger clasts at the bar head. These data strongly indicate the following scenario: larger sized clasts deposited at the upstream portion of the gravel bar reflects deposition during highly turbulent flow conditions which kept all finer grained sediments in transport. During these high discharge events, both light and heavy sediment remained in suspension. As a result of the highly turbulent flow conditions acting on the bar head, this sediment was not able to be deposited at this location. However, with the development of lower energy conditions downstream, heavier detrital sediments were then able to accumulate together with finer clasts through the process of hydraulic equivalence as the gravel bar was forming. Only with a reduction in river discharge are less dense sediments able to infiltrate the remaining open pore spaces located between the larger clasts previously deposited at the bar head. This process typically results in the accumulation of finer grained and better-sorted sediments in these open framework gravels. In the river systems studied, these processes generally resulted in higher percentages of heavy detrital sediments being deposited with finer grained gravels. This scenario as outlined above best explains the data obtained from the Jackpine, Agawa, and Mississagi River study. Data collected from the North Saskatchewan River also supports the above proposed sequence of events. An interpretation of all graphs indicates that the highest percentage of magnetite was generally deposited with coarse to very coarse-grained, poorly sorted matrix sediments that were deposited in areas of the bar where the smallest clasts accumulated. In the longitudinal bars studied, this resulted in heavy mineral content generally increasing toward the tail of the bar. In the North Saskatchewan, despite much lower heavy mineral contents, the same trends exist whereby the highest percentage of heavy minerals are deposited with the smallest clasts found on the bar. Matrix sediments, where present, often showed grading in the upper few centimetres suggesting final pore-space infilling during waning flows.

Of the bar edge and bar tail sand wedges sampled, they were generally composed of well to very well sorted, medium- to fine-grained sands. Some of these deposits were gradually formed as a result of the process of matrix flushing (or washing) where water seeping into the bar flows through pore spaces in the gravel framework entraining and flushing out finer grained sediments which are subsequently deposited upon emergence from the bar (see Figure 6). These fine-grained sediments accumulate in deep, low energy pools of water along the edges of abandoned chute channels or the sides and tails of longitudinal bars. This flushing process can result in the matrix adopting a post-depositional reverse grading as fine sediments are removed from the

upper matrix and either deposited deeper in the framework or along the periphery of the bar. This process presents an alternative mode of formation of bar edge and bar tail formation and matrix reverse grading. Bar edge and bar tail sand wedges are thought to form as a result of sediments being swept over the surface of the bar and subsequently deposited along the sides and tails of bars where the depth of water typically increases and the velocity decreases. Several bar edge and tail sand wedges sampled on the North Saskatchewan River were actually observed forming as a result of river water seeping into the bar and flushing out finer grained sediments previously deposited during turbulent flow conditions (see Figure 6). This process presents an alternative mode for formation of bar edge and bar tail formation and matrix reverse grading. Following an analysis of all samples collected in the field, relatively low concentrations of heavy minerals were found to be associated with both bar edge and bar tail sand wedges.

6.3: Discussion of Flume Data

Detrital sediments used in the flume were deposited by one of two mechanisms: 1) suspension rain out, and 2) avalanche face progradation. Sediments deposited by avalanche face progradation were found to contain significantly higher concentrations of heavy minerals than those deposited through the process of suspension rain out. This phenomenon was shown to be the result of the processes operating at the site where sediment was being eroded.

During the early erosive stripping of the medium- and coarse-grained sands, heavier detrital sediments often formed an erosive lag on the bottom of the flume as individual grains settled into interstitial spaces between the few remaining larger sized quartz grains. This process of winnowing away the finer grained portion of the less dense sediments, results in the development of a thickly armoured bed composed almost entirely of heavy minerals. Throughout this winnowing process, the forces necessary to overcome the high pivot angles produced between heavy and light grains resulted in the lighter grains being eroded first as the forces required to move these grains was reached much sooner (Middleton and Southard, 1984, p.167). Thus, the sand in transport was predominantly quartz-rich which resulted in few heavy minerals being deposited in the gravel bed from the initial suspension rain out processes. However, once the majority of quartz grains at the surface had been stripped away leaving behind a heavy mineral rich lag deposit, there were no longer sufficient quartz grains to shield the remaining heavy minerals. This process resulted in the eventual initiation of heavy mineral transport downstream (see Figure 34) and their subsequent deposition in the avalanche bedform

prograding over the gravel bar. This often resulted in the burying of sediments previously deposited through suspension rain out (see Figure 37). Sediments which accumulated from avalanche face progradation were therefore found to contain higher concentrations of heavy minerals than those previously deposited from suspension rain out (see also Minter and Toens, 1970).

The fine and medium sand deposited from suspension rain out showed a slight positive correlation between the percentage of heavy minerals deposited and velocity whereas coarse sand shows no correlation at all (see Appendix 2, pages 113, 119, and 125). This is likely the result of heavy minerals moving in both bed load and near-bed suspension while quartz sand moved predominately in suspension during moderate to high flow velocities above the bed. Obviously there is a velocity which result in an optimal separation of these two populations. The curves indicate that this optimal velocity is higher than could be obtained during present flume experimentation. The lack of correlation with the coarse sand indicates that the large quartz grains and heavy mineral components behaved similarly at the velocities attained. This is an expected result for at these flow velocities, grain sizes, and densities, both coarse sand and heavy minerals would not have had a sizable component moving in suspension transport.

Overall, the highest concentration of lead was deposited amongst pebble-sized clasts during the fastest velocity runs. The highest concentration of magnetite was deposited amongst large pebble to cobble-sized clasts. The coarser sediment grain size requires a corresponding increase in velocity in order to achieve the optimal conditions which will result in complete density segregation. There were few significant trends with the less dense pyroxene grains which overall behaved similarly to quartz grains.

It would appear that dissimilar results obtained while using detrital lead and magnetite under controlled conditions casts some doubt as to the validity in using less dense magnetite grains to simulate very dense heavy minerals such as uraninite and gold. Detrital lead makes a much better analogue in these types of experiments as it behaves more hydraulically similar to the heavy minerals typically recovered from placer deposits.

6.4: Discussion of Results

As a result of the processes discussed in the previous section, depositional placer formation in longitudinal gravel bars appears to be dependent upon the separation of heavy minerals from light minerals (Slingerland, 1984, p.140). This results from heavy minerals being transported in bed load while lighter minerals are kept mostly in

suspension. However, this separation often leads to heavy minerals being preferentially deposited with coarser grained sediments and clasts that are similarly unable to remain in suspension (see Figure 3, Tourtelot, 1986). Such a condition makes the formation of an economic placer deposit very unlikely unless coarse-grained, hydraulically equivalent sized and less dense minerals are noticeably absent while heavier minerals are being transported by the river system.

An examination of Rouse Z values calculated from data obtained from selected experimental runs reveals several interesting trends (see Appendix 4). Again, most medium- and coarse-grained sediments remained in bed load transport as the energy required to transport these sediments in suspension was not attained. Accordingly, this condition would make the separation of less dense sediments from heavier ones difficult. However, experimental runs using fine-grained sediments reveal a differential transport mechanism operating based on density. Data in Appendix 4 reveal that less dense quartz sediments were kept in suspension over the entire length of the flume as indicated by Rouse Z values less than 2.5, the value at which sediments go into suspension (see Middleton and Southard, 1984, p. 200). Somewhat denser pyroxene sediments were initially transported in bed load but with increasing turbulence over the gravel bar, these grains were subsequently transported in suspension (Z values greater than 2.5). The denser magnetite and lead grains remained almost exclusively in bed load transport during all experimental runs as there was insufficient energy in the system to transport these grains in suspension (Z values greater than 2.5). It can therefore be seen that the primary reason for this segregation of sediments in transport to have occurred is due to differences in energy levels, particularly over the gravel bar during various runs.

Extremely high flow velocities also make placer formation difficult as the preferential deposition of heavy minerals is not likely to occur. The majority of grains in both the heavy and light fractions will travel in suspension and thus not be separated until there is a decrease in energy in the system. Moreover, lower flow velocities, such as those obtained during most flume experimentation, will also not result in the preferential deposition of heavy minerals. During low flows, the critical velocity required to keep light grains in suspension transport is not available and therefore, these conditions are unable to separate the heavy fraction from the light fraction in transport. This results in an uneconomic deposit where heavy minerals, although present, have not experienced the hydraulic conditions necessary to maximise placer formation.

6.5: Possible Modes of Formation of Placer Accumulations in Coarse-Grained Alluvium

Three possible syngenetic models for palaeoplacer formation in conglomerates at Elliot Lake were suggested by Fralick and Miall (1981) These are:

> 1) the uraninite and quartz pebbles both came from the same source material and thus the uraniferous conglomerate packages represent erosion of small sources and local deposition of the material (mineralisation and pebbles genetically linked).
>
> 2) the uraninite was deposited in the pores of an openwork gravel due to special hydraulic conditions which were created by the gravel bed (mineralisation caused by the pebbles).
>
> 3) both pebbles and uraninite represent heavy material which only extended down gradient and into the basin area during times of intense flow velocity (mineralisation and pebbles causatively linked).

The third mechanism is most probable and supports Pretorius' (1981) views that an increase in gradient played an important role in the formation of some conglomeratic Witwatersrand palaeoplacers and Fralick and Miall's (1987) contention that Elliot Lake palaeoplacers were created by catastrophic flood events that carried coarse detritus into the basin.

Fralick and Miall (1987) used Zr/Hf ratios in samples from uraniferous conglomerates and non-mineralised sandstones of the Matinenda Formation to show how the sediments at Elliot Lake had been well mixed prior to sedimentation and that processes operating in the area of conglomeratic deposition resulted in the formation of uraniferous palaeoplacers. Thus, the conditions outlined in Hypothesis One did not occur. Hypothesis Two attributes the deposition of uraninite in an open framework gravel to hydraulic conditions created over the gravel bar. In order for this hypothesis to be correct, clast size would have to control the hydraulic conditions generated over a gravel bar and thus control the percentage of heavy minerals deposited therein. The previous discussion of data obtained from the flume reveals that this did not occur. The percentage of heavy minerals which accumulated in the gravel bar showed little correlation with clast size. Therefore, based on flume experimentation, Hypothesis Two can be rejected. However, clast size and the deposition of heavy minerals are in fact related in the longitudinal gravel bars sampled in the field. This is at variance with flume data results and must be further explained.

It is of the author's opinion that clast size and the percentage of heavy minerals deposited show a correlation in natural systems because they are both related to a third

hypothesis is supported by flume data which show flow velocity has controlled the amount of heavy minerals deposited in the bar. In a natural system, it is therefore logical to assume that flow velocity controls the amount of heavy minerals accumulating and also controls the size of the clasts being sedimented at that site. Thus, flow velocity influences both of these variables and leads to a correlation between them. In order for this to occur, the clasts must have been in transport and subsequently deposited at the same time as the heavy minerals were accumulating. Therefore, Hypothesis Two is once again rejected and Hypothesis Three is left as the most probable process that resulted in the formation of the Witwatersrand and Elliot Lake palaeoplacers. An interpretation of all graphs indicates that the highest concentration of heavy minerals was found amongst the coarsest and most poorly sorted sediments deposited in areas of the bar where the smallest clasts tend to accumulate. In the longitudinal bars studied, this resulted in heavy mineral content increasing towards the tail of the bar.

This study has highlighted two processes which result in the formation of alluvial depositional placer accumulations in coarse-grained braided river systems. The first process results from heavy minerals travelling in bed load transport, while less dense sediments are kept mostly in suspension. With a decrease in velocity, heavy minerals are sedimented with hydraulically equivalent sized, less dense sediments in open framework gravels. The second process occurs as a result of heavy minerals in channel bottom sediments becoming progressively enriched through the winnowing of less dense sediments, resulting in the formation of an erosional placer deposit. Flume experimentation revealed that when high concentrations of heavy minerals armouring the stream-bed were reached, this often resulted in the initiation of their movement downstream. This process can also be triggered by catastrophic events such as large floods or regional tectonic uplift. A sudden increase in energy typically associated with such events results in the flushing of erosional placers and their eventual deposition in areas of higher preservation potential. Therefore, a catastrophic adjustment helps to flush out erosional placer deposits into the basin to form a depositional placer accumulation.

CHAPTER 7: REFERENCES

ADAMS, J., ZIMPFER, G. L., and McLANE, C. F. 1978. Basin dynamics, channel processes, and placer formation: a model study. Economic Geology, **73**, pp. 416-426.

ASHLEY, G. M., SHAW, J., and SMITH, N. D. 1985. Glacial Sedimentary Environments. Society of Economic Paleontologists and Mineralogists Short Course Number **16**, Tulsa, 246p.

BATEMAN, A. M. 1951. The Formation of Mineral Deposits. 2nd Edition. John Wiley and Sons, Inc., New York, 371p.

BESCHTA, R. L., and JACKSON, W. L. 1979. The intrusion of fine sediments into a stable gravel bed. Canadian Journal of Fisheries Research and Aquatic Sciences, **36**, pp. 204-210.

BOOTHROYD, J. C., and ASHLEY, G. M. 1975. Process, bar morphology, and sedimentary structures on braided outwash fans, Northeastern Gulf of Alaska. *In* Glaciofluvial and Glaciolacustrine Sedimentation. *Edited by* A. V. Jopling and B.C. McDonald. Society of Paleontologists and Mineralogists Special Publication **23**, Tulsa, pp. 193-222.

BOOTHROYD, J. C., and NUMMEDAL, D. 1978. Proglacial braided outwash: a model for humid alluvial-fan deposits. *In* Fluvial Sedimentology. *Edited by* A. D. Miall. Canadian Society of Petroleum Geologists Memoir **5**, pp. 641-668.

BREWSTER, R., and BARNETT, R. L. 1979. Magnetites from a new unidentified tephra source, Banff National Park, Alberta. Canadian Journal of Earth Science, **16**, pp. 1294-1297.

BURTON, J. P. 1986. A comparative analysis of diurnal stream flow regime: a study of sites in high alpine and temperate continental environments. Unpublished H.B.Sc. Thesis, Lakehead University, 78p.

BURTON, J. P., and FRALICK, P. W. 1988. Placer formation in braided river systems. *In* Geoscience Research Grant Program, Summary of Research, 1987-88. *Edited by* V. G. Milne. Ontario Geological Survey, Miscellaneous Paper **140**, pp. 205-216.

CARLING, P. A. 1984. Deposition of fine and coarse sand in an open-work gravel bed. Canadian Journal of Fisheries and Aquatic Sciences, **41**, pp. 263-270.

CARY, A. S. 1951. Origin and significance of open-work gravels. Transactions of the American Society of Civil Engineers, **116**, pp. 1296-1308.

CHENEY, E. S., and PATTON, T. C. 1967. Origin of the bedrock values of placer deposits. Economic Geology, **62**, pp. 852-853.

CHURCH, M. A. 1972. Baffin Island sandurs: a study of Arctic fluvial processes. Geological Survey of Canada Bulletin **216**, 208p.

CHURCH, M. A., and GILBERT, R. 1975. Proglacial fluvial and lacustrine environments. *In* Glaciofluvial and Glaciolacustrine Sedimentation. *Edited by* A. V. Jopling and B. C. McDonald. Society of Paleontologists and Mineralogists Special Publication **23**, Tulsa, pp. 22-100.

CRAMPTON, F. A. 1937. Occurrence of gold in stream placers. Mining Journal, **20**, pp. 3-4, 33-34.

DERIKX, L., and LOIJENS, H. 1970. Hydrology of glacierized basins-summary of research by Glaciology Subdivision, Inland Waters Branch. Department of Energy, Mines and Resources, Ottawa, Ontario, pp. 33-35.

DUNNE, T., and LEOPOLD, L. B. 1978. Water in Environmental Planning. W. H. Freeman and Co., San Francisco, 818p.

DYER, K. R. 1970. Grain-size parameters for sandy gravels. Journal of Sedimentary Petrology, **40**, pp. 616-620.

EINSTEIN, H. A. 1968. Deposition of suspended particles in a gravel bed. Journal of the Hydraulics Division, Proceedings of the American Society of Civil Engineers, **94**, No. HY5, pp. 1197-1205.

FRALICK, P. W., and MIALL, A. D. 1981. Sedimentology of the Matinenda Formation. *In* Geoscience Research Grant Program, Summary of Research 1980-81. *Edited by* E. G. Pye, Ontario Geological Survey, Miscellaneous Paper **98**, pp. 80-89.

FRALICK, P. W., and MIALL, A. D. 1987. Glacial outwash uranium placers? Evidence from the Lower Huronian Supergroup, Ontario, Canada. *In* Uranium Deposits in Proterozoic Quartz-Pebble Conglomerates. *Edited by* D. Pretorius, International Atomic Energy Agency Technical Document **427**, Vienna, 459p.

FRASER, H. J. 1935. Experimental study of the porosity and permeability of clastic sediments. Journal of Geology, **43**, pp. 910-1010.

FROSTICK, L. E., LUCAS, P. M., and REID, I. 1984. The infiltration of fine matrices into coarse-grained alluvial sediments and its implications for stratigraphical interpretation. Geological Society of London. Journal, **141**, pp. 955-965.

GLADWELL, D. R., and HALE, M. 1981. Multifractional analyses in geochemical exploration for tin mineralization. Unpublished manuscript, Imperial College, London, U.K., 30p.

GREGORY, K. J., and WALLING, D. E. 1973. Drainage Basin Form and Process. Edward Arnold Ltd., London, 456p.

GUNN, C. B. 1968. Origin of the bedrock values of placer deposits. Economic Geology, **63**, p. 86.

GUSTAVSON, T. C. 1974. Sedimentation on gravel outwash fans, Malaspina Glacier foreland, Alaska. Journal of Sedimentary Petrology, **44**, pp. 374-389.

HALLBAUER, D. K., and UTTER, T. 1977. Geochemical and morphological characteristics of gold particles from recent river deposits and the fossil placers of the Witwatersrand. Mineralium Deposita, **12**, pp. 293-306.

HAMMER, K. M., and SMITH, N. D. 1983. Sediment production and transport in a proglacial stream: Hilda Glacier, Alberta, Canada. Boreas, **12**, pp. 91-106.

HEIN, F. J., and WALKER, R. G. 1977. Bar evolution and development of stratification in the gravelly braided Kicking Horse River, B.C. Canadian Journal of Earth Science, **14**, pp. 562-570.

HENLEY, R. W., and ADAMS, J. 1979. On the evolution of giant gold placers. Transactions of the Institution of Mineralogy and Metallurgy (Section B: Applied Earth Science), **79**, pp. 41-50.

KARTASHOV, I. P. 1971. Geological features of alluvial placers. Economic Geology, **66**, pp. 879-885.

KEHEW, A. E., and LORD, M. L. 1987. Glacial-lake outbursts along the mid-continent margins of the Laurentide ice-sheet. *In* Catastrophic Flooding. *Edited by* L. Mayer and D. Nash. 18th Annual Geomorphology Symposium, Allen and Unwin, Winchester, MA, pp. 95-120.

KOLESOV, S. V. 1975. Subsidence of gold grains in allochthonous alluvial and coastal-marine placers. International Geology Review, **17**, pp. 951-953.

KOSTER, E. H. 1978. Transverse ribs: their characteristics, origin, and paleohydraulic significance. *In* Fluvial Sedimentology. *Edited by* A. D. Miall. Canadian Society of Petroleum Geologists Memoir **5**, pp. 161-186.

KRAPEZ, B. 1985. The Ventersdorp Contact placer: a gold-pyrite placer of stream debris-flow origins from the Archean Witwatersrand Basin of South Africa. Sedimentology, **32**, pp. 223-234.

KROOK, L. 1968. Origin of bedrock values of placer deposits. Economic Geology, **63**, pp. 844-846.

LEOPOLD, L. B., and WOLMAN, M. G. 1957. River channel patterns: braided, meandering, and straight. U.S. Geological Survey Professional Paper **282-B**, 85p.

McDONALD, B. C., and BANERJEE, I. 1971. Sediments and bedforms on a braided outwash plain. Canadian Journal of Earth Science, **8**, pp. 1281-1301.

MEEHAN, W. R., and SWANSTON, D. N. 1977. Effects of gravel morphology on fine sediment accumulation and survival of incubating salmon eggs. United States Department of Agriculture, Forestry Service Research Paper, PNW-220, 16p.

MEIER, M. F. 1960a. Mode of flow of Saskatchewan glacier, Alberta, Canada. U.S. Geological Survey Professional Paper **351**, 70p.

MIALL, A. D. 1977. A review of the braided-river depositional environment. Earth Science Reviews, **13**, pp. 1-62.

MIALL, A. D. 1984. Glaciofluvial transport and depostion. *In* Glacial Geology. *Edited by* N. Eyles. Pergamon Press, New York, pp. 168-183.

MIDDLETON, G. V., and SOUTHARD, J. B. 1984. Mechanics of Sediment Movement. Society of Economic Paleontologists and Mineralogists Short Course Number **3**, 2nd edition, Tulsa, 401p.

MINTER, W. E. L. 1970. Gold distribution related to the sedimentology of a Precambrian Witwatersrand conglomerate, South Africa, as outlined by moving-average analysis. Economic Geology, **65**, pp. 963-969.

MINTER, W. E. L. 1976. Detrital gold, uranium, and pryrite concentrations related to sedimentology in the Precambrian Vaal Reef placer, Witwatersrand, South Africa. Economic Geology, **71**, pp. 157-176.

MINTER, W. E. L. 1978. A sedimentological synthesis of placer gold, uranium and pyrite concentration in Proterozoic Witwatersrand sediments. *In* Fluvial Sedimentology. *Edited by* A. D. Miall. Canadian Society of Petroleum Geologists Memoir **5**, pp. 801-830.

MINTER, W. E. L., and TOENS, P. D. 1970. Experimental simulation of gold deposition in gravel beds. Transactions of the Geological Society of South Africa, **73**, pp. 89-99.

MOSLEY, M. P., and SCHUMM, S. A. 1977. Stream junctions - a probable location for bedrock placers. Economic Geology, **72**, pp. 691-694.

ONTARIO GEOLOGICAL SURVEY, 1986. Geological Highway Map, Northern Ontario, Map 2506.

PARK, C. F., and MacDIARMID, R. S. 1964. Ore Deposits. W. H. Freeman and Company, San Francisco, 475p.

PRETORIUS, D. A. 1976. The nature of the Witwatersrand gold-uranium deposits. *In* Handbook of Stratabound and Stratiform Ore Deposits, Volume **7**. *Edited by* K. H.Wolf. Elsevier, Amsterdam, pp. 29-88.

PRETORIUS, D. A. 1981. Gold and uranium in quartz-pebble conglomerates. Economic Geology, **75**, pp. 117-138.

RUST, B. R. 1972a. Structure and process in a braided river. Sedimentology, **18**, pp. 221-245.

RUST, B. R., and KOSTER, E. H. 1984. Coarse alluvial deposits. *In* Facies Models, Second Edition. *Edited by* R. G. Walker. Geoscience Canada, Reprint Series 1, pp. 53-69.

SCHUMM, S. A. 1977. The Fluvial System. John Wiley and Sons, Inc., New York, 338p.

SHREVE, R. L. 1972. Movement of water in glaciers. Journal of Glaciology, **11**, pp. 205-214.

SLINGERLAND, R. L. 1977. The effects of entrainment on the hydraulic equivalence relationships of light and heavy minerals in sands. Journal of Sedimentary Petrology, **47**, pp. 753-770.

SLINGERLAND, R. L. 1984. Role of hydraulic sorting in the origin of fluvial placers. Journal of Sedimentary Petrology, **54,** pp. 137-150.

SLINGERLAND, R. L., and SMITH, N. D. 1986. Occurrence and formation of water-laid placers. Annual Review of Earth and Planetary Science, **14**, pp. 113-147.

SMITH, D. G. 1972. Aggradation and channel patterns of the Alexandra - North Saskatchewan River, Banff National Park, Alberta. *In* Mountain Geomorphology. *Edited by* H. O. Slaymaker and H. J. McPherson. Tantalus Press, pp. 177-185.

SMITH, D. G. 1973. Aggradation of the Alexandra - North Saskatchewan River, Banff Park, Alberta. *In* Fluvial Geomorphology. *Edited by* M. Morisawa. Proceedings of the 4th Annual Geomorphology Symposium. Binghamton, New York, pp. 201-219.

SMITH, N. D. 1970. The braided stream depositional environment: comparison of the Platte River with some Silurian clastic rocks, North-Central Appalachians. Geological Society of America Bulletin, **81**, pp. 2993-3014.

SMITH, N. D. 1974. Sedimentology and bar formation in the upper Kicking Horse River, a braided outwash stream. Journal of Geology, **82**, pp. 205-223.

SMITH, N. D. 1985. Proglacial fluvial environment. *In* Glacial Sedimentary Environments. *Edited by* G. M. Ashley, J. Shaw, and N. D. Smith. Society of Economic Paleontologists and Mineralogists Short Course Number **16**, Tulsa, pp. 85-134.

SMITH, N. D., and MINTER, W. E. L. 1980. Sedimentological controls of gold and uranium in two Witwatersrand paleoplacers. Economic Geology, **75**, pp. 1-14.

SMITH, N. D., and BEUKES, N. J. 1983. Bar to bank flow convergence zones: a contribution to the origin of alluvial placers. Economic Geology, **78**, pp. 1342-1349.

SMITH, N. D., and SMITH, D. G. 1984. Williams River: an outstanding example of channel widening and braiding caused by bed-load addition. Geology, **12**, pp. 78-82.

SMITH, N. D., and ASHLEY, G. M. 1985. Proglacial lacustrine environments. *In* Glacial Sedimentary Environments. *Edited by* G. M. Ashley, J. Shaw, and N. D. Smith. Society of Economic Paleontologists and Mineralogists Short Course Number **16**, Tulsa, pp. 135-216.

SUGDEN, D. E., and JOHN, B. S. 1976. Glaciers and Landscape. Edward Arnold Ltd., London, 376p.

TOURTELOT, H. A. 1968. Hydraulic equivalence of grains of quartz and heavier minerals, and implications for the study of placers. U.S. Geological Survey Professional Paper **594-F**, 13p.

TUCK, K. 1968. Origin of the bedrock values of placer deposits. Economic Geology, **63**, pp. 191-193.

WILLIAMS, P. F., and RUST, B. R. 1969. The sedimentology of a braided river. Journal of Sedimentary Petrology, **39**, pp. 649-679.

APPENDICES

APPENDIX 1

Flume data tables

Appendix 1.1: Data derived from fine-grained surficial sediments.
Appendix 1.2: Data derived from fine-grained matrix sediments.
Appendix 1.3: Data derived from medium-grained surficial sediments.
Appendix 1.4: Data derived from medium-grained matrix sediments.
Appendix 1.5: Data derived from coarse-grained surficial sediments.
Appendix 1.6: Data derived from coarse-grained matrix sediments.

Appendix 1.1

Run Parameters	Sample Number	Mean Quartz	Sorting of Quartz	Mean Pyroxene	Sorting of Pyroxene	Percent Pyroxene	Mean Magnetite	Sorting of Magnetite	Percent Magnetite	Percent Lead	Percent Lead pellet	Velocity m/s	Clast Size cm2	Mean Quartz
-fine sand, small pebbles	19.1	2.46	0.34	2.31	0.25	65.50	2.36	0.39	11.26	1.71	0.00	0.41	11	2.59
slow velocity	19.2	2.46	0.34	2.32	0.26	66.23	2.35	0.39	8.75	0.62	0.00	0.41	11	2.59
-fine sand, small pebbles	20.1	2.58	0.42	2.35	0.29	40.68	2.35	0.38	7.31	35.78	0.00	0.83	11	2.59
medium velocity	20.2	2.58	0.42	2.36	0.29	58.12	2.39	0.36	6.89	13.65	0.00	0.83	11	2.59
-fine sand, small pebbles	18.1	2.70	0.46	2.46	0.35	15.74	2.48	0.36	1.95	60.61	11.11	1.24	11	2.59
fast velocity	18.2	2.69	0.47	2.49	0.39	23.72	2.43	0.40	3.53	54.42	1.04	1.24	11	2.59
-fine sand, large pebbles	17.1	2.55	0.41	2.35	0.29	47.39	2.34	0.40	18.12	19.16	0.00	0.56	32	2.59
slow velocity	17.2	2.51	0.39	2.31	0.26	58.61	2.33	0.41	17.85	1.73	0.00	0.56	32	2.59
-fine sand, large pebbles	16.1	2.52	0.39	2.33	0.28	52.52	2.33	0.40	10.32	2.82	0.00	0.86	32	2.59
medium velocity	16.2	2.58	0.42	2.37	0.29	39.25	2.38	0.38	3.67	0.19	0.00	0.86	32	2.59
-fine sand, large pebbles	15.1	2.55	0.41	2.37	0.31	46.15	2.35	0.40	8.17	16.51	0.00	1.13	32	2.59
fast velocity	15.2	2.59	0.42	2.38	0.33	49.29	2.31	0.41	11.12	4.07	0.00	1.13	32	2.59
-fine sand, cobbles	12.1	2.66	0.46	2.40	0.33	51.62	2.41	0.37	7.79	19.30	0.00	0.48	82	2.59
slow velocity	12.2	2.74	0.49	2.38	0.31	52.39	2.36	0.39	9.78	21.98	0.00	0.48	82	2.59
-fine sand, cobbles	14.1	2.53	0.40	2.34	0.28	48.89	2.33	0.39	11.77	2.65	0.00	0.83	82	2.59
medium velocity	14.2	2.63	0.44	2.41	0.34	46.56	2.40	0.38	4.37	0.32	0.00	0.83	82	2.59
-fine sand, cobbles	13.1	2.72	0.48	2.45	0.36	32.42	2.41	0.39	4.96	39.03	0.00	1.16	82	2.59
fast velocity	13.2	---	---	---	---	---	---	---	---	---	0.00	1.16	82	2.59

Appendix 1.2

Run Parameters	Sample Number	Mean Quartz	Sorting of Quartz	Mean Pyroxene	Sorting of Pyroxene	Percent Pyroxene	Mean Magnetite	Sorting of Magnetite	Percent Magnetite	Percent Lead	Percent Lead pellet	Velocity m/s	Clast Size cm2	Mean Quartz
-fine sand, small pebbles	19.3	2.47	0.33	2.43	0.33	39.38	2.42	0.36	2.10	0.27	0.00	0.41	11	2.59
slow velocity	19.4	2.49	0.35	2.42	0.32	40.45	2.43	0.37	2.03	0.61	0.00	0.41	11	2.59
-fine sand, small pebbles	20.3	2.50	0.35	2.41	0.31	41.08	2.41	0.37	2.72	1.00	0.00	0.83	11	2.59
medium velocity	20.4	2.54	0.38	2.41	0.32	46.69	2.41	0.38	3.63	0.41	0.00	0.83	11	2.59
-fine sand, small pebbles	18.3	2.45	0.31	2.34	0.28	53.46	2.36	0.39	7.18	2.72	0.00	1.24	11	2.59
fast velocity	18.4	2.49	0.34	2.39	0.31	43.23	2.41	0.37	3.66	5.45	0.00	1.24	11	2.59
-fine sand, large pebbles	17.3	2.49	0.34	2.42	0.31	38.19	2.43	0.37	2.42	0.84	0.00	0.56	32	2.59
slow velocity	17.4	2.47	0.34	2.38	0.30	44.23	2.40	0.37	3.88	0.48	0.00	0.56	32	2.59
-fine sand, large pebbles	16.3	2.52	0.37	2.38	0.31	45.70	2.35	0.39	6.76	0.46	0.00	0.86	32	2.59
medium velocity	16.4	2.58	0.40	2.45	0.36	41.22	2.47	0.39	1.78	0.45	0.00	0.86	32	2.59
-fine sand, large pebbles	15.3	2.47	0.33	2.41	0.32	42.19	2.41	0.38	3.32	0.62	0.00	1.13	32	2.59
fast velocity	15.4	2.54	0.37	2.44	0.35	41.31	2.38	0.40	4.55	1.87	0.00	1.13	32	2.59
-fine sand, cobbles	12.3	2.51	0.36	2.44	0.33	36.75	2.43	0.37	2.57	1.00	0.00	0.48	82	2.59
slow velocity	12.4	2.49	0.36	2.39	0.28	37.99	2.41	0.37	2.50	0.87	0.00	0.48	82	2.59
-fine sand, cobbles	14.3	2.59	0.41	2.44	0.35	42.21	2.44	0.38	2.96	0.47	0.00	0.83	82	2.59
medium velocity	14.4	2.66	0.44	2.46	0.36	39.21	2.46	0.39	2.32	0.20	0.00	0.83	82	2.59
-fine sand, cobbles	13.3	2.53	0.36	2.41	0.30	33.12	2.39	0.40	3.73	13.17	0.00	1.16	82	2.59
fast velocity	13.4	2.68	0.46	2.50	0.39	36.35	2.53	0.39	2.64	12.98	0.00	1.16	82	2.59

Appendix 1.3

Run Parameters	Sample Number	Mean Quartz	Sorting of Quartz	Mean Pyroxene	Sorting of Pyroxene	Percent Pyroxene	Mean Magnetite	Sorting of Magnetite	Percent Magnetite	Percent Lead	Percent Lead pellet	Velocity m/s	Clast Size cm2	Mean Quartz
-med sand, small pebbles	8.1	1.88	0.24	1.95	0.22	23.03	2.21	0.38	4.66	56.63	0.00	0.51	11	1.84
slow velocity	8.2	1.86	0.24	1.92	0.22	39.68	2.17	0.38	8.29	28.11	0.00	0.51	11	1.84
-med sand, small pebbles	10.1	1.87	0.23	1.93	0.22	49.51	2.20	0.37	9.37	11.05	0.37	0.85	11	1.84
medium velocity	10.2	1.85	0.23	1.92	0.21	51.42	2.17	0.38	8.55	1.78	0.00	0.85	11	1.84
-med sand, small pebbles	9.1	1.90	0.24	1.96	0.22	53.96	2.38	0.46	10.39	7.19	0.73	1.11	11	1.84
fast velocity	9.2	1.88	0.24	1.93	0.22	53.93	2.18	0.38	8.70	1.32	0.00	1.11	11	1.84
-med sand, large pebbles	6.1	1.85	0.24	1.93	0.22	36.39	2.17	0.38	6.95	35.94	0.00	0.52	32	1.84
slow velocity	6.2	1.84	0.23	1.90	0.22	49.33	2.14	0.38	9.82	14.46	0.00	0.52	32	1.84
-med sand, large pebbles	4.1	1.84	0.22	1.90	0.21	56.97	2.20	0.38	10.58	6.54	0.00	0.73	32	1.84
medium velocity	4.2	1.81	0.22	1.89	0.22	47.50	2.20	0.39	8.08	0.57	0.00	0.73	32	1.84
-med sand, large pebbles	5.1	1.88	0.24	1.93	0.23	18.64	2.22	0.40	4.54	63.48	0.11	1.14	32	1.84
fast velocity	5.2	1.87	0.24	1.93	0.23	42.28	2.56	0.41	9.70	13.63	0.00	1.14	32	1.84
-med sand, cobbles	2.1	1.85	0.23	1.90	0.21	40.45	2.15	0.38	7.10	24.09	0.00	0.51	82	1.84
slow velocity	2.2	1.83	0.22	1.89	0.21	50.24	2.11	0.37	9.81	11.25	0.00	0.51	82	1.84
-med sand, cobbles	3.1	1.82	0.22	1.90	0.22	50.25	2.17	0.39	9.68	3.47	0.00	0.83	82	1.84
medium velocity	3.2	1.84	0.23	1.92	0.22	55.30	2.18	0.38	11.97	3.10	0.00	0.83	82	1.84
-med sand, cobbles	11.1	1.86	0.23	1.91	0.23	49.88	2.20	0.40	9.31	1.23	0.00	1.25	82	1.84
fast velocity	11.2	1.87	0.24	1.89	0.23	62.24	2.20	0.40	9.54	1.00	0.00	1.25	82	1.84

Appendix 1.4

Run Parameters	Sample Number	Mean Quartz	Sorting of Quartz	Mean Pyroxene	Sorting of Pyroxene	Percent Pyroxene	Mean Magnetite	Sorting of Magnetite	Percent Magnetite	Percent Lead	Percent Lead pellet	Velocity m/s	Clast Size cm2	Mean Quartz
-med sand, small pebbles	8.3	1.85	0.23	1.91	0.22	29.28	2.19	0.40	4.09	0.49	0.00	0.51	11	1.84
slow velocity	8.4	1.85	0.23	1.92	0.22	26.82	2.15	0.38	3.75	0.95	0.00	0.51	11	1.84
-med sand, small pebbles	10.3	1.82	0.22	1.88	0.22	28.23	2.19	0.42	4.16	0.07	0.00	0.85	11	1.84
medium velocity	10.4	1.84	0.23	1.88	0.21	30.04	2.15	0.39	5.42	0.10	0.00	0.85	11	1.84
-med sand, small pebbles	9.3	1.82	0.22	1.89	0.21	30.83	2.17	0.40	5.01	0.27	0.00	1.11	11	1.84
fast velocity	9.4	1.84	0.22	1.90	0.22	24.64	2.16	0.41	2.94	0.06	0.00	1.11	11	1.84
-med sand, large pebbles	6.3	1.84	0.22	1.94	0.22	24.10	2.15	0.39	3.22	0.34	0.00	0.52	32	1.84
slow velocity	6.4	1.86	0.23	1.93	0.22	24.47	2.15	0.39	3.73	0.10	0.00	0.52	32	1.84
-med sand, large pebbles	4.3	1.83	0.22	1.88	0.22	24.45	2.14	0.41	3.17	0.05	0.00	0.73	32	1.84
medium velocity	4.4	1.85	0.23	1.92	0.23	27.33	2.16	0.40	3.73	0.22	0.00	0.73	32	1.84
-med sand, large pebbles	5.3	1.82	0.22	1.88	0.21	34.85	2.14	0.40	5.29	0.45	0.03	1.14	32	1.84
fast velocity	5.4	1.84	0.22	1.89	0.22	32.16	2.16	0.41	4.50	0.90	0.00	1.14	32	1.84
-med sand, cobbles	2.3	1.81	0.21	1.89	0.21	26.79	2.14	0.40	4.67	0.51	0.00	0.51	82	1.84
slow velocity	2.4	1.83	0.22	1.87	0.21	33.91	2.16	0.41	7.70	0.09	0.00	0.51	82	1.84
-med sand, cobbles	3.3	1.83	0.22	1.90	0.21	27.35	2.14	0.40	4.39	0.68	0.00	0.83	82	1.84
medium velocity	3.4	1.85	0.23	1.93	0.22	30.08	2.15	0.39	5.31	0.35	0.00	0.83	82	1.84
-med sand, cobbles	11.3	1.81	0.22	1.89	0.22	37.22	2.16	0.39	5.54	1.28	0.00	1.25	82	1.84
fast velocity	11.4	1.87	0.24	1.94	0.22	42.73	2.21	0.40	6.61	0.38	0.00	1.25	82	1.84

Appendix 1.5

Run Parameters	Sample Number	Mean Quartz	Sorting of Quartz	Mean Pyroxene	Sorting of Pyroxene	Percent Pyroxene	Mean Magnetite	Sorting of Magnetite	Percent Magnetite	Percent Lead	Percent Lead pellet	Velocity m/s	Clast Size cm2	Mean Quartz
-coarse sand, small pebbles	28.1	1.09	0.48	1.48	0.43	15.25	3.01	0.62	5.79	23.93	0.00	0.42	11	0.97
slow velocity	28.2	0.74	0.63	1.66	0.45	12.83	2.08	0.56	6.30	16.92	0.00	0.42	11	0.97
-coarse sand, small pebbles	27.1	1.21	0.45	1.63	0.43	25.57	2.07	0.55	12.65	13.07	0.20	0.89	11	0.97
medium velocity	27.2	1.12	0.49	1.52	0.40	25.11	2.00	0.59	10.01	0.22	0.00	0.89	11	0.97
-coarse sand, small pebbles	29.1	1.34	0.35	1.71	0.40	4.94	2.23	0.46	4.07	81.22	3.56	1.21	11	0.97
fast velocity	29.2	0.95	0.61	1.60	0.42	4.80	2.10	0.57	4.29	63.81	13.30	1.21	11	0.97
-coarse sand, large pebbles	25.1	0.96	0.59	1.58	0.44	12.33	2.11	0.58	6.31	41.09	0.00	0.43	32	0.97
slow velocity	25.2	1.24	0.40	1.56	0.40	17.61	2.12	0.54	8.36	24.21	0.00	0.43	32	0.97
-coarse sand, large pebbles	26.1	1.66	0.49	1.56	0.40	15.88	2.04	0.56	7.77	39.29	0.56	0.91	32	0.97
medium velocity	26.2	0.97	0.55	1.43	0.41	22.96	1.94	0.64	9.39	1.48	0.00	0.91	32	0.97
-coarse sand, large pebbles	24.1	1.21	0.46	1.61	0.42	28.28	2.08	0.52	13.34	1.88	0.96	1.09	32	0.97
fast velocity	24.2	0.87	0.63	1.54	0.43	21.26	2.01	0.58	10.94	3.08	0.00	1.09	32	0.97
-coarse sand, cobbles	21.1	1.19	0.45	1.60	0.42	14.99	2.16	0.50	7.01	38.04	0.00	0.48	82	0.97
slow velocity	21.2	1.21	0.44	1.74	0.43	14.01	2.21	0.46	7.56	53.40	0.00	0.48	82	0.97
-coarse sand, cobbles	23.1	0.97	0.56	1.51	0.45	16.54	1.98	0.63	8.17	21.55	0.00	0.93	82	0.97
medium velocity	23.2	0.92	0.58	1.41	0.40	23.05	1.92	0.66	9.69	0.44	0.00	0.93	82	0.97
-coarse sand, cobbles	22.1	0.86	0.62	1.42	0.40	17.04	1.92	0.67	9.22	3.30	0.00	1.27	82	0.97
fast velocity	22.2	0.68	0.64	1.37	0.41	15.13	1.86	0.70	6.58	0.63	0.00	1.27	82	0.97

Appendix 1.6

Run Parameters	Sample Number	Mean Quartz	Sorting of Quartz	Mean Pyroxene	Sorting of Pyroxene	Percent Pyroxene	Mean Magnetite	Sorting of Magnetite	Percent Magnetite	Percent Lead	Percent Lead pellet	Velocity m/s	Clast Size cm2	Mean Quartz
-coarse sand, small pebbles	28.3	1.17	0.45	1.26	0.43	11.06	1.63	0.80	4.63	1.18	0.00	0.42	11	0.97
slow velocity	28.4	0.83	0.59	1.29	0.40	7.47	1.69	0.79	4.27	0.60	0.00	0.42	11	0.97
-coarse sand, small pebbles	27.3	0.89	0.56	1.24	0.41	9.10	1.40	0.76	1.74	0.06	0.00	0.89	11	0.97
medium velocity	27.4	1.08	0.51	1.07	0.43	17.43	1.67	0.70	3.13	0.11	0.00	0.89	11	0.97
-coarse sand, small pebbles	29.3	0.85	0.57	1.33	0.41	11.50	1.72	0.74	3.85	1.16	1.56	1.21	11	0.97
fast velocity	29.4	0.99	0.52	1.39	0.39	12.91	1.82	0.70	3.98	2.47	0.18	1.21	11	0.97
-coarse sand, large pebbles	25.3	0.84	0.57	1.21	0.37	10.47	1.66	0.78	3.45	0.40	0.00	0.43	32	0.97
slow velocity	25.4	0.77	0.59	1.16	0.36	14.45	1.59	0.80	3.49	0.16	0.00	0.43	32	0.97
-coarse sand, large pebbles	26.3	0.83	0.58	1.21	0.36	10.43	2.47	0.74	2.86	0.57	0.00	0.91	32	0.97
medium velocity	26.4	0.88	0.57	1.30	0.39	18.41	1.76	0.73	4.94	0.07	0.00	0.91	32	0.97
-coarse sand, large pebbles	24.3	0.79	0.56	1.33	0.40	11.65	1.72	0.73	4.08	1.22	0.46	1.09	32	0.97
fast velocity	24.4	0.94	0.55	1.40	0.42	10.40	1.81	0.71	3.42	0.31	0.00	1.09	32	0.97
-coarse sand, cobbles	21.3	0.86	0.59	1.28	0.39	12.83	1.93	0.69	5.78	0.25	0.00	0.48	82	0.97
slow velocity	21.4	1.00	0.55	1.38	0.40	18.96	1.97	0.62	6.63	0.91	0.00	0.48	82	0.97
-coarse sand, cobbles	23.3	0.87	0.59	1.27	0.38	12.19	1.80	0.72	3.85	0.04	0.00	0.93	82	0.97
medium velocity	23.4	0.96	0.55	1.38	0.38	12.05	1.86	0.69	3.98	0.01	0.00	0.93	82	0.97
-coarse sand, cobbles	22.3	0.90	0.56	1.39	0.41	9.10	1.82	0.72	3.38	0.14	0.00	1.27	82	0.97
fast velocity	22.4	0.93	0.56	1.42	0.44	7.31	1.75	0.76	2.65	0.21	0.00	1.27	82	0.97

APPENDIX 2

Scatter diagrams derived from flume data

Legend:

a) Fine-grained Surficial Sediments
b) Fine-grained Matrix Sediments
c) Medium-grained Surficial Sediments
d) Medium-grained Matrix Sediments
e) Coarse-grained Surficial Sediments
f) Coarse-grained Matrix Sediments

a) % Magnetite vs % Pyroxene

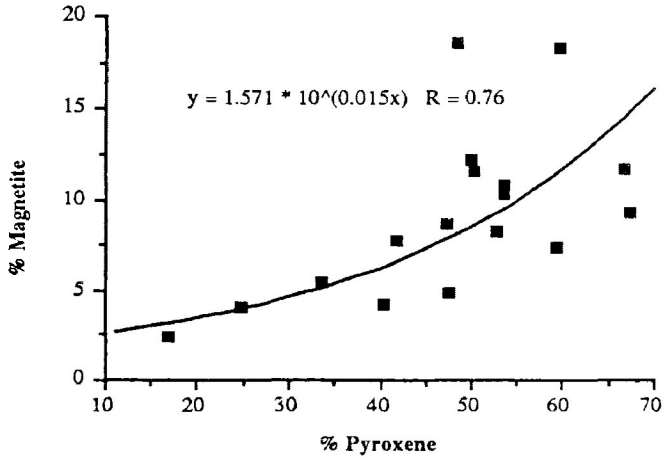

b) % Magnetite vs % Pyroxene

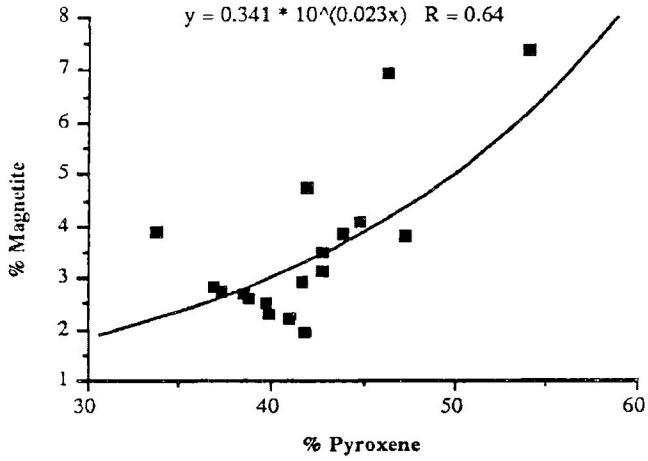

c) % Magnetite vs % Pyroxene

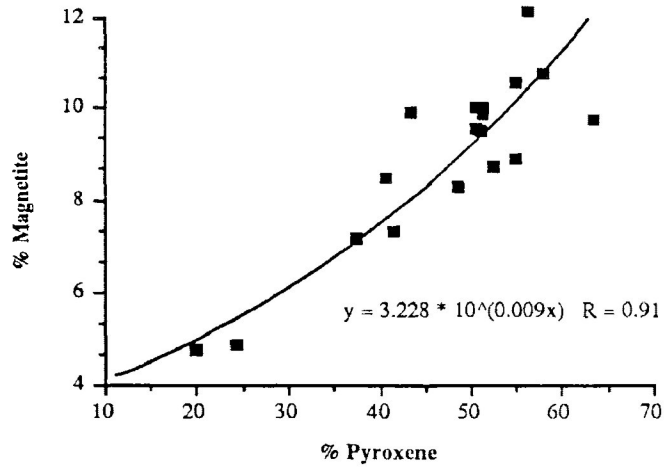

d) % Magnetite vs % Pyroxene

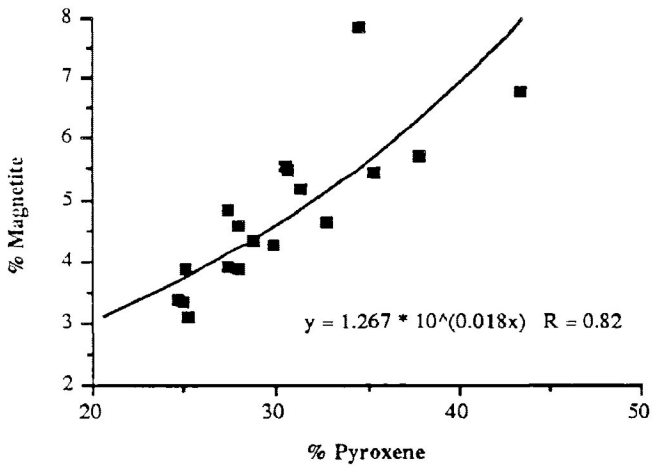

e) % Magnetite vs % Pyroxene

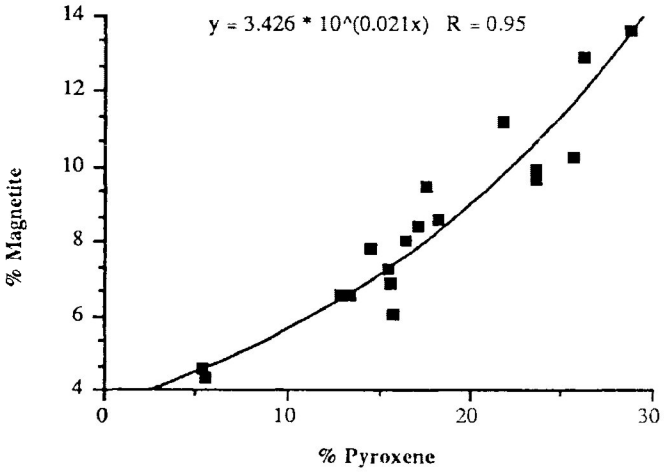

f) % Magnetite vs % Pyroxene

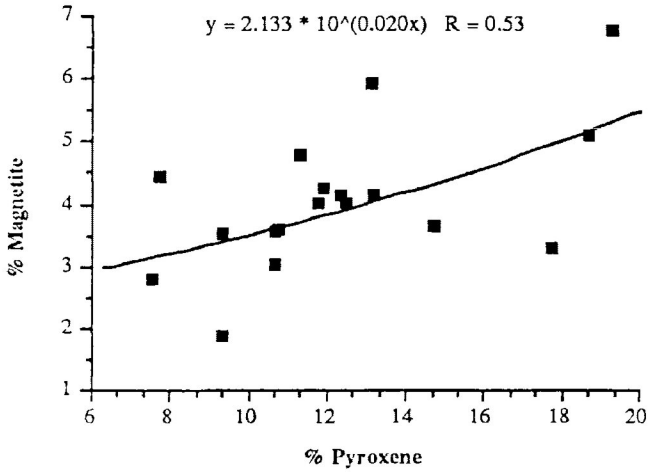

Appendix 2.1

a) % Lead vs % Pyroxene

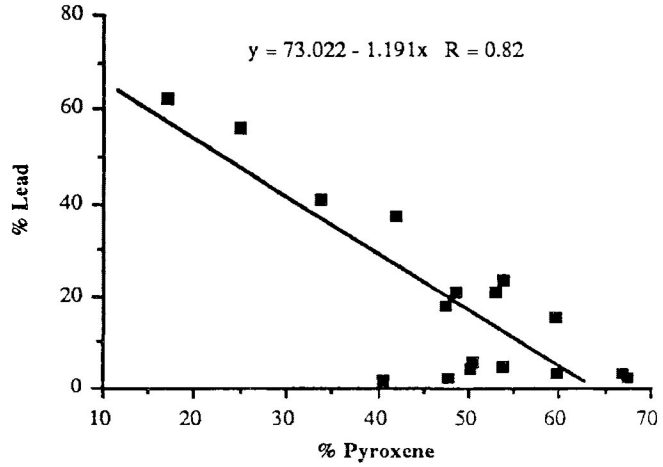

b) % Lead vs % Pyroxene

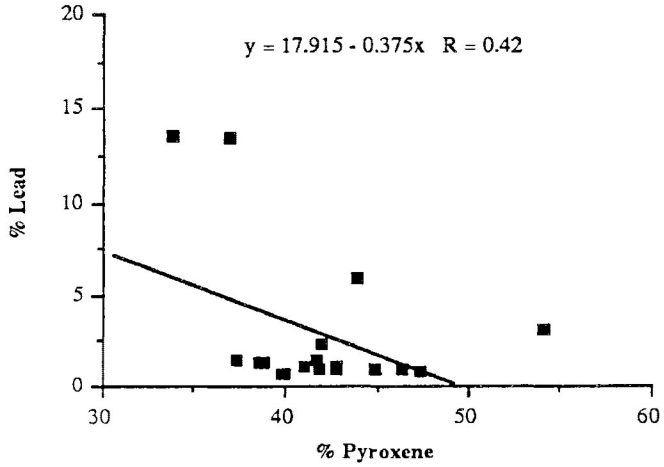

c) % Lead vs % Pyroxene

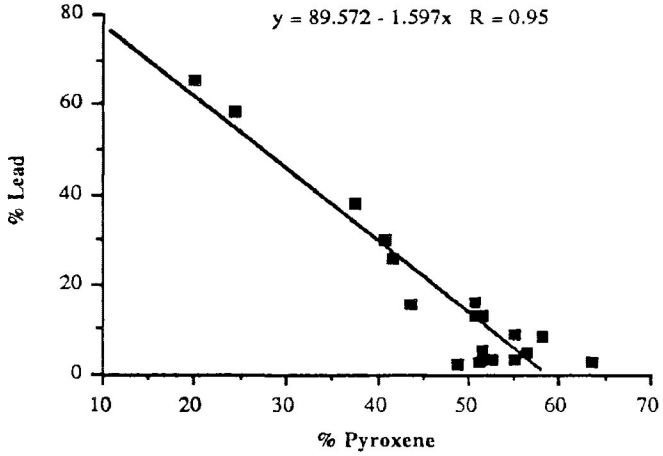

d) % Lead vs % Pyroxene

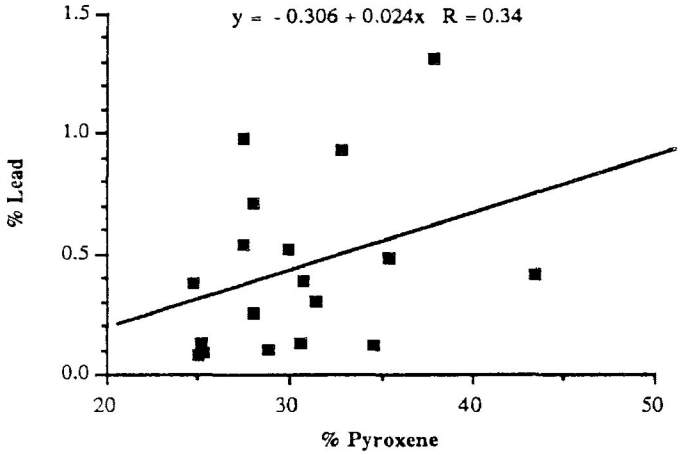

e) % Lead vs % Pyroxene

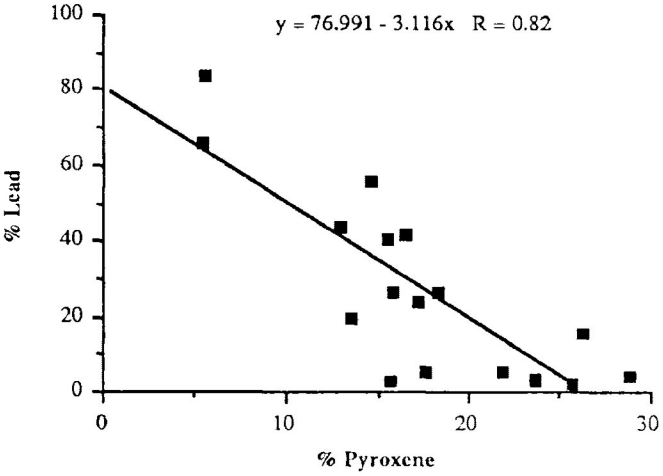

f) % Lead vs % Pyroxene

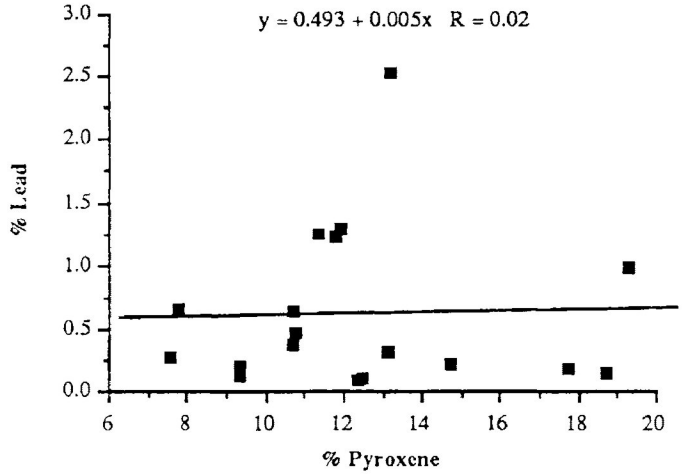

Appendix 2.2

a) % Lead vs % Magnetite

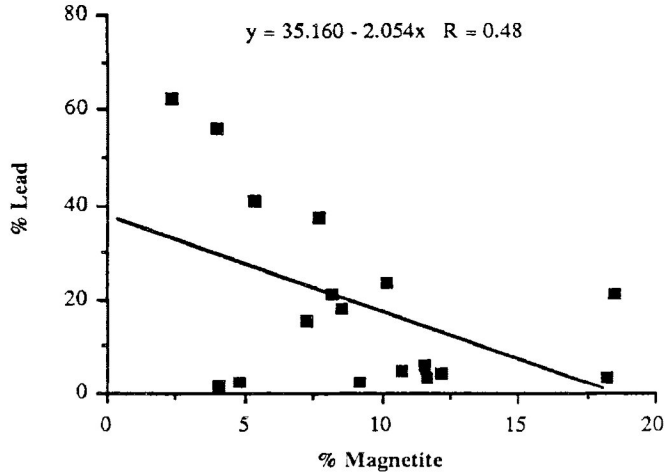

b) % Lead vs % Magnetite

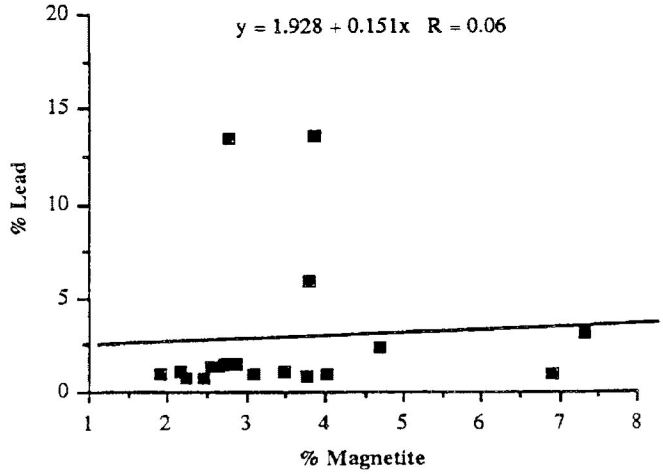

c) % Lead vs % Magnetite

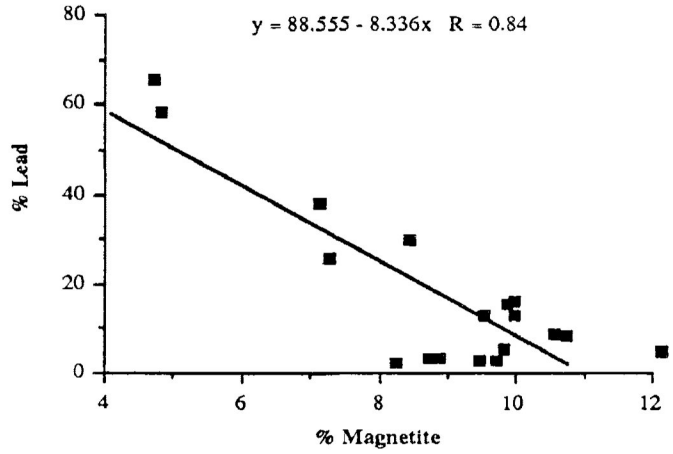

d) % Lead vs % Magnetite

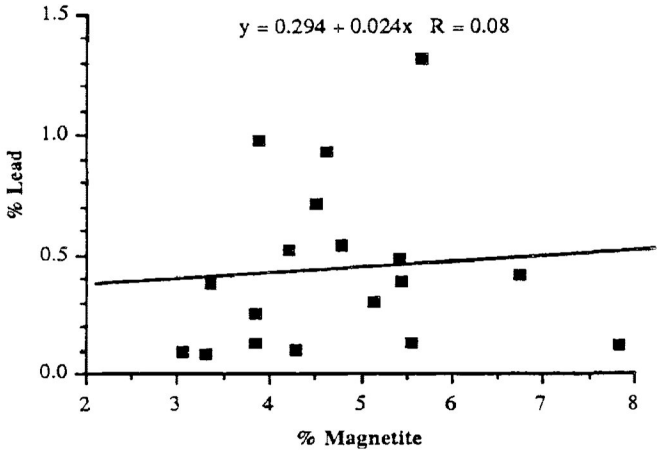

e) % Lead vs % Magnetite

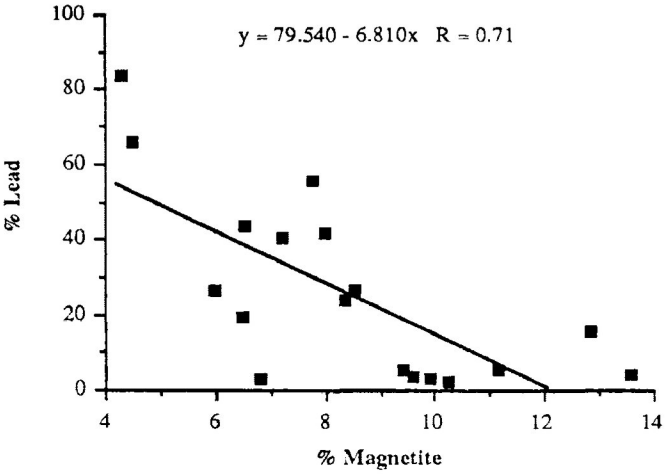

f) % Lead vs % Magnetite

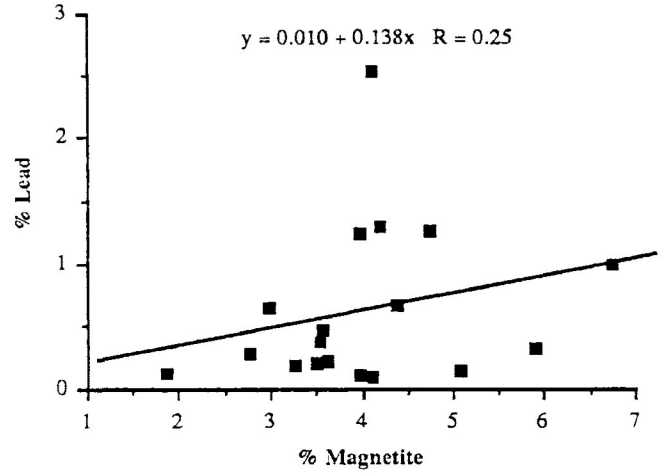

Appendix 2.3

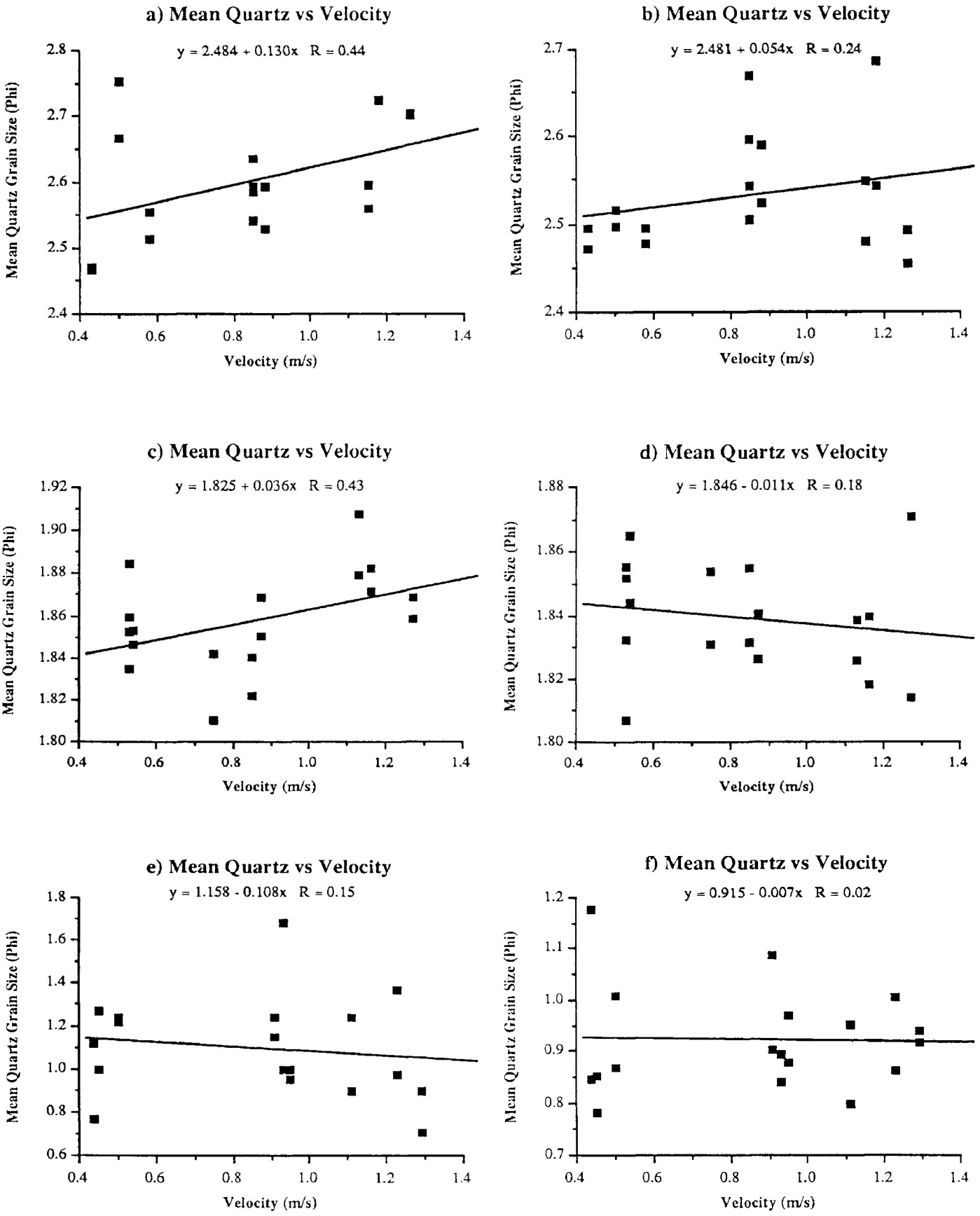
a) Mean Quartz vs Velocity
y = 2.484 + 0.130x R = 0.44
Mean Quartz Grain Size (Phi)
Velocity (m/s)
b) Mean Quartz vs Velocity
y = 2.481 + 0.054x R = 0.24
Mean Quartz Grain Size (Phi)
Velocity (m/s)
c) Mean Quartz vs Velocity
y = 1.825 + 0.036x R = 0.43
Mean Quartz Grain Size (Phi)
Velocity (m/s)
d) Mean Quartz vs Velocity
y = 1.846 - 0.011x R = 0.18
Mean Quartz Grain Size (Phi)
Velocity (m/s)
e) Mean Quartz vs Velocity
y = 1.158 - 0.108x R = 0.15
Mean Quartz Grain Size (Phi)
Velocity (m/s)
f) Mean Quartz vs Velocity
y = 0.915 - 0.007x R = 0.02
Mean Quartz Grain Size (Phi)
Velocity (m/s)

Appendix 2.4

a) Sorting of Quartz vs Velocity

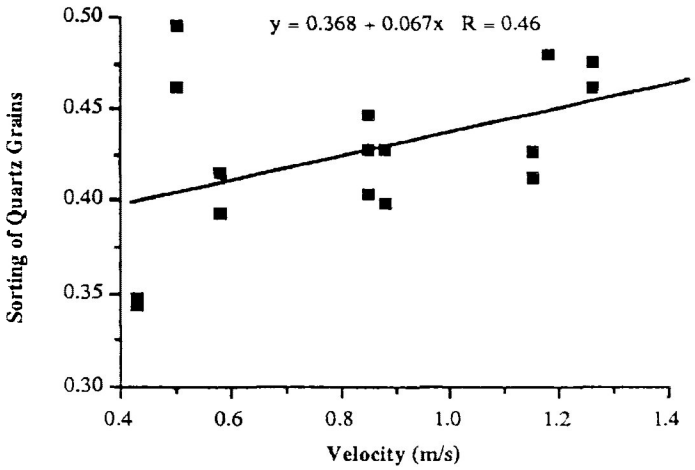

b) Sorting of Quartz vs Velocity

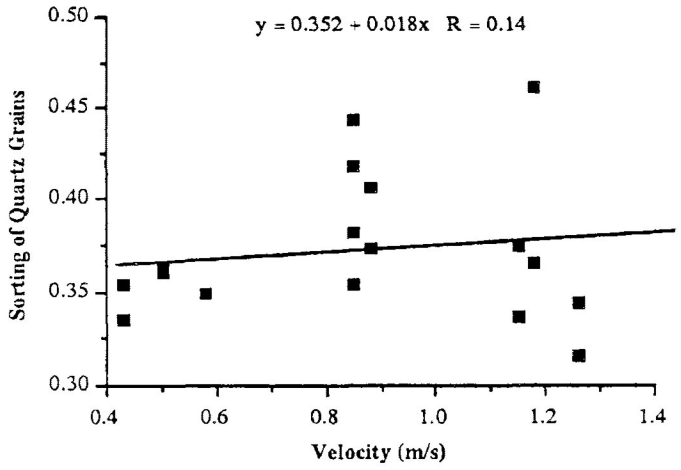

c) Sorting of Quartz vs Velocity

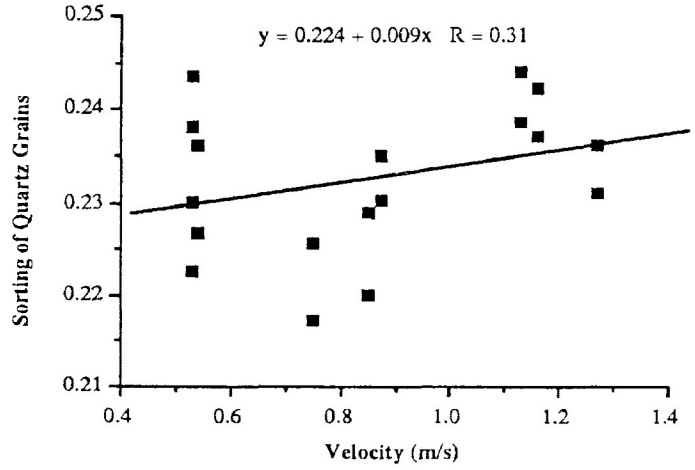

d) Sorting of Quartz vs Velocity

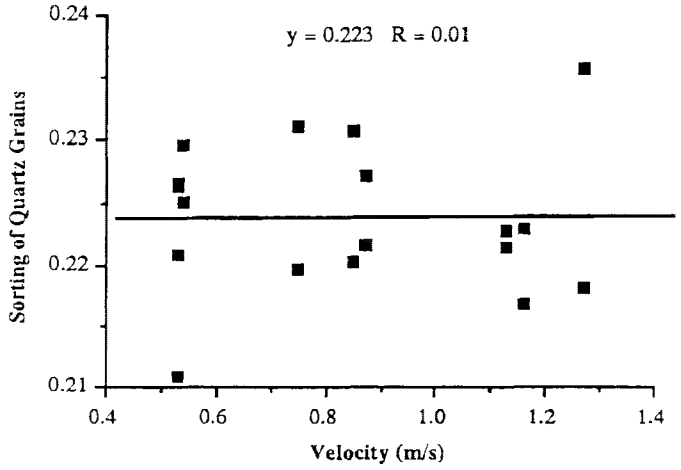

e) Sorting of Quartz vs Velocity

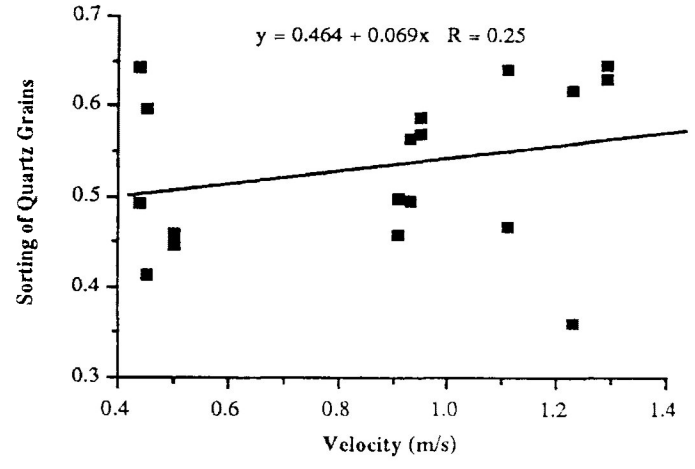

f) Sorting of Quartz vs Velocity

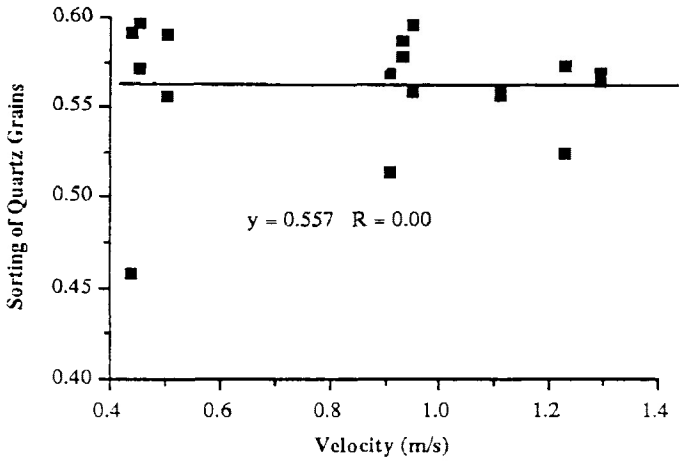

Appendix 2.5

a) % Pyroxene vs Velocity

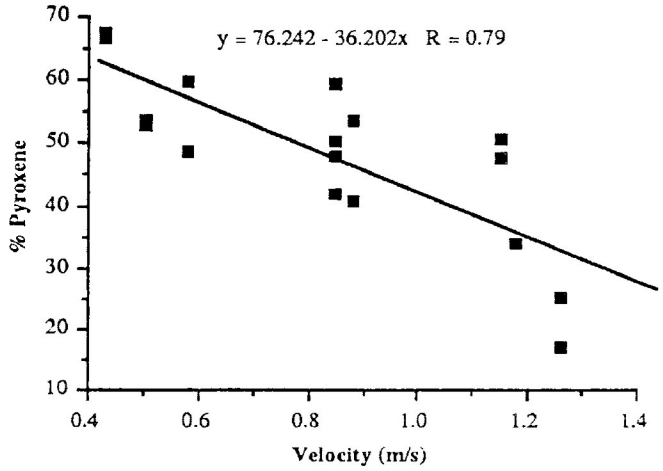

b) % Pyroxene vs Velocity

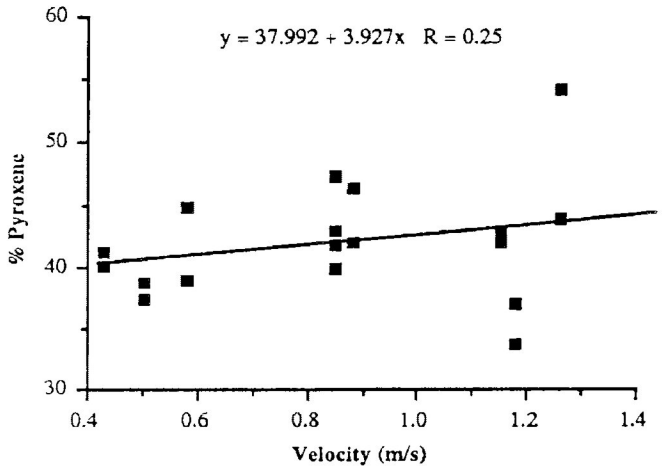

c) % Pyroxene vs Velocity

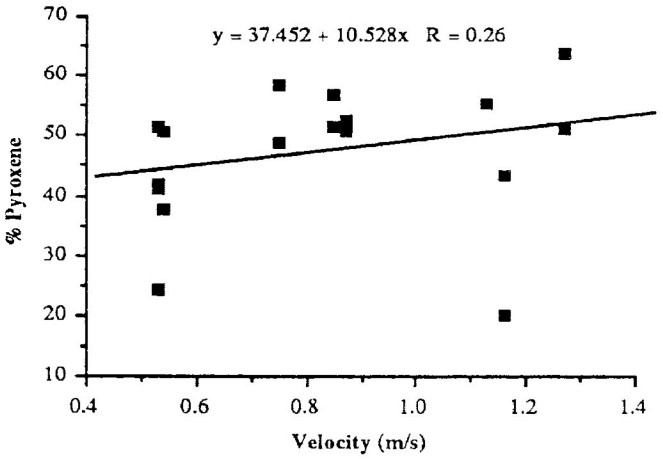

d) % Pyroxene vs Velocity

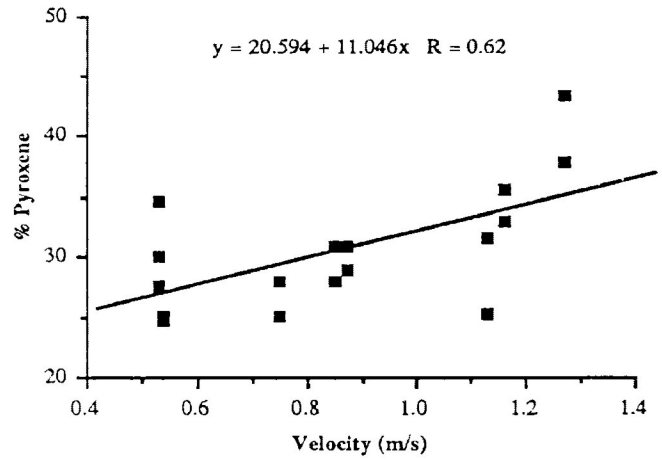

e) % Pyroxene vs Velocity

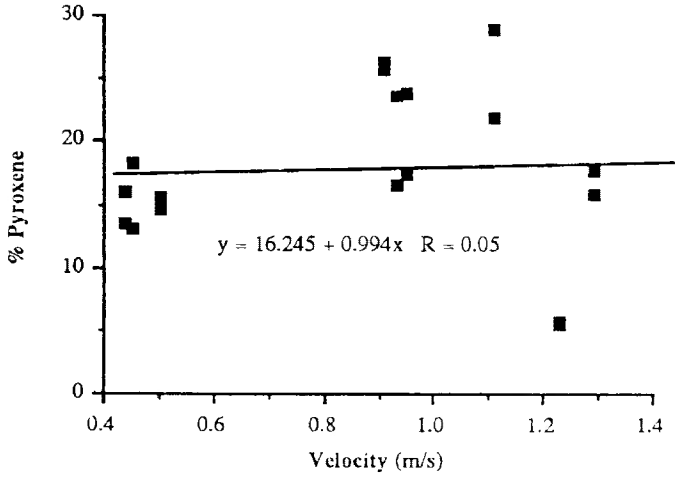

f) % Pyroxene vs Velocity

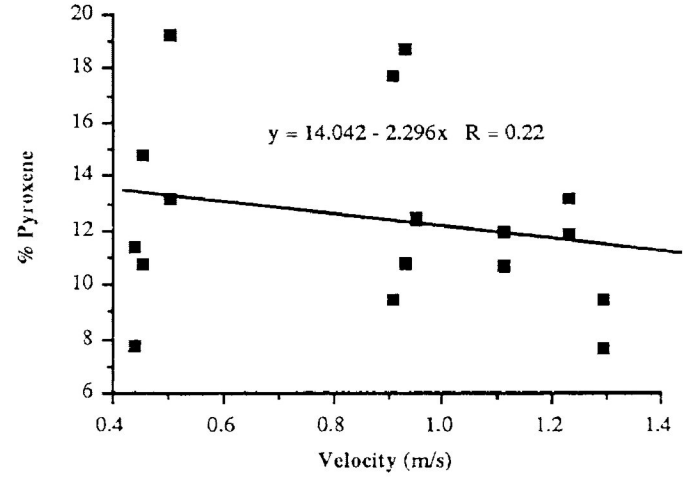

Appendix 2.6

a) % Pyroxene vs Clast Size

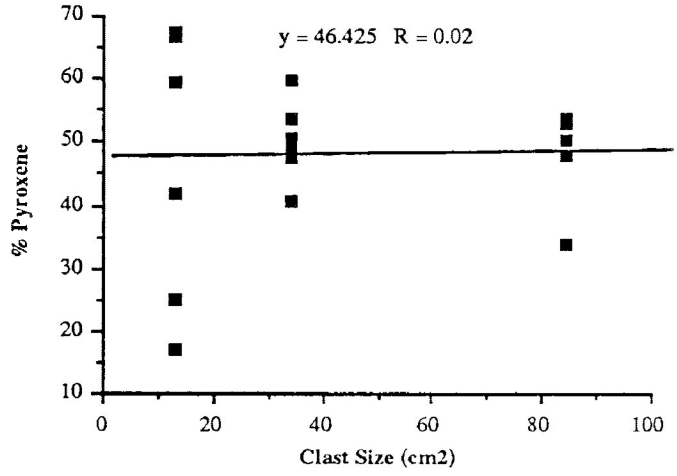

b) % Pyroxene vs Clast Size

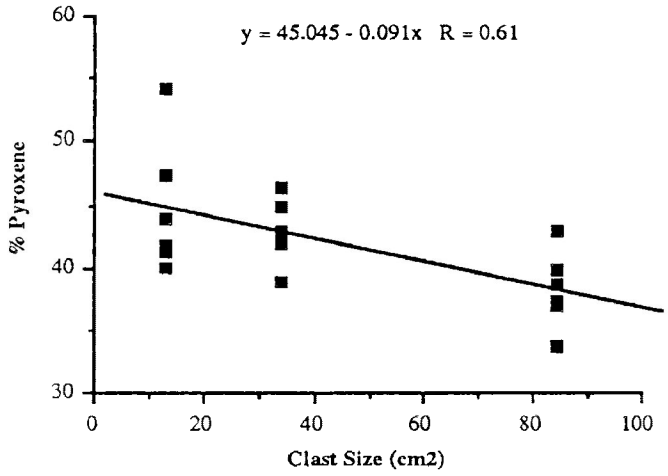

c) % Pyroxene vs Clast Size

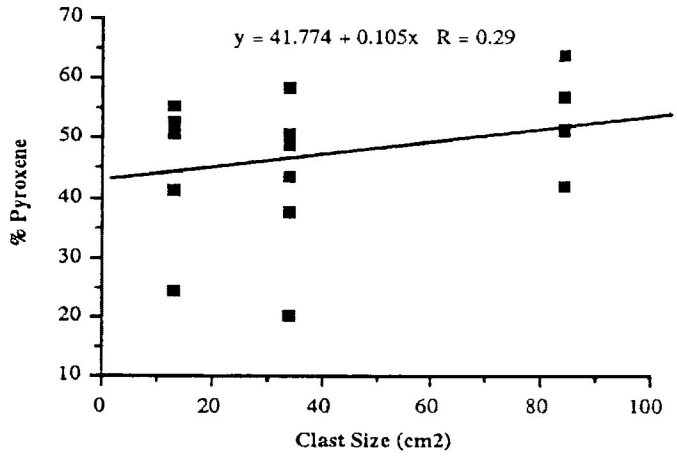

d) % Pyroxene vs Clast Size

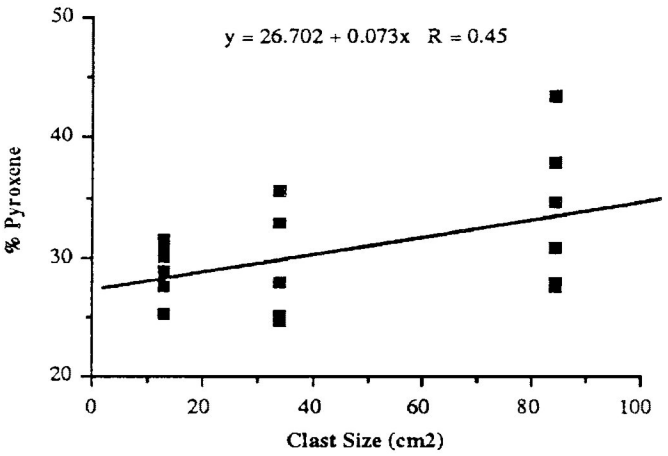

e) % Pyroxene vs Clast Size

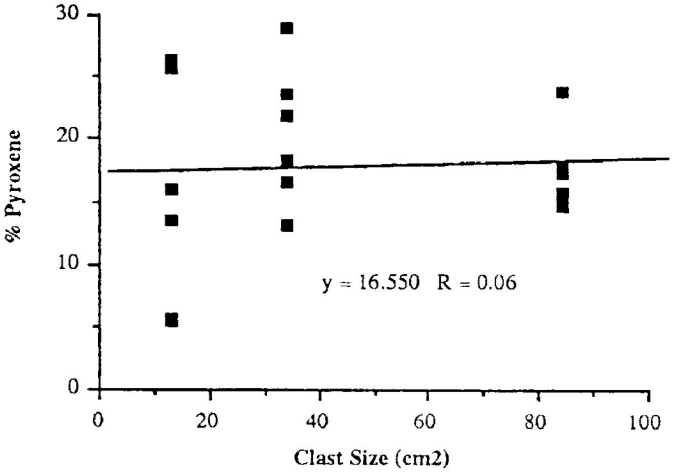

f) % Pyroxene vs Clast Size

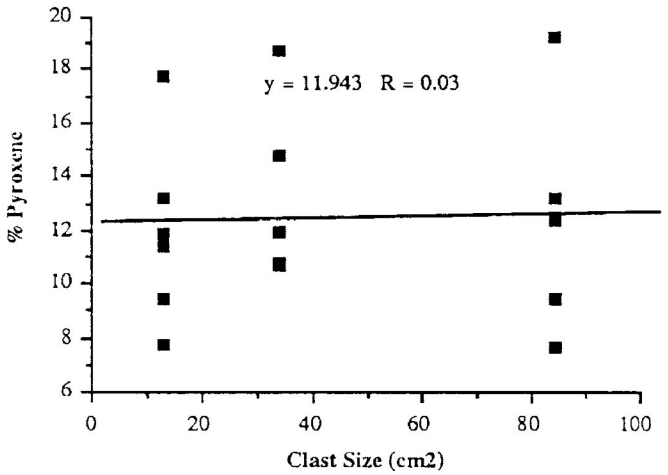

Appendix 2.7

a) % Pyroxene vs Mean Quartz

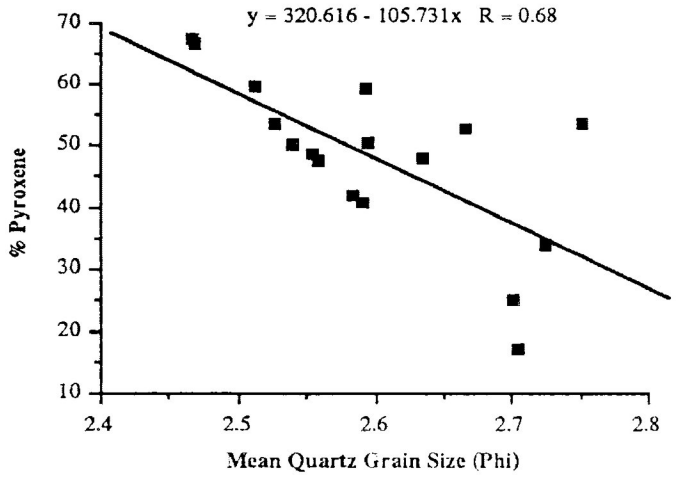

b) % Pyroxene vs Mean Quartz

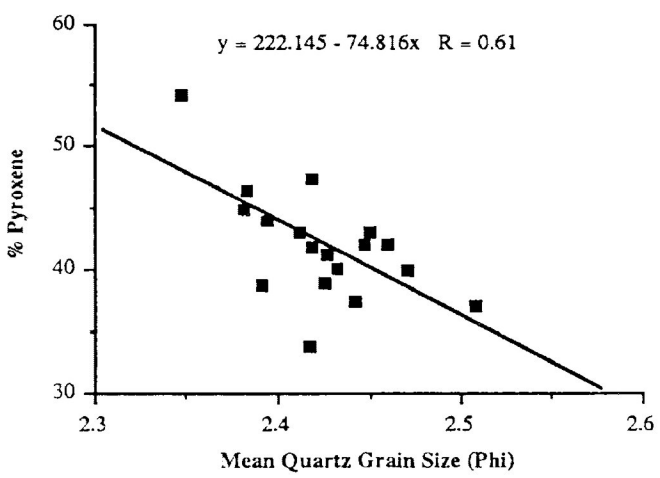

c) % Pyroxene vs Mean Quartz

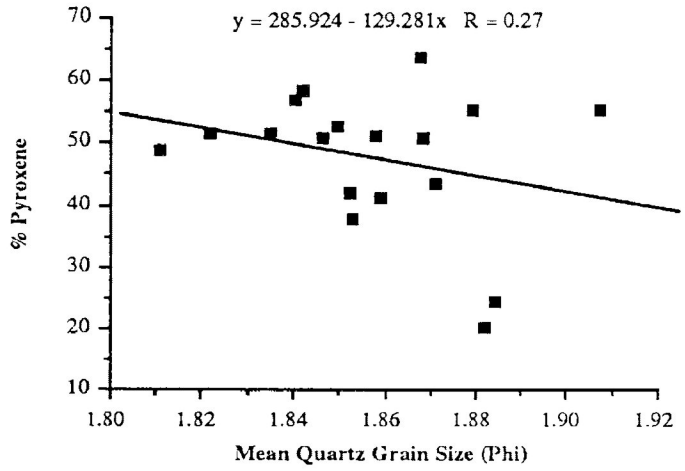

d) % Pyroxene vs Mean Quartz

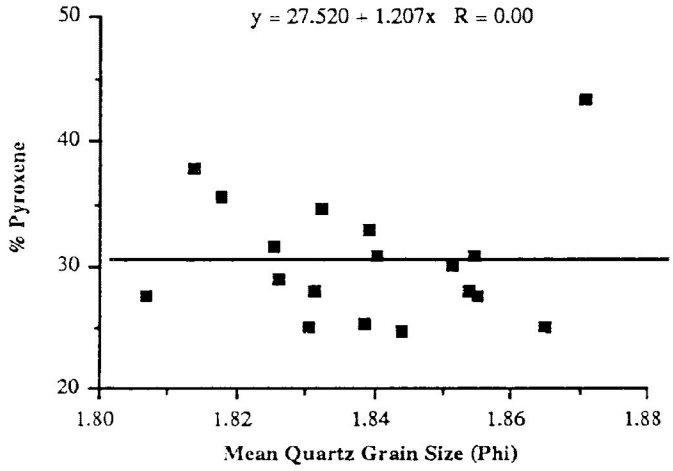

e) % Pyroxene vs Mean Quartz

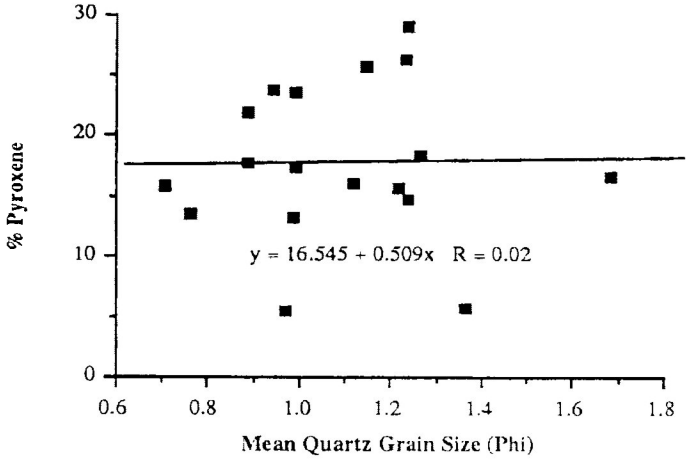

f) % Pyroxene vs Mean Quartz

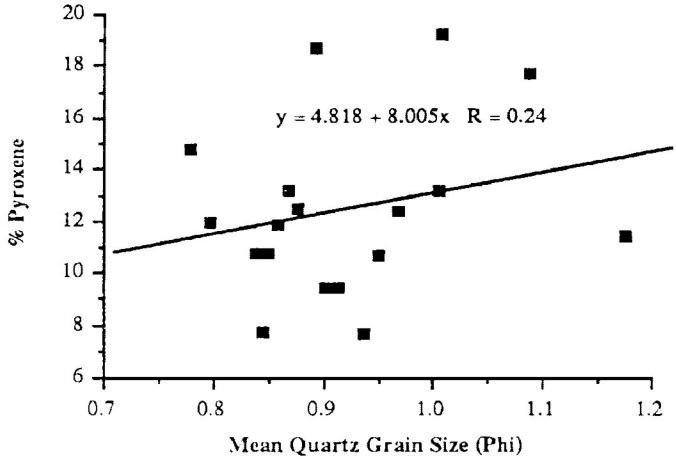

Appendix 2.8

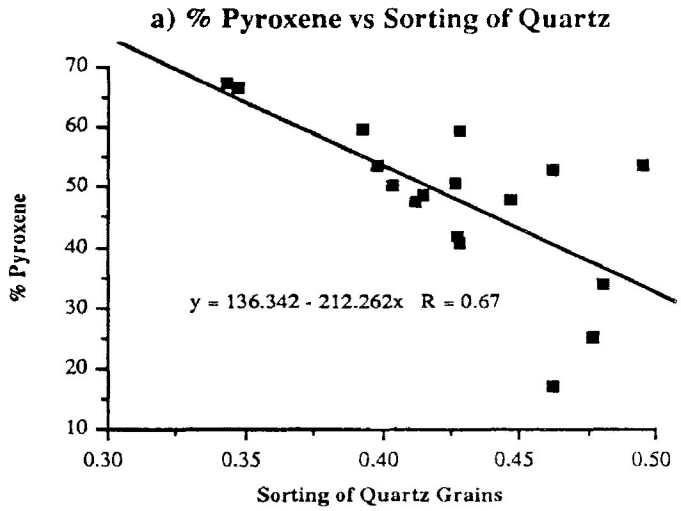
a) % Pyroxene vs Sorting of Quartz
y = 136.342 - 212.262x R = 0.67
% Pyroxene
Sorting of Quartz Grains

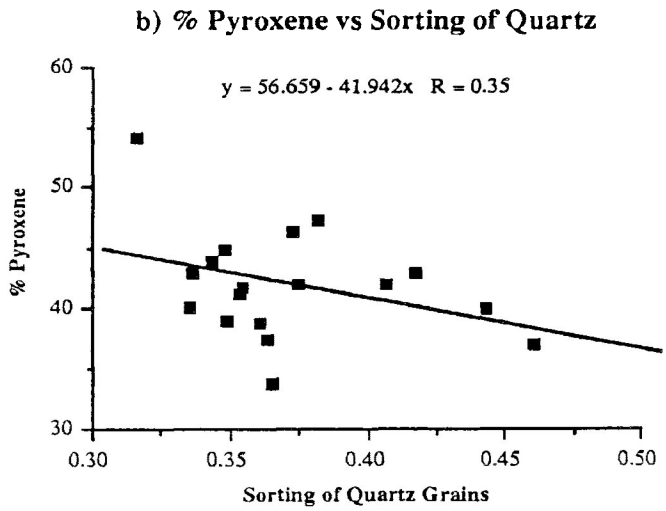
b) % Pyroxene vs Sorting of Quartz
y = 56.659 - 41.942x R = 0.35
% Pyroxene
Sorting of Quartz Grains

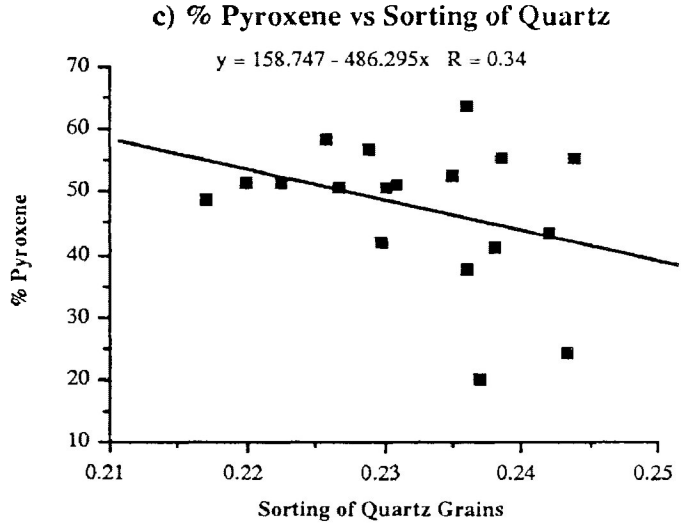
c) % Pyroxene vs Sorting of Quartz
y = 158.747 - 486.295x R = 0.34
% Pyroxene
Sorting of Quartz Grains

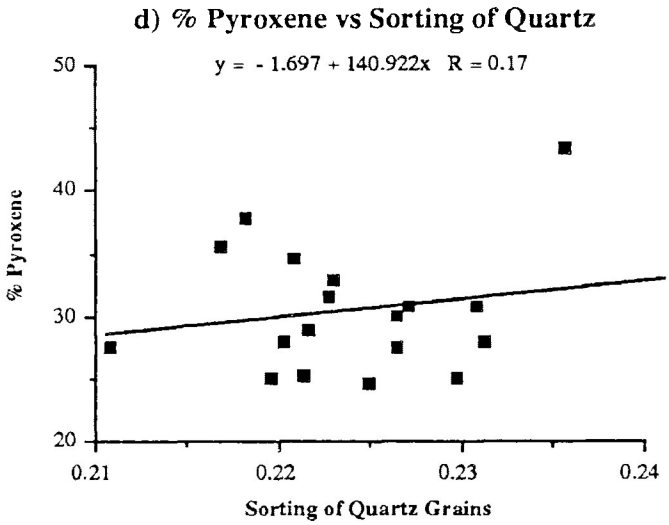
d) % Pyroxene vs Sorting of Quartz
y = - 1.697 + 140.922x R = 0.17
% Pyroxene
Sorting of Quartz Grains

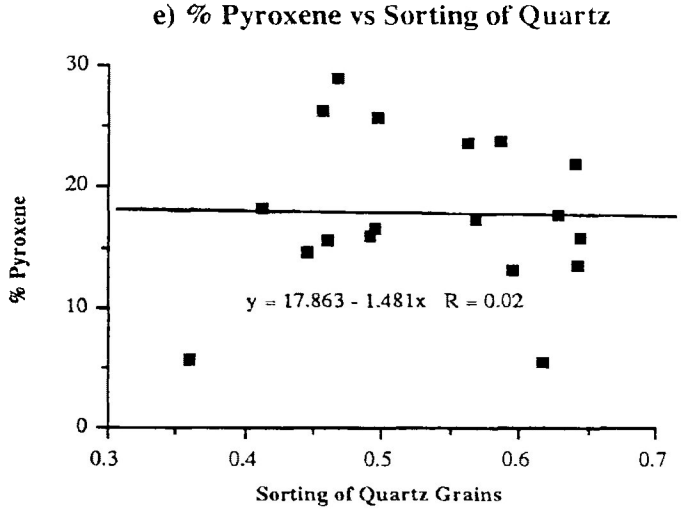
e) % Pyroxene vs Sorting of Quartz
y = 17.863 - 1.481x R = 0.02
% Pyroxene
Sorting of Quartz Grains

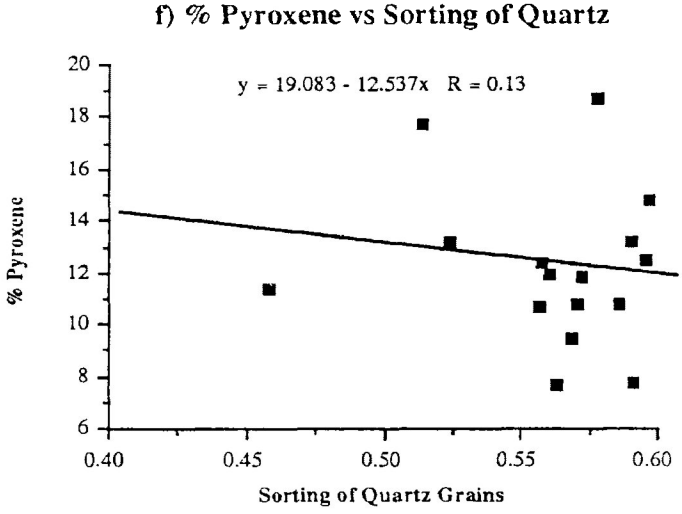
f) % Pyroxene vs Sorting of Quartz
y = 19.083 - 12.537x R = 0.13
% Pyroxene
Sorting of Quartz Grains

Appendix 2.9

a) Mean Pyroxene vs Velocity

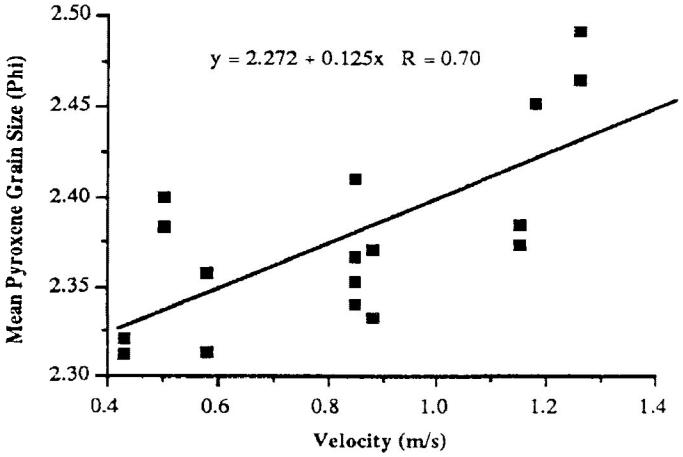

b) Mean Pyroxene vs Velocity

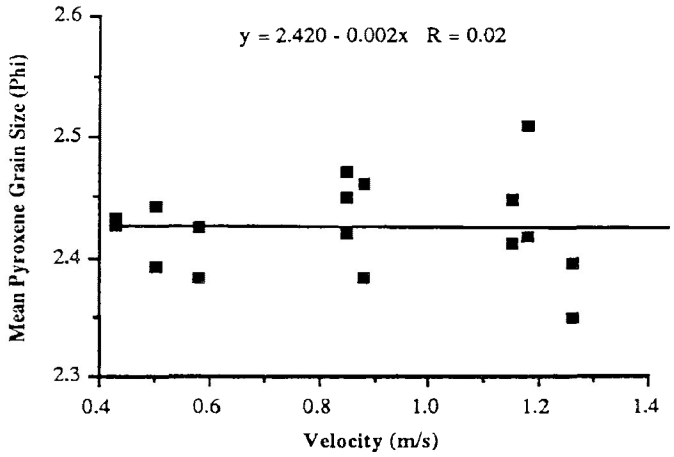

c) Mean Pyroxene vs Velocity

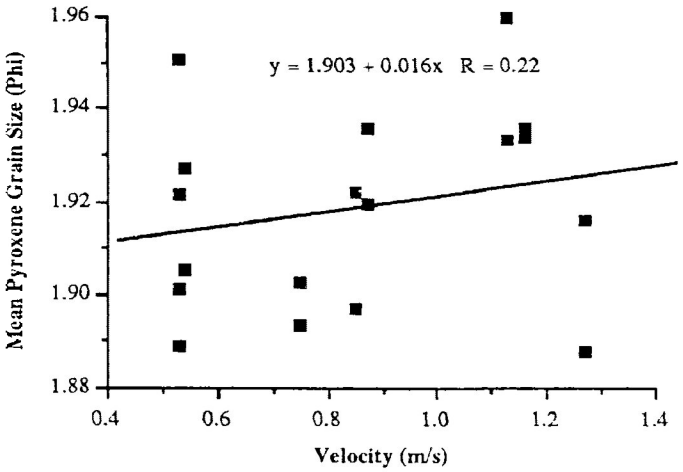

d) Mean Pyroxene vs Velocity (Bot Med)

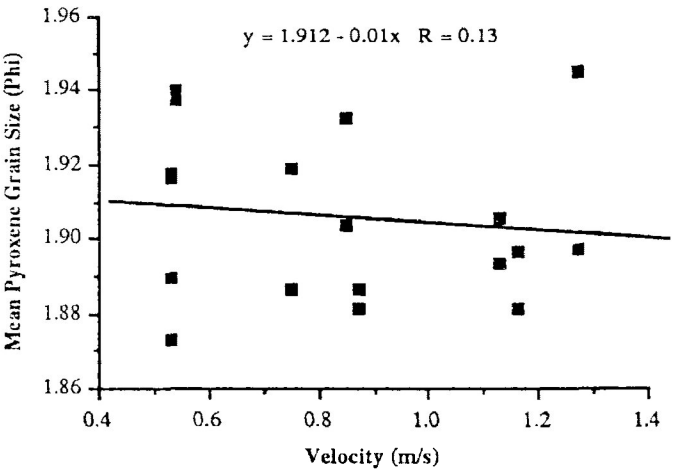

e) Mean Pyroxene vs Velocity

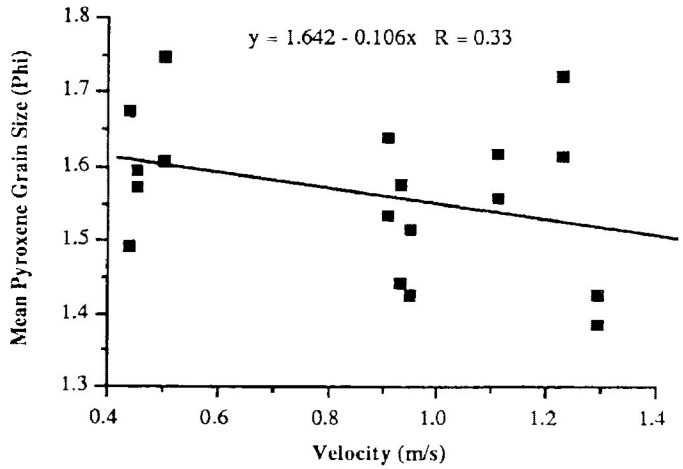

f) Mean Pyroxene vs Velocity

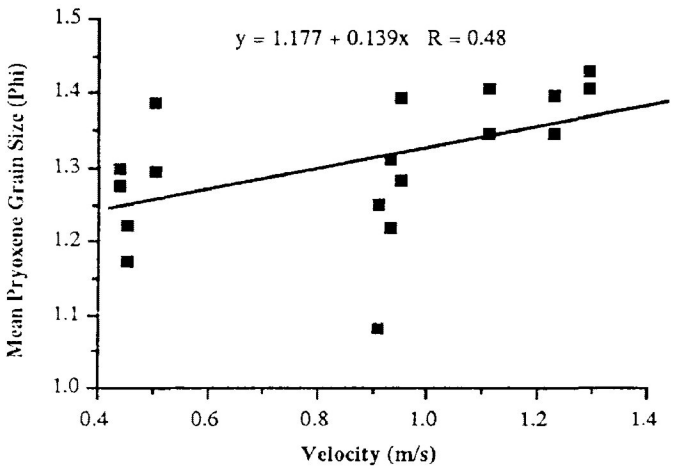

Appendix 2.10

a) Sorting of Pyroxene vs Velocity

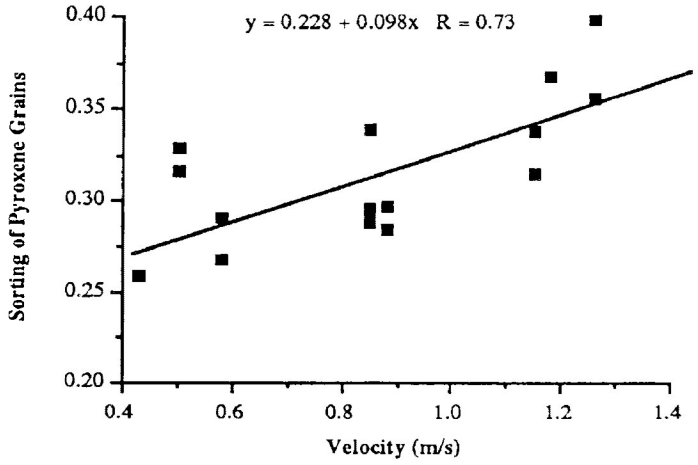

b) Sorting of Pyroxene vs Velocity

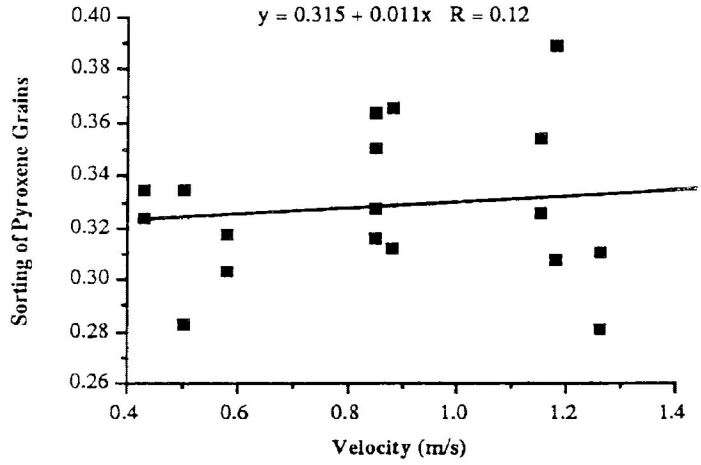

c) Sorting of Pyroxene vs Velocity

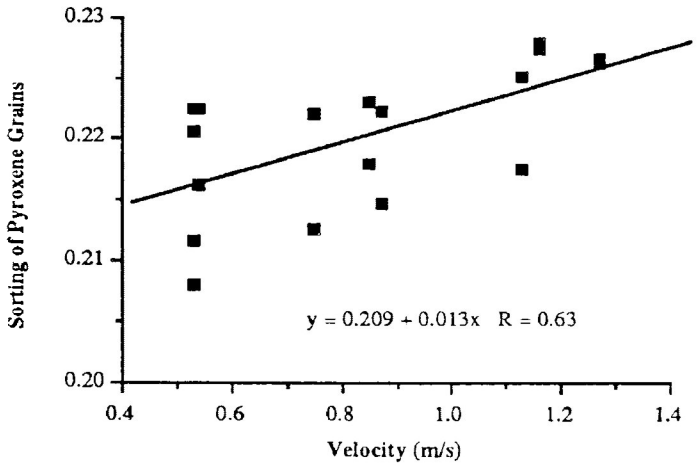

d) Sorting of Pyroxene vs Velocity

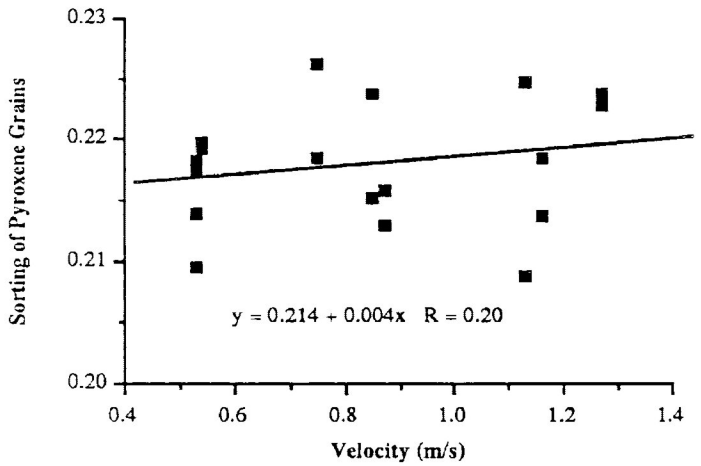

e) Sorting of Pyroxene vs Velocity

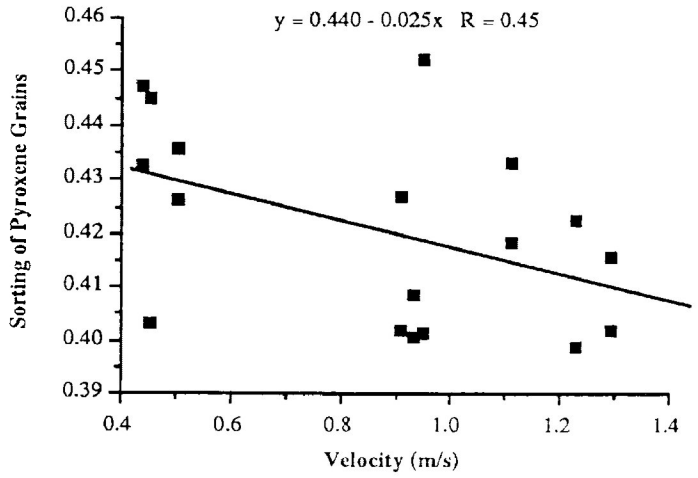

f) Sorting of Pyroxene vs Velocity

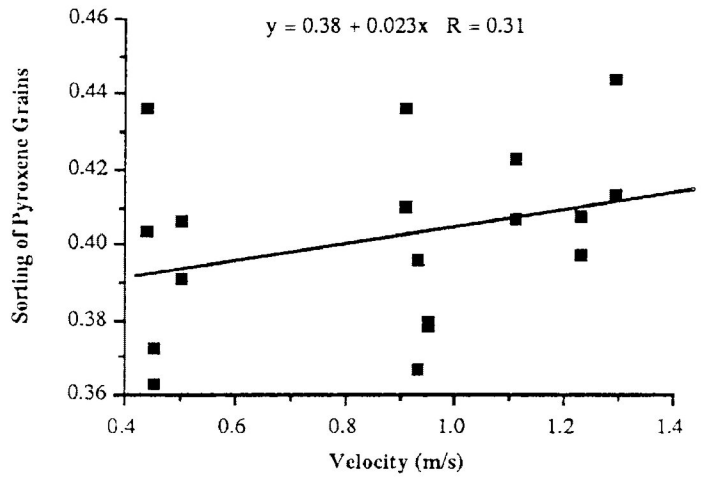

Appendix 2.11

a) % Magnetite vs Velocity

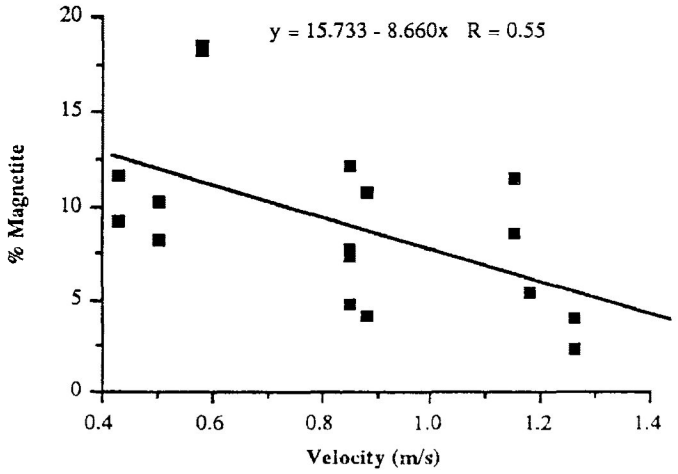

b) % Magnetite vs Velocity

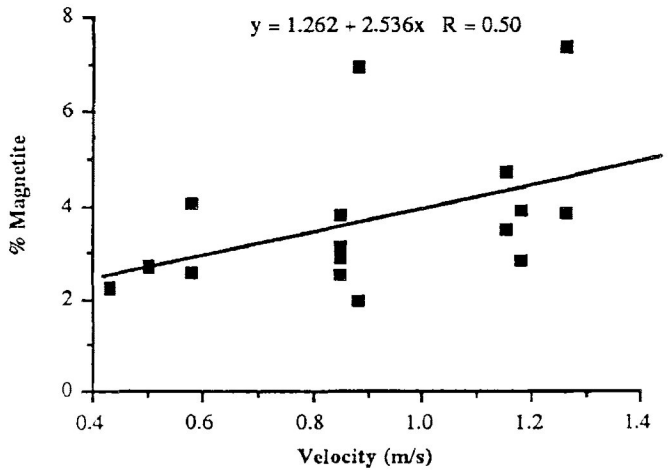

c) % Magnetite vs Velocity

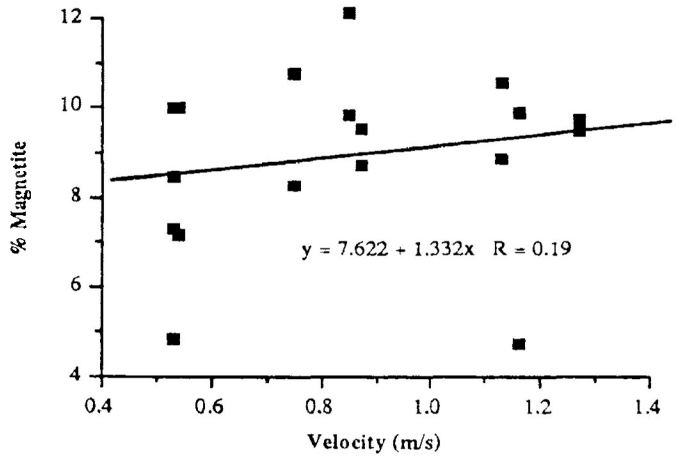

d) % Magnetite vs Velocity

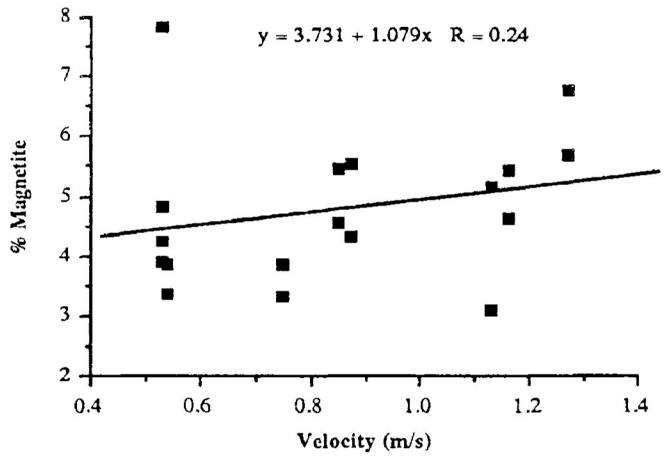

e) % Magnetite vs Velocity

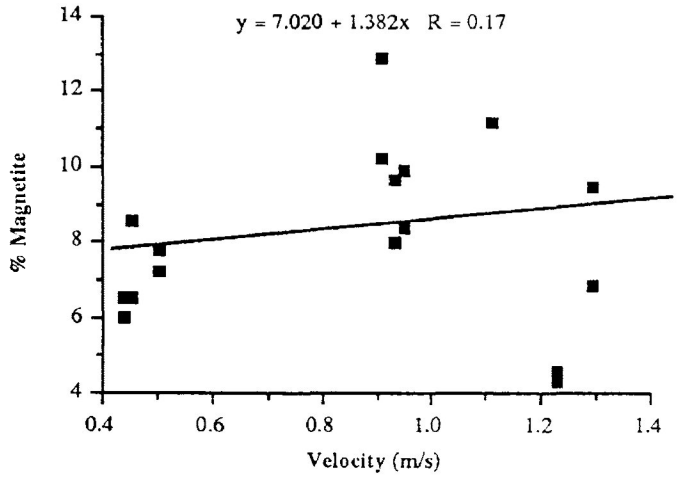

f) % Magnetite vs Velocity

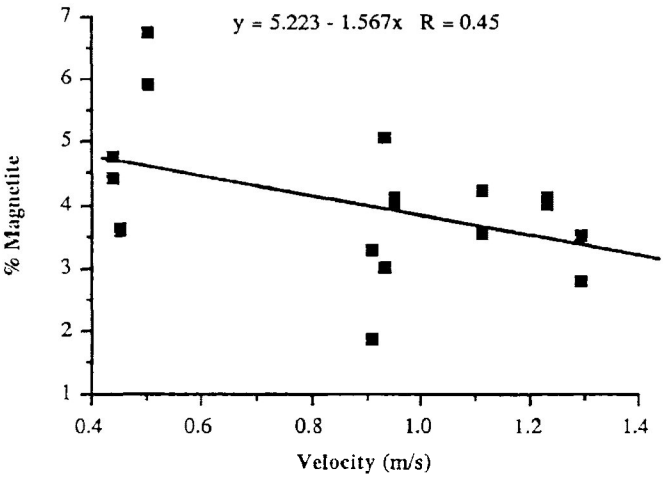

Appendix 2.12

a) % Magnetite vs Clast Size

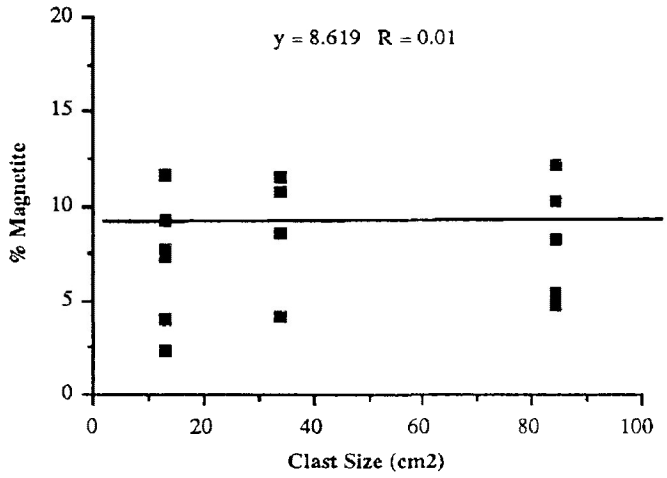

b) % Magnetite vs Clast Size

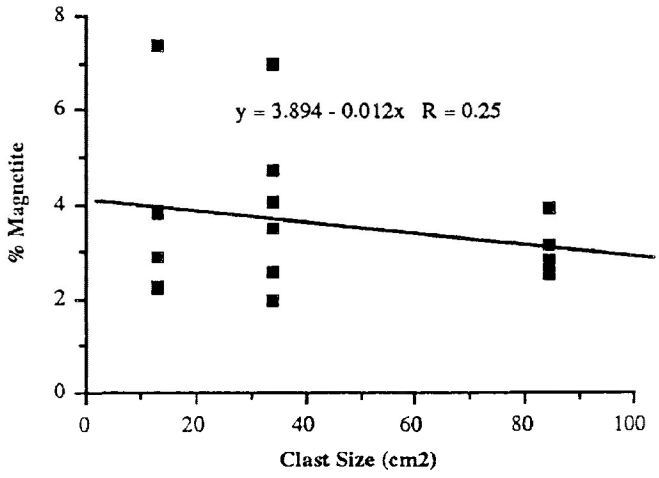

c) % Magnetite vs Clast Size

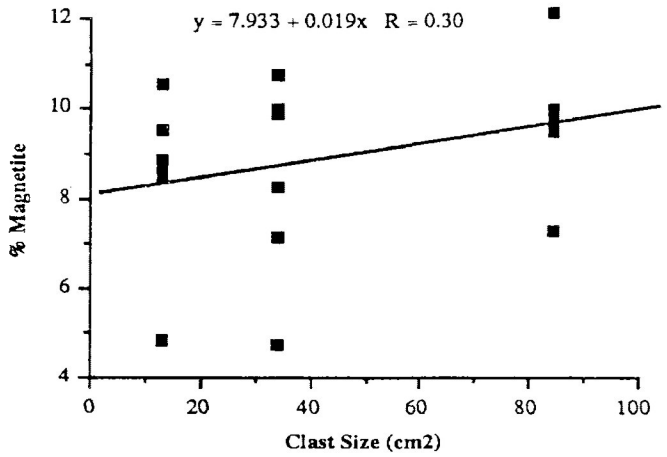

d) % Magnetite vs Clast Size

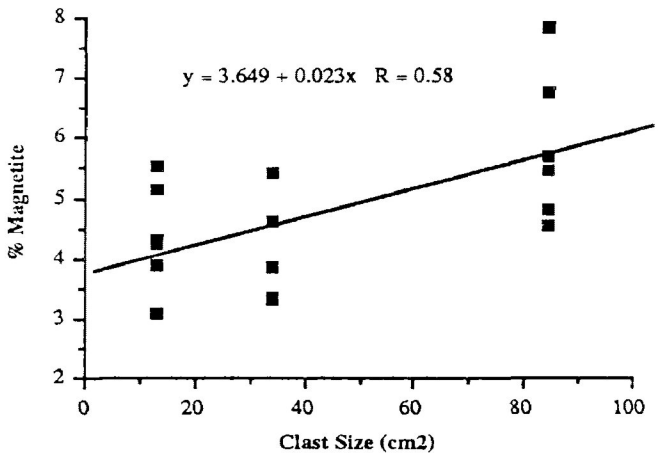

e) % Magnetite vs Clast Size

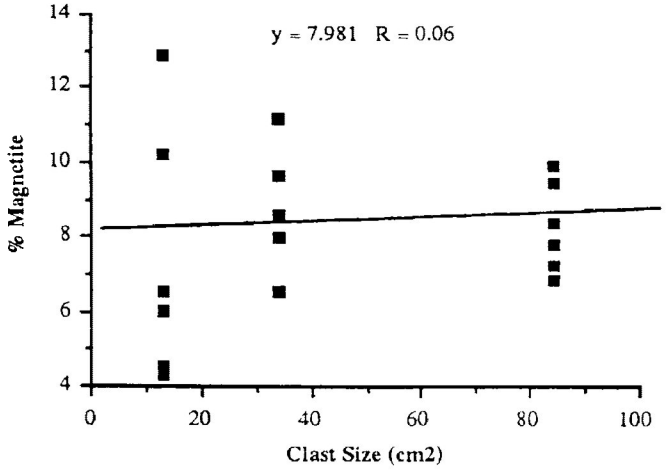

f) % Magnetite vs Clast Size

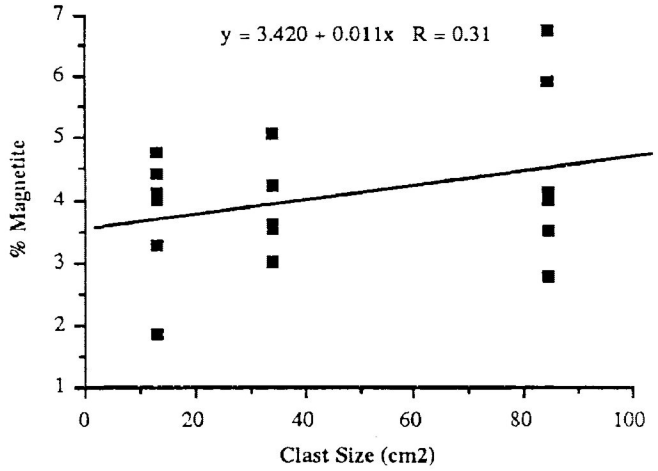

Appendix 2.13

a) % Magnetite vs Mean Quartz

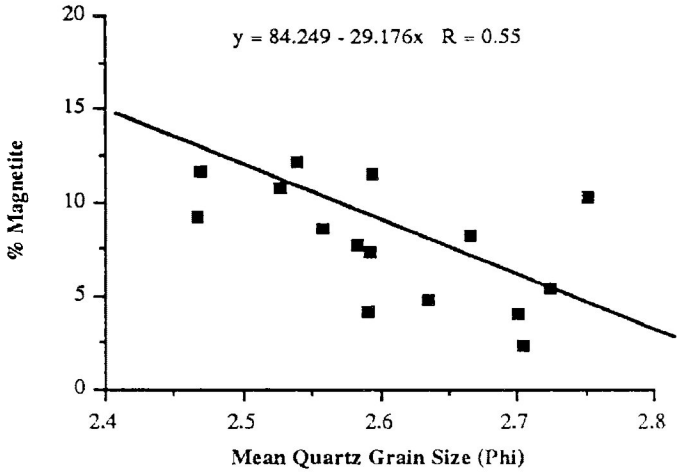

b) % Magnetite vs Mean Quartz

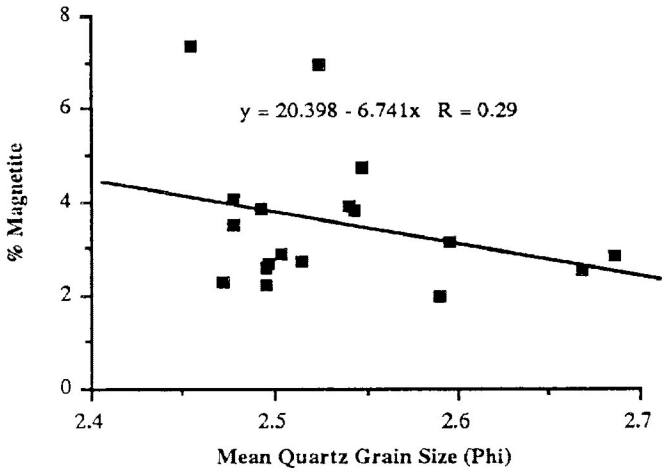

c) % Magnetite vs Mean Quartz

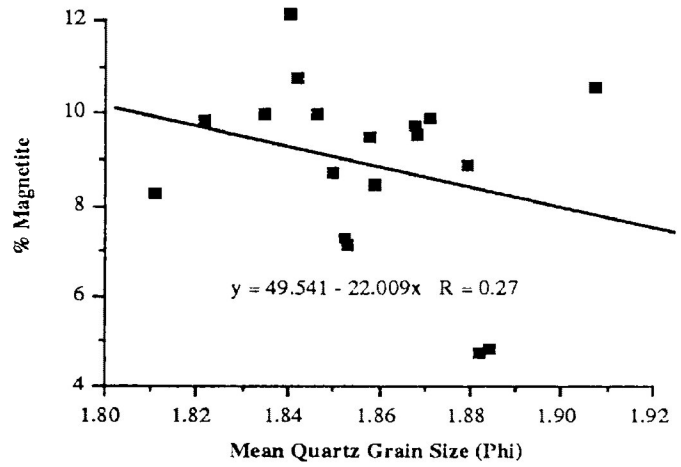

d) % Magnetite vs Mean Quartz

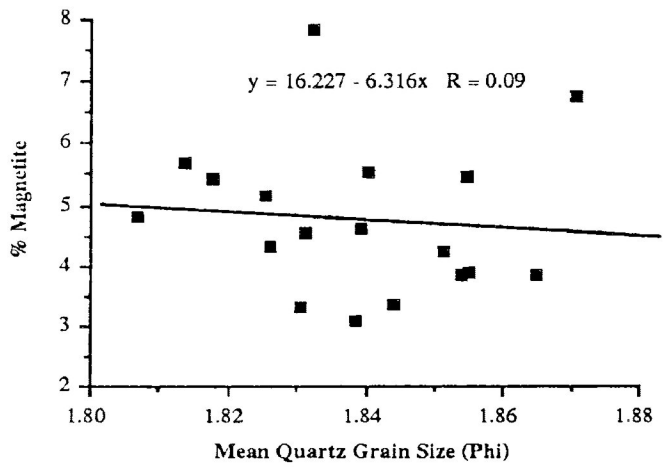

e) % Magnetite vs Mean Quartz

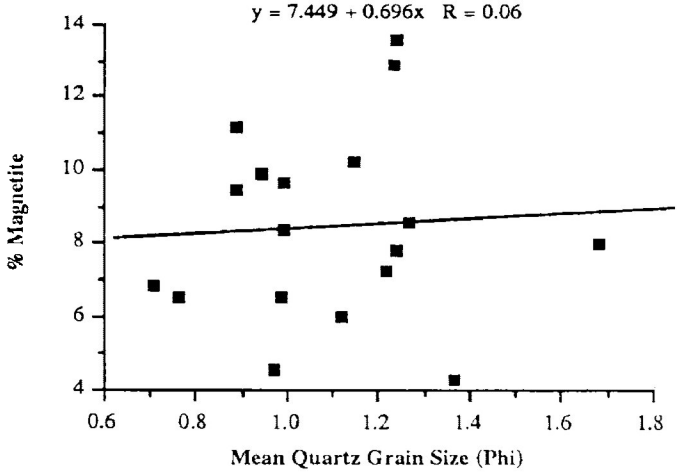

f) % Magnetite vs Mean Quartz

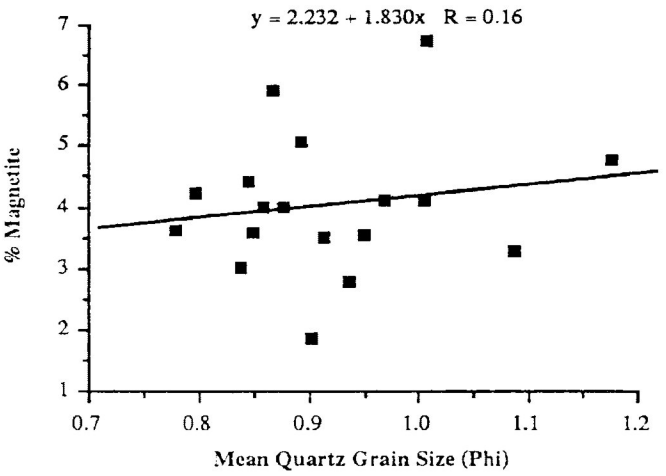

Appendix 2.14

a) % Magnetite vs Quartz Sorting

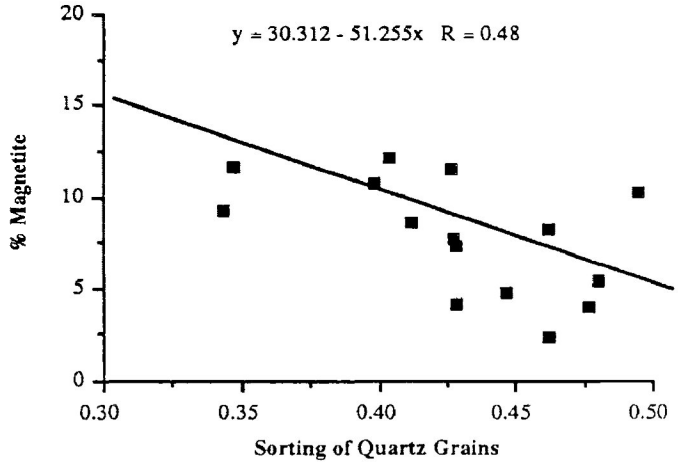

b) % Magnetite vs Sorting of Quartz

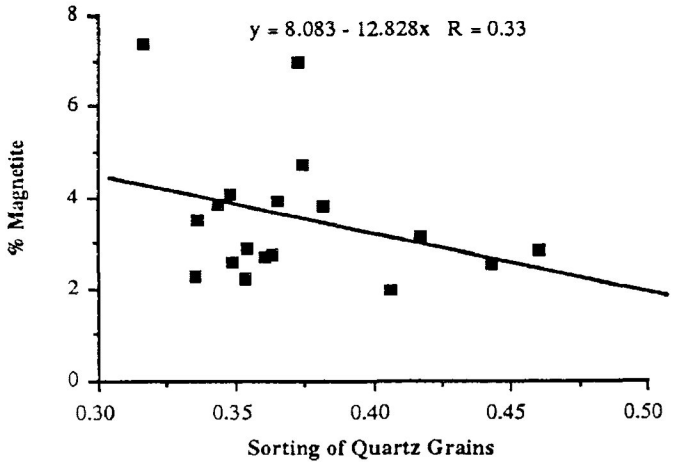

c) % Magnetite vs Sorting of Quartz

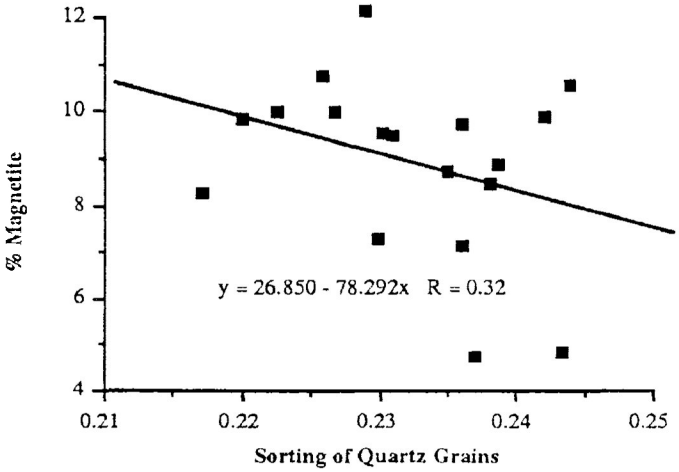

d) % Magnetite vs Sorting of Quartz

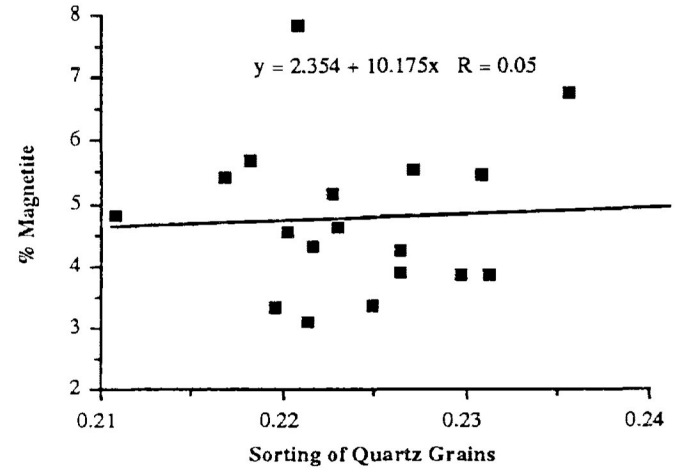

e) % Magnetite vs Sorting of Quartz

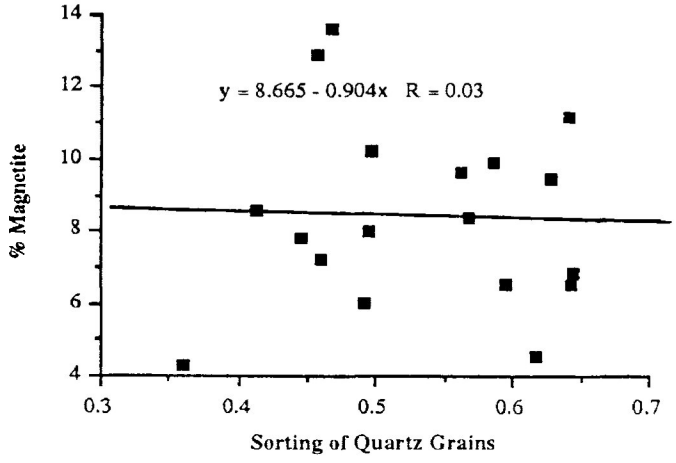

f) % Magnetite vs Sorting of Quartz

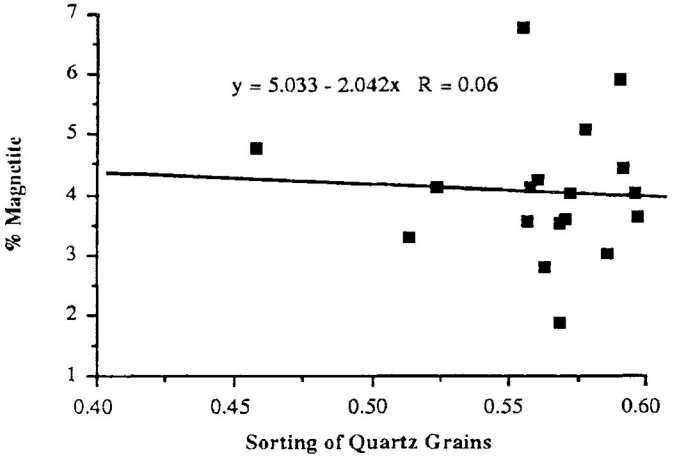

Appendix 2.15

a) Mean Magnetite vs Velocity

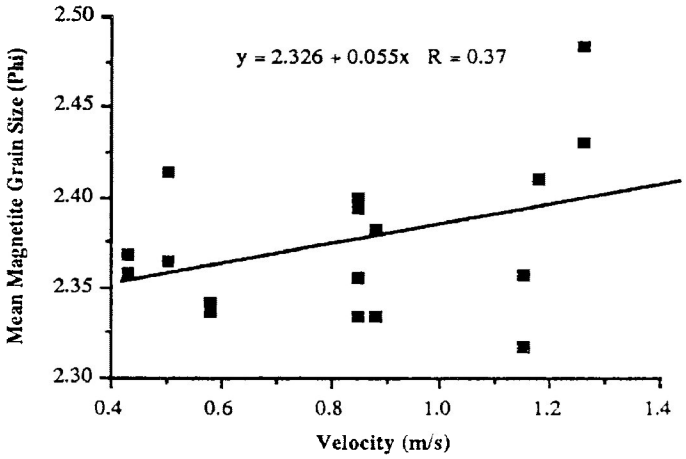

b) Mean Magnetite vs Velocity

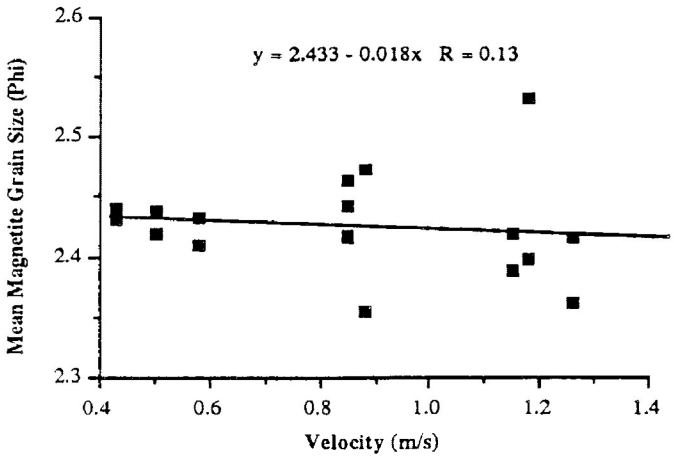

c) Mean Magnetite vs Velocity

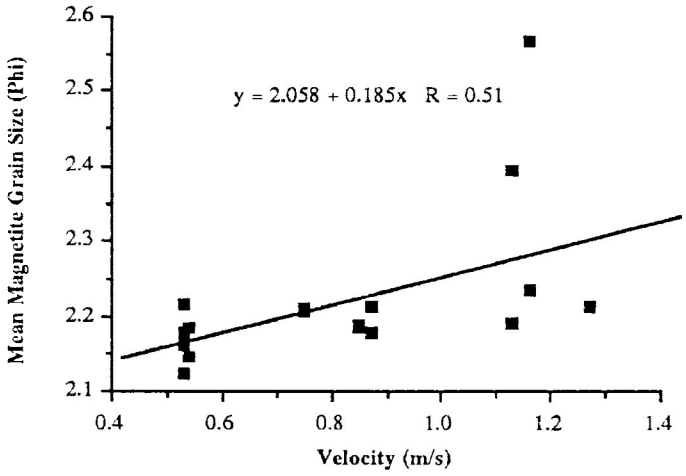

d) Mean Magnetite vs Velocity

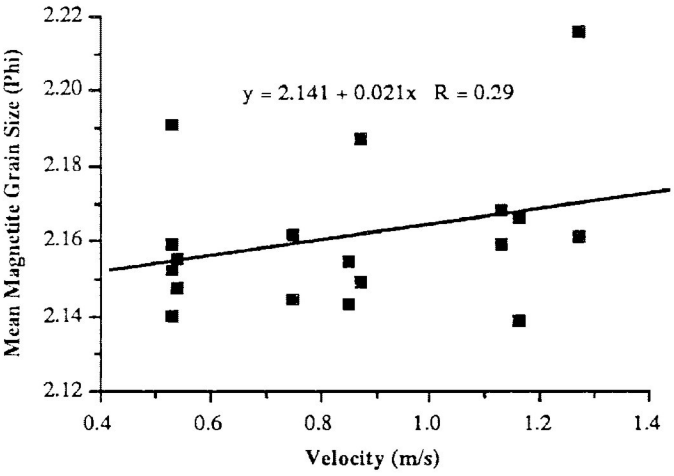

e) Mean Magnetite vs Velocity

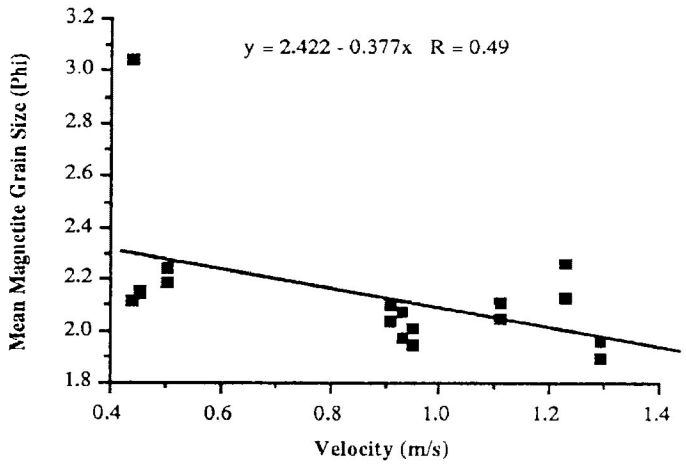

f) Mean Magnetite vs Velocity

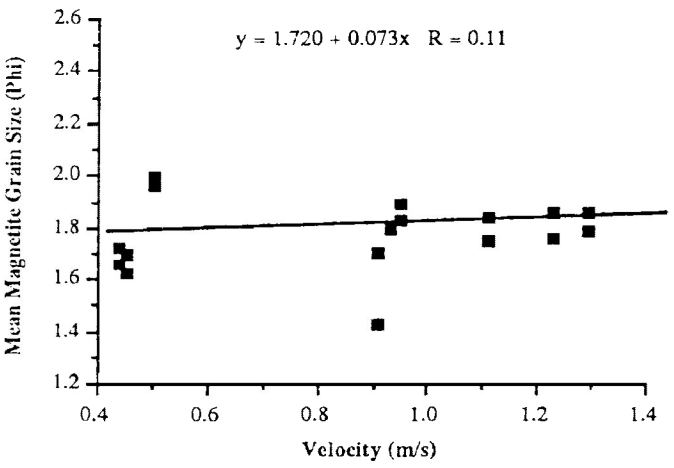

Appendix 2.16

a) Sorting of Magnetite vs Velocity

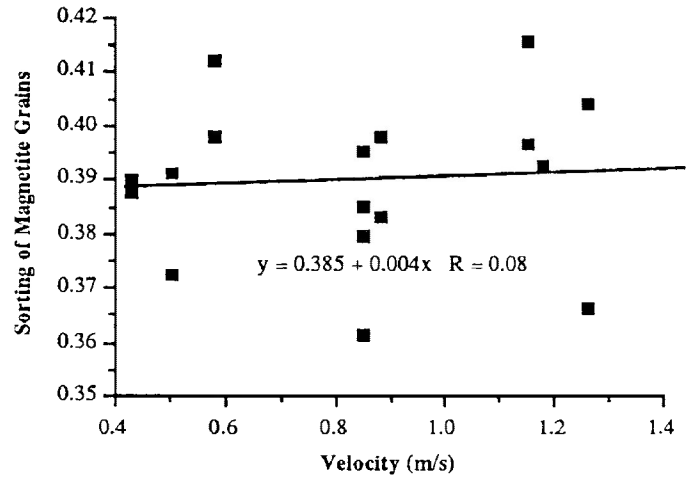

b) Sorting of Magnetite vs Velocity

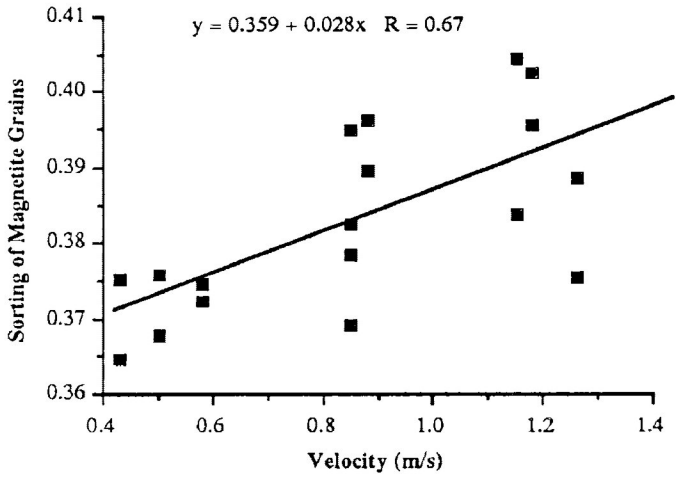

c) Sorting of Magnetite vs Velocity

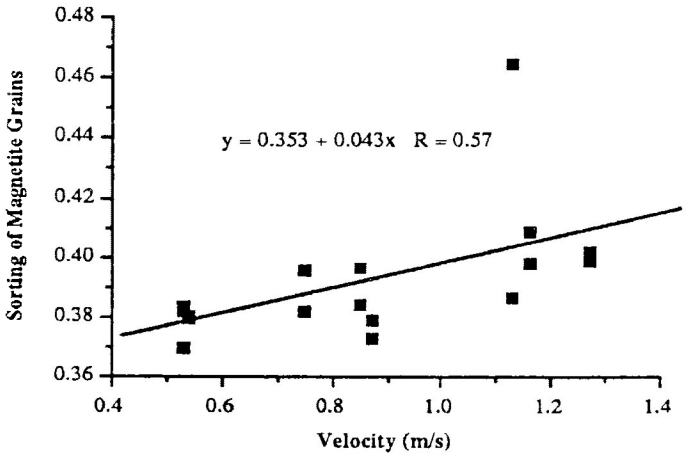

d) Sorting of Magnetite vs Velocity

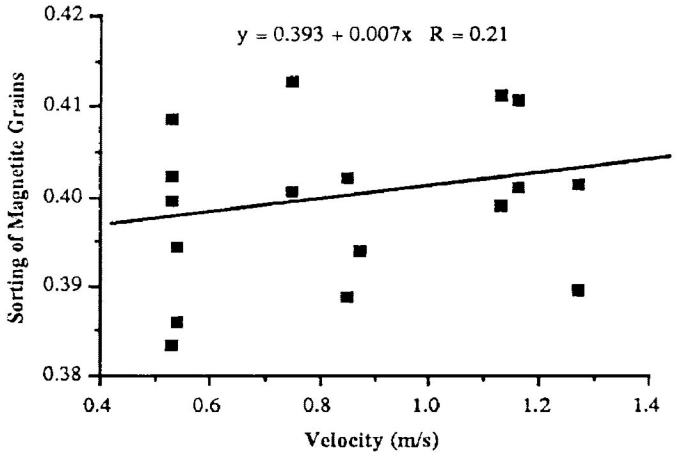

e) Sorting of Magnetite vs Velocity

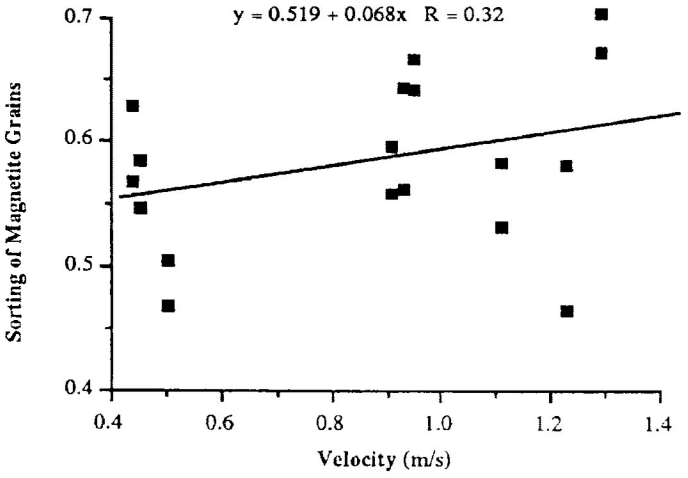

f) Sorting of Magnetite vs Velocity

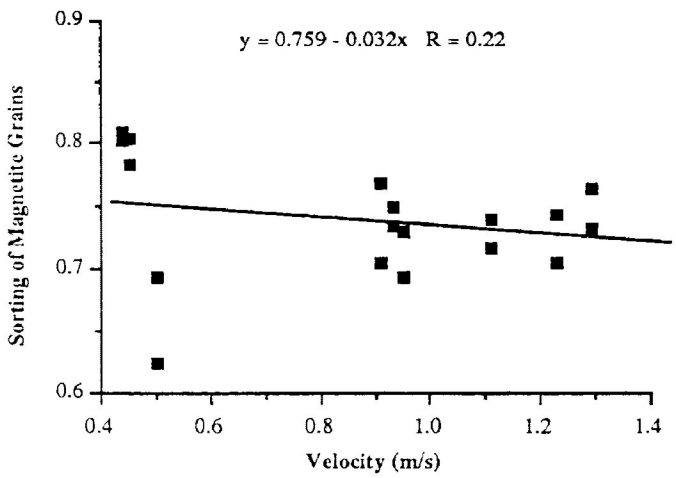

Appendix 2.17

a) % Lead vs Velocity

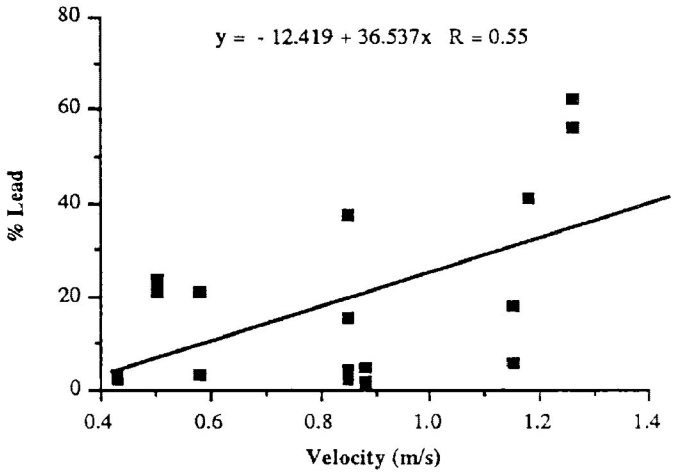

b) % Lead vs Velocity

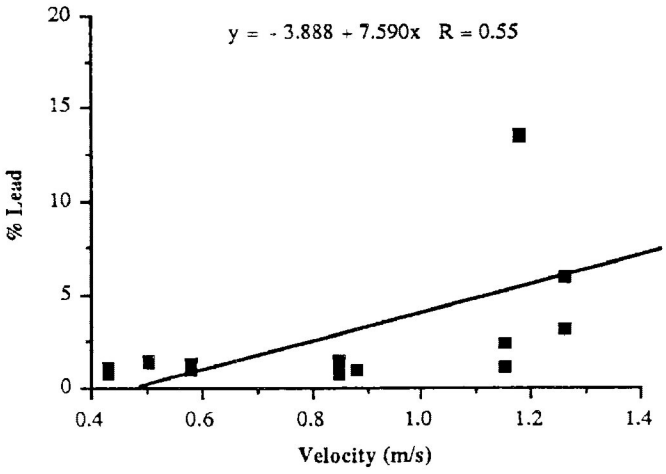

c) % Lead vs Velocity

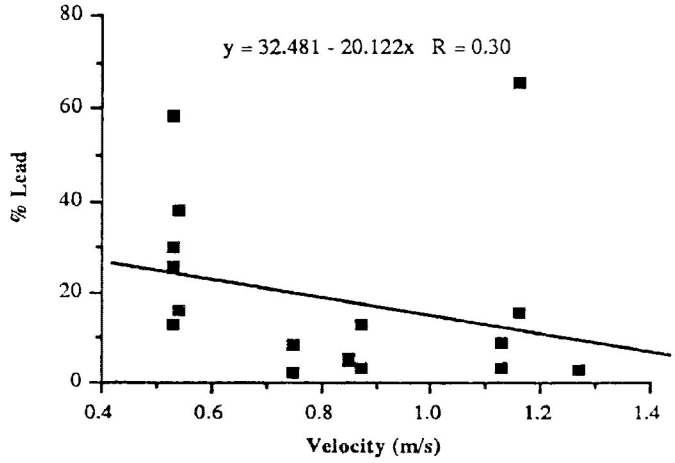

d) % Lead vs Velocity

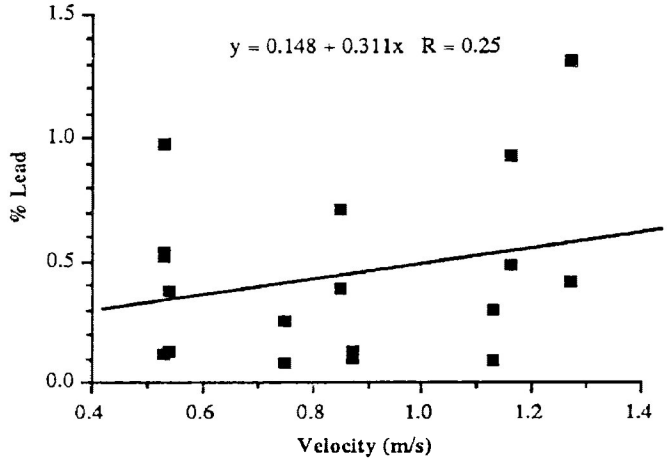

e) % Lead vs Velocity

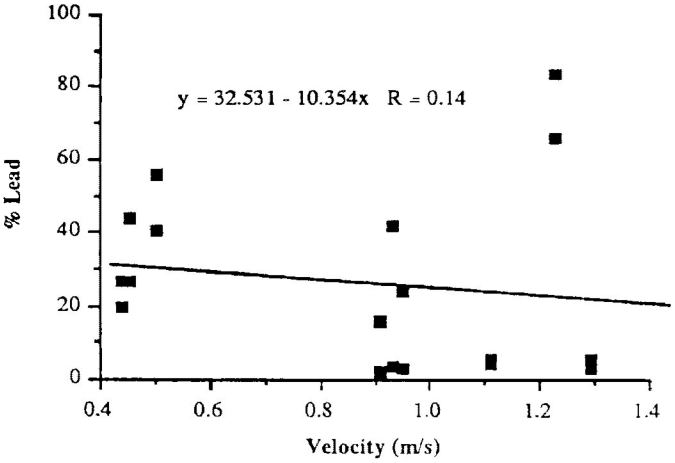

f) % Lead vs Velocity

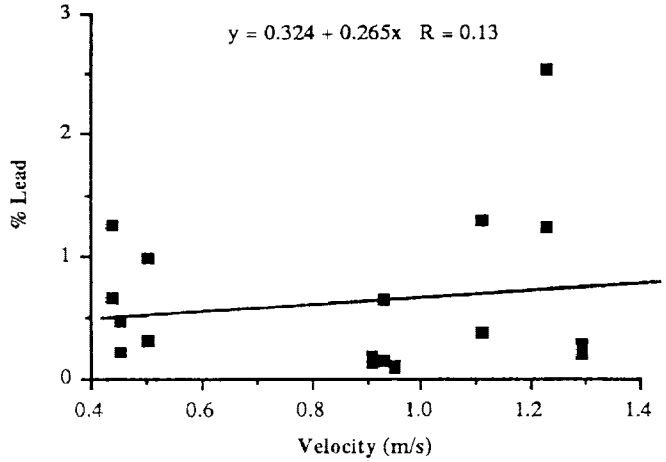

Appendix 2.18

a) % Lead vs Clast Size

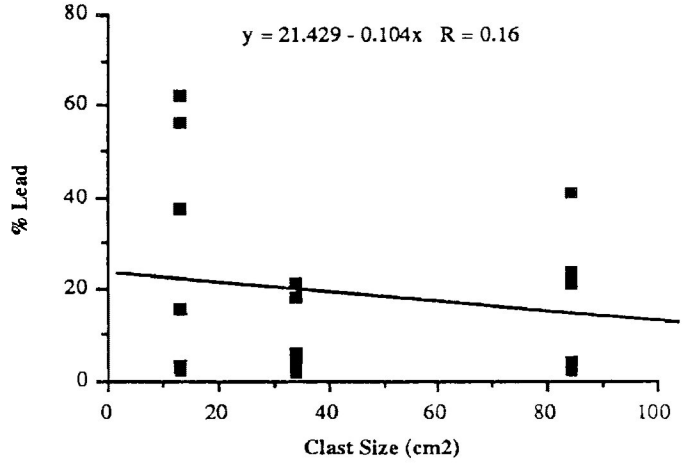

b) % Lead vs Clast Size

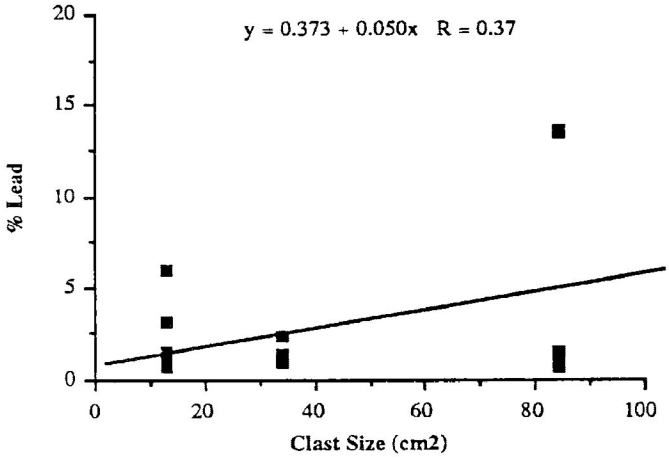

c) % Lead vs Clast Size

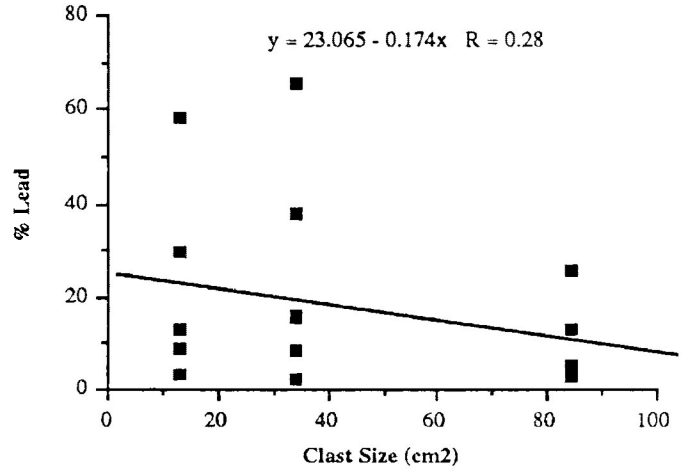

d) % Lead vs Clast Size

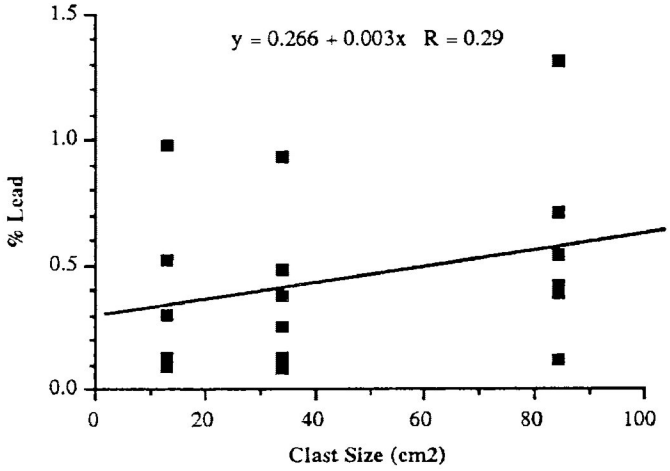

e) % Lead vs Clast Size

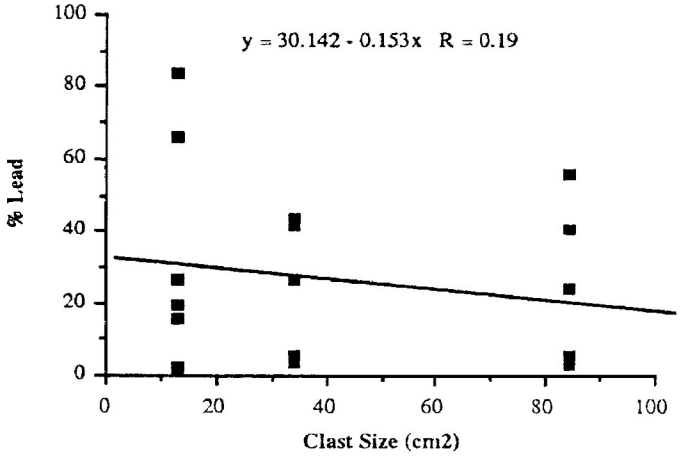

f) % Lead vs Clast Size

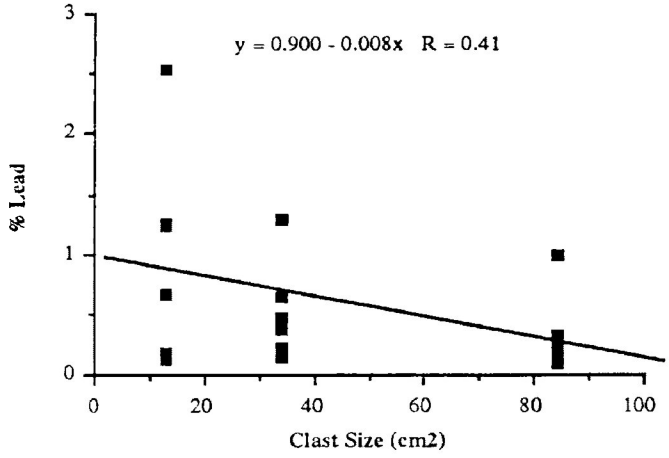

Appendix 2.19

a) % Lead vs Mean Quartz

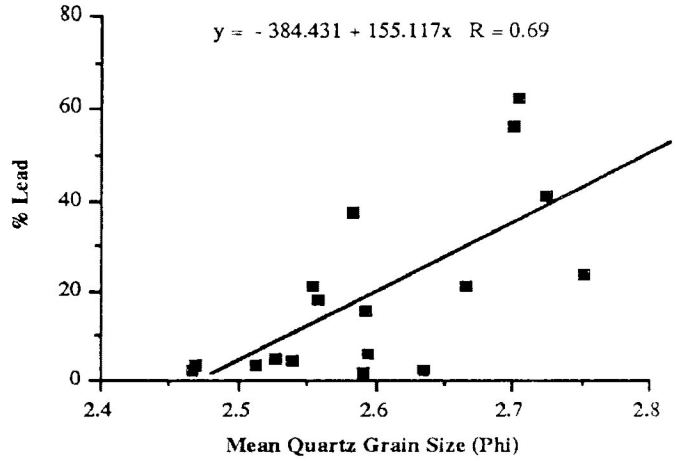

b) % Lead vs Mean Quartz

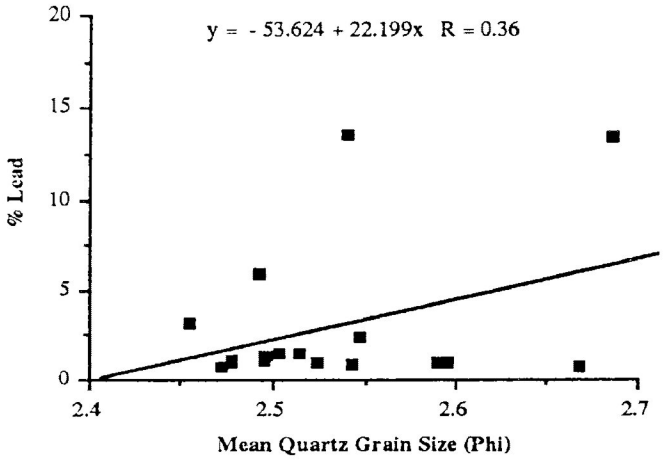

c) % Lead vs Mean Quartz

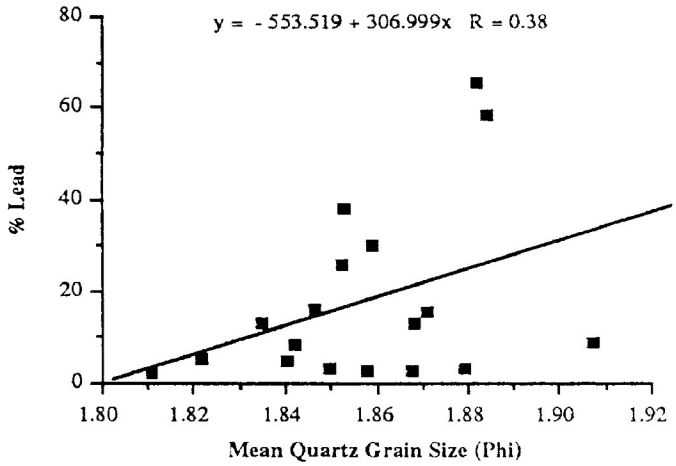

d) % Lead vs Mean Quartz

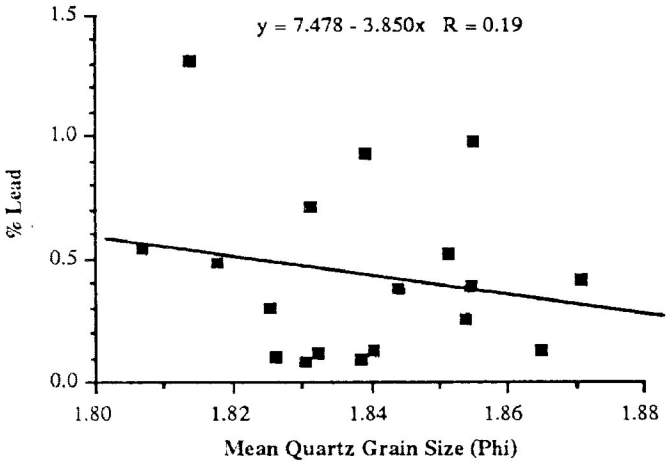

e) % Lead vs Mean Quartz

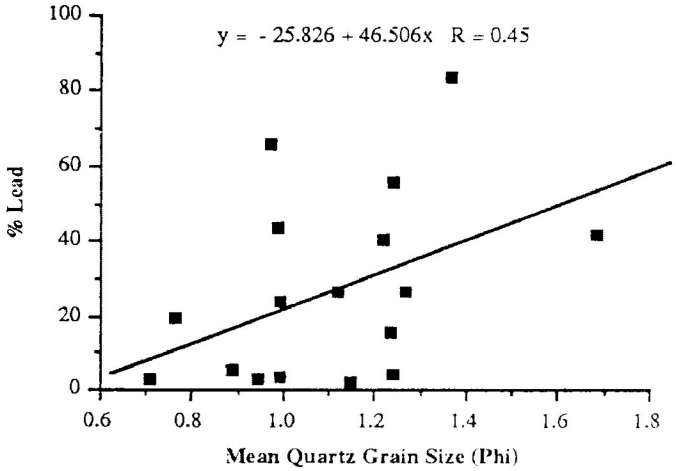

f) % Lead vs Mean Quartz

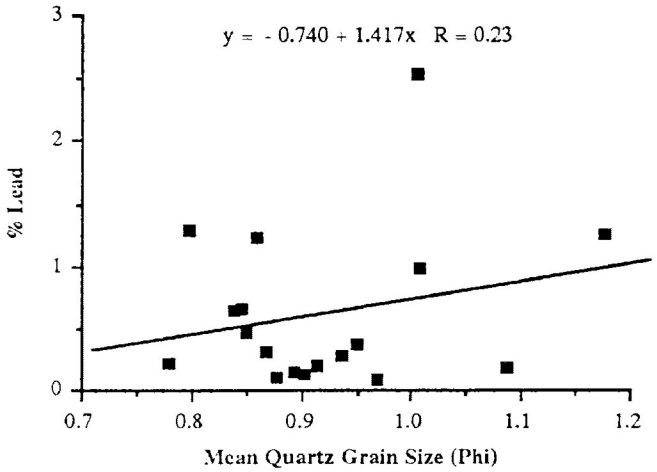

Appendix 2.20

a) % Lead vs Sorting of Quartz

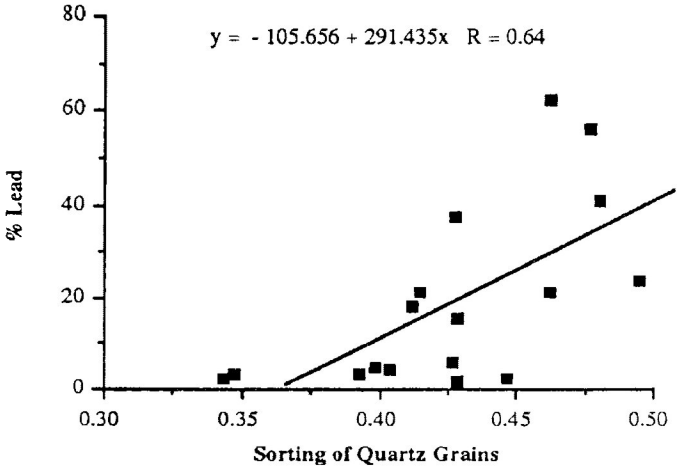

b) % Lead vs Sorting of Quartz

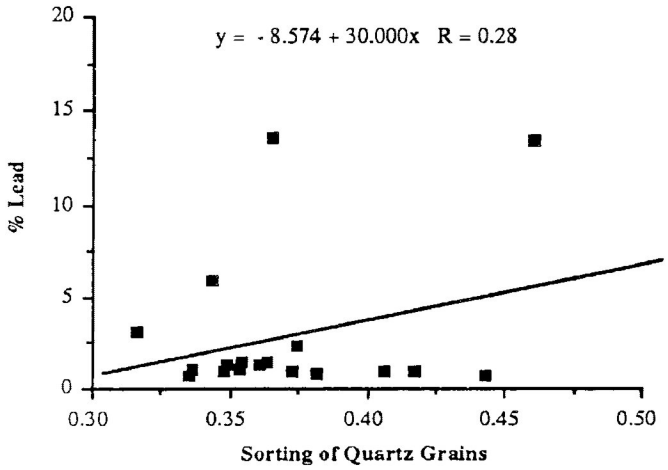

c) % Lead vs Sorting of Quartz

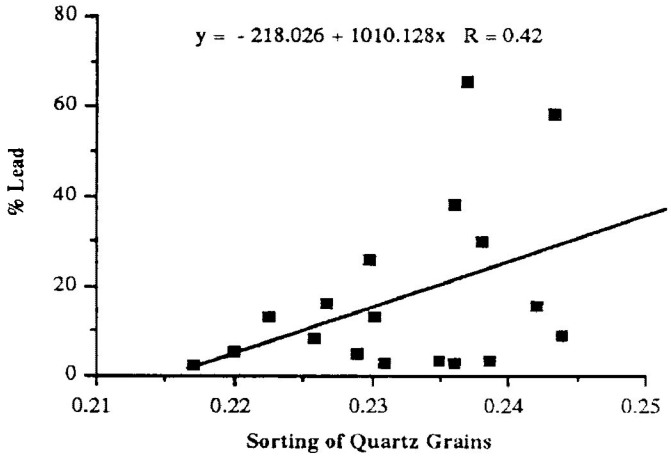

d) % Lead vs Sorting of Quartz

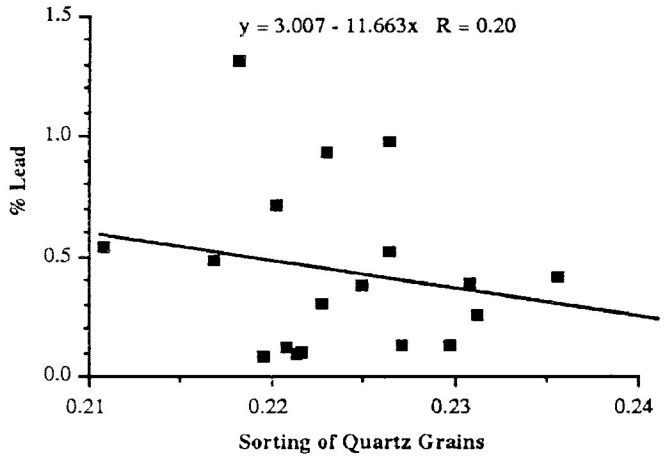

e) % Lead vs Sorting of Quartz

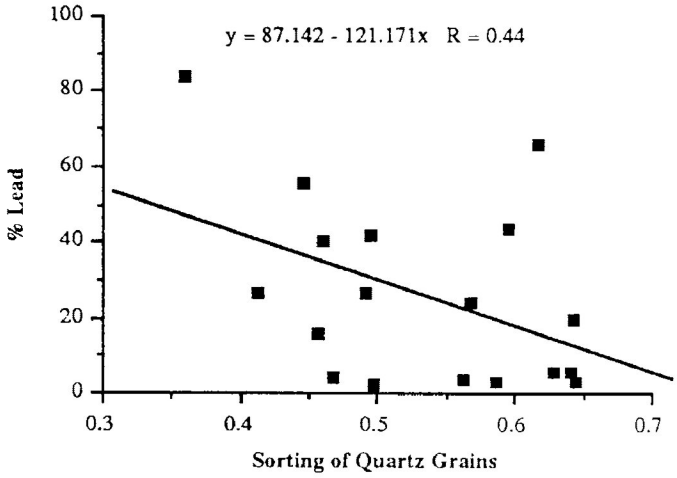

f) % Lead vs Sorting of Quartz

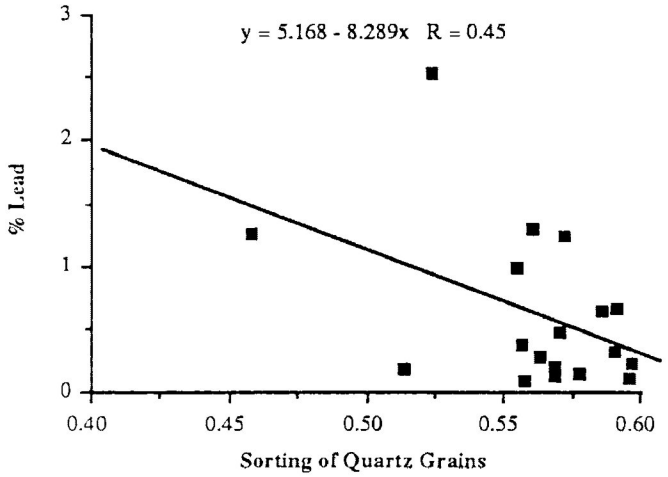

Appendix 2.21

APPENDIX 3

Data derived from selected experimental flume runs according to velocity

Run 19: Slowest Low velocity run (0.41 m/s)
Run 17: Fastest Low velocity run (0.56 m/s)
Run 4: Slowest Medium velocity run (0.73 m/s)
Run 23: Fastest Medium velocity run (0.93 m/s)
Run 24: Slowest High velocity run (1.09 m/s)
Run 22: Fastest High velocity run (1.27 m/s)

Site Number	Location (cm)	**Slow Run 19**	**Slow Run 17**	**Medium Run 4**	**Medium Run 23**	**Fast Run 24**	**Fast Run 22**
		Depth (cm)	Depth (cm)	Depth (cm)	Depth (cm)	Depth (cm)	Depth (cm)
1	0	10.0	10.0	3.5	12.0	10.0	9.0
2	150	9.0	8.5	3.5	9.5	9.0	9.0
3	214	11.0	10.0	4.0	9.0	9.0	9.5
4	250	11.0	9.5	3.0	9.0	8.5	10.0
5	271	11.0	10.0	2.5	10.5	9.0	7.0
6	303	19.0	19.0	9.0	18.0	13.0	15.0
		Vel (m/s)	Vel (m/s)	Vel (m/s)	Vel (m/s)	Vel (m/s)	Vel (m/s)
1	0	0.52	0.57	0.77	0.69	0.89	0.74
2	150	0.48	0.62	0.77	1.00	1.16	1.05
3	214	0.43	0.57	0.60	0.87	1.00	1.22
4	250	0.42	0.55	0.74	0.89	1.19	1.21
5	271	0.38	0.55	0.85	1.04	1.09	1.37
6	303	0.37	0.47	0.57	0.77	0.79	0.90
		Froude #	Froude #	Froude #	Froude #	Froude #	Froude #
1	0	0.63	0.69	1.41	0.79	1.08	0.93
2	150	0.60	0.80	1.41	1.24	1.46	1.32
3	214	0.51	0.69	1.04	1.10	1.26	1.51
4	250	0.49	0.68	1.45	1.12	1.53	1.47
5	271	0.45	0.67	1.81	1.24	1.37	1.89
6	303	0.37	0.47	0.72	0.78	0.88	0.96
		Slope	Slope	Slope	Slope	Slope	Slope
1.5	72.5	0.002	0.001	0.014	0.002	0.003	0.001
2.5	200	0.001	0.001	0.007	0.005	0.008	0.002
3.5	264	0.006	0.011	0.022	0.006	0.017	0.022
4.5	282	0	0.003	0.044	0.011	0.039	0.033
		Bed Shear	Bed Shear	Bed Shear	Bed Shear	Bed Shear	Bed Shear
1.5	72.5	13.1	6.43	41.6	14.2	19.7	6.31
2.5	200	6.78	6.43	22.1	32.2	50.5	12.9
3.5	264	43.5	74.7	73.4	37.9	107	147
4.5	282	0	20	106	73.4	241	200

APPENDIX 4

Data derived from selected experimental flume runs according to sediment grain size

Run 19: Fine-grained; Slow Velocity (0.41 m/s); Small Pebbles
Run 20: Fine-grained; Medium Velocity (0.83 m/s); Small Pebbles
Run 18: Fine-grained; Fast Velocity (1.24 m/s); Small Pebbles
Run 2: Medium-grained; Slow Velocity (0.51 m/s); Cobbles
Run 3: Medium-grained; Medium Velocity (0.83 m/s); Cobbles
Run 11: Medium-grained; Fast Velocity (1.25 m/s); Cobbles
Run 28: Coarse-grained; Slow Velocity (0.42 m/s); Small Pebbles
Run 26: Coarse-grained; Medium Velocity (0.91 m/s); Large Pebbles
Run 22: Coarse-grained; Fast Velocity (1.27 m/s); Cobbles

Run 19	To	U*	ßKU*	w Quartz	z Quartz	w Pyroxene	z Pyroxene	w Magnetite	z Magnetite	w Lead	z Lead
1.5	13.10	3.62	1.45	2.30	1.59	4.10	2.83	9.20	6.34	18.50	12.76
2.5	6.79	2.61	1.04	2.30	2.21	4.10	3.94	9.20	8.85	18.50	17.79
3.5	43.50	6.60	2.64	2.30	0.87	4.10	1.55	9.20	3.48	18.50	7.01
4.5	0.00	0.00	0.00	2.30	-	4.10	-	9.20	-	18.50	-

Run 20	To	U*	ßKU*	w Quartz	z Quartz	w Pyroxene	z Pyroxene	w Magnetite	z Magnetite	w Lead	z Lead
1.5	6.79	2.60	1.04	2.30	2.21	4.10	3.94	9.20	8.85	18.50	17.79
2.5	14.10	3.75	1.50	2.30	1.53	4.10	2.73	9.20	2.73	18.50	12.33
3.5	42.10	6.49	2.60	2.30	0.88	4.10	1.58	9.20	3.54	18.50	7.12
4.5	44.80	6.69	2.68	2.30	0.86	4.10	1.53	9.20	3.43	18.50	6.90

Run 18	To	U*	ßKU*	w Quartz	z Quartz	w Pyroxene	z Pyroxene	w Magnetite	z Magnetite	w Lead	z Lead
1.5	5.79	2.41	0.96	2.30	2.40	4.10	4.27	9.20	9.58	18.50	19.27
2.5	27.10	5.21	2.08	2.30	1.11	4.10	1.97	9.20	4.42	18.50	8.89
3.5	78.50	8.86	3.54	2.30	0.65	4.10	1.16	9.20	2.60	18.50	5.23
4.5	151.90	12.30	4.92	2.30	0.47	4.10	0.83	9.20	1.87	18.50	3.76

Run 2	To	U*	ßKU*	w Quartz	z Quartz	w Pyroxene	z Pyroxene	w Magnetite	z Magnetite	w Lead	z Lead
1.5	48.40	6.96	2.78	6.30	2.27	8.10	2.91	9.20	3.31	18.50	6.65
2.5	11.60	3.41	1.36	6.30	4.63	8.10	5.96	9.20	6.76	18.50	13.60
3.5	40.00	6.32	2.53	6.30	2.49	8.10	3.20	9.20	3.64	18.50	7.31
4.5	42.10	6.49	2.60	6.30	2.42	8.10	3.12	9.20	3.54	18.50	7.12

Run 3	To	U*	ßKU*	w Quartz	z Quartz	w Pyroxene	z Pyroxene	w Magnetite	z Magnetite	w Lead	z Lead
1.5	28.00	5.29	2.12	6.30	2.97	8.10	3.82	9.20	4.34	18.50	8.73
2.5	13.30	3.65	1.46	6.30	4.32	8.10	5.55	9.20	6.30	18.50	12.67
3.5	93.40	9.66	3.86	6.30	1.63	8.10	2.10	9.20	2.38	18.50	4.79
4.5	72.80	8.53	3.41	6.30	1.85	8.10	2.38	9.20	2.70	18.50	5.43

Run 11	To	U*	ßKU*	w Quartz	z Quartz	w Pyroxene	z Pyroxene	w Magnetite	z Magnetite	w Lead	z Lead
1.5	47.50	6.89	2.76	6.30	2.28	8.10	2.93	9.20	3.33	18.50	6.70
2.5	19.70	4.44	1.78	6.30	3.54	8.10	4.55	9.20	5.17	18.50	10.39
3.5	98.40	9.92	3.97	6.30	1.59	8.10	2.04	9.20	2.32	18.50	4.66
4.5	360.20	18.98	7.59	6.30	0.83	8.10	1.07	9.20	1.21	18.50	2.44

Run 28	To	U*	ßKU*	w Quartz	z Quartz	w Pyroxene	z Pyroxene	w Magnetite	z Magnetite	w Lead	z Lead
1.5	4.65	2.16	0.86	22.00	25.58	22.00	25.58	9.20	10.70	18.50	21.51
2.5	12.10	3.48	1.39	22.00	15.83	22.00	15.83	9.20	6.62	18.50	13.31
3.5	44.10	6.64	2.66	22.00	8.27	22.00	8.27	9.20	3.46	18.50	6.95
4.5	0.00	0.00	0.00	22.00	-	22.00	-	9.20	-	18.50	-

Run 26	To	U*	ßKU*	w Quartz	z Quartz	w Pyroxene	z Pyroxene	w Magnetite	z Magnetite	w Lead	z Lead
1.5	12.60	3.55	1.42	22.00	15.49	22.00	15.49	9.20	6.48	18.50	13.03
2.5	26.20	5.12	2.05	22.00	10.73	22.00	10.73	9.20	4.49	18.50	9.02
3.5	74.70	8.64	3.46	22.00	6.36	22.00	6.36	9.20	2.66	18.50	5.35
4.5	40.70	6.38	2.55	22.00	8.63	22.00	8.63	9.20	3.61	18.50	7.25

Run 22	To	U*	ßKU*	w Quartz	z Quartz	w Pyroxene	z Pyroxene	w Magnetite	z Magnetite	w Lead	z Lead
1.5	6.31	2.51	1.00	22.00	22.00	22.00	22.00	9.20	9.20	18.50	18.50
2.5	12.90	3.59	1.44	22.00	15.28	22.00	15.28	9.20	6.39	18.50	12.85
3.5	146.80	12.1	4.84	22.00	4.55	22.00	4.55	9.20	1.90	18.50	3.82
4.5	199.70	14.1	5.64	22.00	3.90	22.00	3.90	9.20	1.63	18.50	3.28

Legend

To: Bed Shear Stress
U*: Shear Velocity
ß: Constant (~1)
K: von Karman's constant (~0.4)
w: Settling Velocity
z: Rouse Z value